

Republic of Iraq
Ministry of Higher Education and Scientific Research
University of Misan/Collage of Engineering
Department of Civil Engineering



**STRENGTHENING TECHNIQUES FOR WEB OPENING
SHEAR SPAN OF COMPOSITE ENCASED STEEL-CONCRETE
BEAMS**

by

Khatam Salim Hussein

B.Sc. in Civil Engineering, 2018

A thesis submitted in partial fulfillment
of the requirements for the Master of Science
degree in Civil Engineering
University of Misan

May 2022

Supervisor:- Dr. Nasser Hakeem Tu'ma

سُورَةُ يُوسُفَ

بِسْمِ اللَّهِ الرَّحْمَنِ الرَّحِيمِ

وَلَمَّا بَلَغَ أَشُدَّهُ وَءَاتَيْنَاهُ حُكْمًا وَعِلْمًا وَكَذَلِكَ نَجْزِي

الْمُحْسِنِينَ ﴿٢٢﴾

DEDICATION

To my mother

A strong and gentle soul who taught me to trust in Allah, believe in hard work and that so much could be done with little.

To my supervisor Dr. Nasser Hakeem with respect.

ACKNOWLEDGEMENTS

In the accomplishment of this research successfully, many people have best owned upon me their the heart pledged support.

Primarily I would like to thank Allah, the prophet Muhammad and the family of Muhammad, and especially Imam Mahdi, for facilitating my research.

Then I would like to thank my mother, my father, and my sisters (Nisreen, Naba) who have helped me with their valuable suggestions and guidance has been very helpful in various phases of completion of the research.

Also, I would like to express my gratitude to my supervisor Dr. Nasser Hakeem, and many thanks for Engineer Ali and Raad for their helping.

Last but not the least I would like to thank my friends (Ahmed Kareem, Noora Kadhim) who have helped me a lot.

Supervisor certification

I certify that the preparation of this thesis entitled “Strengthening Techniques for Web Opening Shear Span of Composite Encased Steel–Concrete Beams” was presented by “Khatam Salim Hussein”, and prepared under my supervision at the University of Misan, Department of Civil Engineering, Collage of Engineer, as a partial fulfillment of the requirements for the degree of Master of Science in Civil Engineering (Structures).

Signature:

Dr. Nasser Hakeem Tu`ma

Date:

In view of the available recommendations, I forward this thesis for discussion by the examining committee.

Signature:

Assist. Prof. Dr. Samir M Chassib
(Head of Civil Eng. Department)

Date:

ABSTRACT

This research investigated the strengthening techniques of composite encased steel-concrete beams which have transverse square openings in the shear zone under the effect of four-point loading. Two square openings (50×50)mm and (136×136)mm were studied under the effect of using different strengthening techniques. The experimental program consisted of testing fifteen beams with transverse square openings in the mid-span of the shear zone, three of the beams served as control beams, including one beam without openings, whereas the other two beams had two openings located symmetrically in the shear zone, and twelve beams were strengthened with different techniques in the opening zone such as extruded encasing transversely (EET) technique, reinforcement arrangement, Carbon Fiber Reinforced Polymer CFRP sheets (the CFRP strengthening configuration considered in this study was a fully wrapping system around the square openings and diagonal strengthening sheets around the square openings) and Near Surface Mounted NSM CFRP bars in two different configurations around the square openings (strengthening the specimens with a Rhombus shape strengthening CFRP bar and diagonal strengthening CFRP bars). The structural response has been discussed in terms of the first cracking load, ultimate load, maximum deflection, failure modes, crack patterns, initial stiffness, and energy absorption. Test results indicated that the reinforcement arrangement technique used to strengthening small opening recorded an enhancement in the ultimate load capacity and stiffness of about 15% and 50%; respectively compared to the control beam with a small opening. In addition to the composite encased steel-concrete beam with small square opening in shear zone strengthening by CFRP fully wrapping sheets around openings has improved the shear strength as regards ultimate load capacity and energy absorption by 8% and 48% compared with the control beam with small opening; respectively.

TABLE OF CONTENTS

TABLE OF CONTENTS	vi
LIST OF TABLES	x
LIST OF FIGURES	xi
LIST OF SYMBOLES	1
CHAPTER ONE: INTRODUCTION	3
1.1 Introduction	3
1.2 The shape of opening	3
1.3 The opening’s location	4
1.4 Composite beam	4
1.5 Composite encased steel-concrete beams	5
1.6 Strengthening process	6
1.7 Techniques of strengthening	6
1.8 Fiber reinforced polymer (FRP).....	7
1.9 Near-surface mounted technique (NSM)	8
1.10 CFRP technique.....	9
1.11 Research objectives	9
1.12 Outline of Thesis	10
CHAPTER TWO: LITERATURE REVIEW	11
2.1 Size of opening.....	11
2.2 Shear failure mechanism	13
2.2.1 Shear design of the composite encased steel-concrete beams ...	13

2.3 Shear Capacity of Composite Member	16
2.4 Shear capacity and (CFRP bars/sheets).....	17
2.4.1 Externally bonded reinforcement (EBR) strips/sheets.....	19
2.4.2 Near-surface (NS)	20
2.4.3 CFRP's Contribution in shear capacity.....	20
2.5 Shear connectors.....	24
2.6 Literature review	24
2.6.1 Composite beam with web opening	25
2.6.2 Strengthening and location of transverse openings in shear zone	27
2.6.3 Strengthening techniques for web openings	28
2.6.4 Longitudinal openings of composite beam	30
2.7 Summary	34
CHAPTER THREE: EXPERIMENTAL WORK	35
3.1 General	35
3.2 Descriptions of specimens.....	35
3.3 Material characteristics	37
3.3.1 Material Properties	37
3.4 Geometry of the tested beams	40
3.5 The specimens variables in the present study	42
3.6 Steel materials used in the present work	48
3.6.1 Steel box section	48
3.6.2 Angle shear connector.....	48

3.6.3 Steel reinforcement	49
3.6.4 Reinforcement details of opening	50
3.7 Extruded encasing transversely (EET)	52
3.8 Reinforcement arrangement	53
3.9 Specimens preparation	54
3.9.1 Molds.....	54
3.10 Mixing procedures for the specimens	56
3.11 Workability test	56
3.11.1 The slump test	56
3.12 Pouring of the specimens	57
3.13 Curing and age of testing	57
3.14 Testing for mechanical properties of normal concrete.....	58
3.14.1 Compressive strength.....	58
3.14.2 Splitting tensile strength (fct).....	59
3.14.3 Modulus of rupture (fr)	61
3.15 Carbon fiber reinforced polymer (CFRP)	62
3.15.1 CFRP sheets	62
3.15.2 Adhesive material (epoxy)	63
3.16 Strengthening procedure of CFRP sheets	64
3.17 Strengthening by using NSM CFRP bars.....	66
3.18 Test Procedure	68

CHAPTER FOUR: EXPERIMENTAL RESULTS AND DISCUSSION	70
--	-----------

4.1 Introduction	70
4.2 General structural behavior of beams during the testing	70
4.3 General failure modes in the composite encased steel-concrete beams	72
4.4 Load-deflection behavior and crack patterns for tested beams	72
4.5 Ultimate load	82
4.6 Load-deflection comparisons for tested beam	84
4.7 Initial stiffness comparisons for the tested beams	88
4.8 ENERGY ABSORPTION CAPACITY COMPARISONS FOR THE TESTED BEAMS	92
CHAPTER FIVE: CONCLUSIONS AND RECOMENDATIONS	96
5.1 Conclusions	96
5.2 Recommendations for future works	100
REFERENCES	101
APPENDIX A	111
APPENDIX B	116

LIST OF TABLES

Table 2.1 Comparison between steel-reinforcement and (CFRP types).....	18
Table 3.1 Details of the Tested composite encased steel-concrete beams....	36
Table 3.2 Physical properties of cement	38
Table 3.3 Chemical properties of cement.....	38
Table 3.4 Grading of fine aggregate.....	39
Table 3.5 Grading of coarse aggregate.....	40
Table 3.6 Tensile properties of the steel section.	48
Table 3.7 Tensile test results of steel reinforcing bars	49
Table 3.8 Tensile test results of steel reinforcing bars	50
Table 3.10 Concrete Mix Design	56
Table 3.11 Experimental values of compressive strength.....	59
Table 3.12 Experimental values for the splitting tensile strength.....	60
Table 3.13 Flexural test results.....	61
Table 3.14 Properties of CFRP sheets.....	63
Table 3.15 Properties of CFRP bars.....	67
Table 4.1 Tests results of tested beams	71
Table 5.1 Theoretical and experimental result of CFRP sheet.....	100

LIST OF FIGURES

Figure 1.1 Examples illustrating beams with openings.	3
Figure 1.2 Composite Sections[28].	6
Figure 1.3 The application of FRP compos.....	8
Figure 1.4 NSM FRP bars.	8
Figure 1.5 CFRP sheets.	9
Figure 2.1 Definition of small openings according to Somes and Corley. ...	11
Figure 2.2 Definition of large openings according to Somes and Corley.....	11
Figure 2.3 Rectangular web opening in flexural zone of a simply supported RC beam[47].	12
Figure 2.4 Shear bond failure Interface[48].	13
Figure 2.5 Comparison among (CFRP,GFRP,AFRP, and steel bars) in term of stress-strain relationship ALNATIT 2011.	18
Figure 2.6 Typical wrapping schemes for shear strengthening using FRP laminates[50].	19
Figure 2.7 Illustration of the dimensional variables used in shear-strengthened calculations for repair, retrofit, or strengthening using FRP laminates[50].	19
Figure 2.8 Angle shear connector[62], [63].	24
Figure 2.9 Rectangular web openings in composite beams[64].	25
Figure 2.10 FM model used[66].	26
Figure 2.11 Configuration of experimental specimens[68].	28
Figure 2.12 The beam test setup and the steel reinforcement configuration[69].	29

Figure 2.13 The embedding of NSM steel bars into the grooves by epoxy paste[70].....	30
Figure 2.14 Setup of beams with reinforcement arrangement[71].	31
Figure 2.15 Casting beams with the longitudinal opening[72].	32
Figure 2.16 Beams with openings[73].	33
Figure 3.1 Cement used in the present work.....	39
Figure 3.2 Geometry for control beam.....	41
Figure 3.3 Details of first-group.....	43
Figure 3.4 Details of second-group.....	44
Figure 3.5 Details of third-group.....	45
Figure 3.6 Details of fourth-group.	46
Figure 3.7 Details of fifth-group.	47
Figure 3.8 Angle shear connectors with steel box.	49
Figure 3.9 Steel bars were used in this research.	49
Figure 3.10 Reinforcement details around a small and large opening[16]. ..	50
Figure 3.11 Reinforcement opening details for small and large openings....	51
Figure 3.12 Small square transverse openings strengthening by composite method CIS1.	52
Figure 3.13 Large square transverse openings strengthening by composite method CIS2.	53
Figure 3.14 Small square transverse openings strengthening by reinforcement arrangement RIS1.....	53
Figure 3.15 Large transverse square openings strengthening by reinforcement arrangement RIS2.....	54
Figure 3.16 Molds.	54

Figure 3.17 Preparing the molds.	55
Figure 3.18 Slump test.....	56
Figure 3.19 Curing of specimens.	57
Figure 3.20 Cleaning of specimens by water jet pump.	57
Figure 3.21 Painting the specimens by white color.	58
Figure 3.22 Tests of Normal mixture.	58
Figure 3.23 Compressive Strength Results and failure modes.	59
Figure 3.24 Test results of splitting tensile strength.	60
Figure 3.25 Test results and failure modes of modulus of rupture for prisms.....	62
Figure 3.26 Component A and Component B of Sikadur®-330.	64
Figure 3.27 Light gray paste of Sikadur®-330 components (A+B) mixing.	64
Figure 3.28 Electrical abrasive-paper.....	65
Figure 3.29 Composite encased steel-concrete beams with square openings strengthened by CFRP strips.....	65
Figure 3.30 Grooves installation.	67
Figure 3.31 NSM Installation.....	67
Figure 3.32 Universal Testing Machine.....	68
Figure 3.33 Schematic Testing Setup.....	69
Figure 4.1 Load-deflection behavior and crack patterns for CB.....	73
Figure 4.2 Load-deflection behavior and crack patterns for BW1.....	74
Figure 4.3 Load-deflection behavior and crack patterns for BW2.....	75
Figure 4.4 Load-deflection behavior and crack patterns for CIS1.....	76

Figure 4.5 Load-deflection behavior and crack patterns for CIS2.....	76
Figure 4.6 Load-deflection behavior and crack patterns for RIS1.....	77
Figure 4.7 Load-deflection behavior and crack patterns for RIS2.....	77
Figure 4.8 Load-deflection behavior and crack patterns for ECW1.	78
Figure 4.9 Load-deflection behavior and crack patterns for ECW2.	78
Figure 4.10 Load-deflection behavior and crack patterns for ECS1.....	79
Figure 4.11 Load-deflection behavior and crack patterns for ECS2.....	79
Figure 4.12 Load-deflection behavior and crack patterns for ECR1.	80
Figure 4.13 Load-deflection behavior and crack patterns for ECR2.	80
Figure 4.14 Load-deflection behavior and crack patterns for ECR3.	81
Figure 4.15 Load-deflection behavior and crack patterns for ECR4.	81
Figure 4.16 Load-deflection comparison for Gr.No.1 (effect of opening). ..	85
Figure 4.17 Gr.No.2 (effect of extruded encasing transversely technique) compared with control beams BW1 & BW2.....	85
Figure 4.18 Gr.No.3 (effect technique of reinforcement arrangement) compared with control beams BW1 & BW2.....	86
Figure 4.19 Gr.No.4 (effect technique of CFRP sheets) compared with control beams BW1 & BW2.....	87
Figure 4.20 Gr.No.5 (effect technique of CFRP bar) compared with control beams BW1 & BW2.....	88
Figure 4.21 Gr.No.1 (effect of opening).	89
Figure 4.22 Gr.No.2 (effect of extruded encasing transversely technique) compared with control beams BW1 & BW2.....	89
Figure 4.23 Gr.No.3 (effect technique of reinforcement arrangement) compared with control beams BW1 & BW2.....	90

Figure 4.24 Gr.No.4 (effect technique of CFRP sheets) compared with control beams BW1 & BW2.....	91
Figure 4.25 Gr.No.5 (effect technique of CFRP bar) compared with control beams BW1 & BW2.....	91
Figure 4.26 GR.No.1 (effect of openings).	93
Figure 4.27 GR.No.2 (effect strengthening of extruded encasing transversely) compared with control beams BW1 & BW2.	93
Figure 4.28 GR.No.3 (effect strengthening of reinforcement arrangement) compared with control beams BW1 & BW2.....	94
Figure 4.29 GR.No.4 (effect strengthening of CFRP sheets) compared with control beams BW1 & BW2.....	94
Figure 4.30 GR.No.5 (effect strengthening of CFRP bar) compared with control beams BW1 & BW2.....	95

LIST OF SYMBOLES

a	Shear span
γ_c	Concrete density
d	Effective depth
f_y	Yield stress of steel bars
E_s	Modulus elasticity of steel bars
ϵ_{cu}	Ultimate concrete strain
h_{wc}	Depth web concrete
L	Span length
γ_s	Steel density
ϕ_r	Diameter steel bar
ϕ_s	Diameter of the stirrups
A_{sr}	Steel area
S	Spacing between stirrups
f_y	Yield stress of stirrups
c_v	Web shear coefficient
f_c'	Compressive strength
b	Beam width
H	Overall beam depth
E_c	Concrete modulus of elasticity
t_1	Depth flange concrete
t_3	Width web concrete
A_{sbox}	Area of steel box
F_{ybox}	yield stress of steel box

b_{box}	Width of flange steel box
t	Thickness of flange steel box
h_{box}	Depth of steel box
t_{ws}	Thickness of web steel box
t_w	Thickness steel box
$(V_n)_{rc}$	Shear capacity of RC member
V_r	Shear contribution of the transverse reinforcement
V_c	Shear contribution of the concrete portion
A_v	Area of transverse reinforcement within distance
S	Spacing of transverse reinforcement
N_u	Required axial compression or tension computed at factored loads
A_g	Gross area of RC member
$(V_n)_{comp}$	Shear capacity of the concrete-encased composite member
sV_u	Shear capacity of steel portion
rV_u	Shear capacity of reinforced concrete (RC) portion
sM_u	Flexural capacity of the steel portion
l'	Clear span length of the composite member
t_w	Steel web thickness
d_w	Depth of the steel web
F_{ys}	Yield stress of steel
rM_u	Flexural capacity of RC portion
rV_{su}	Shear capacity in $r V_u$ controlled by the shear failure of RC portion
rV_{su1}	Shear capacity in $r V_{su}$ due to diagonal shear failure of RC portion
rV_{su2}	Shear capacity in $r V_{su}$ due to shear bond failure of RC portion
B	Gross width of composite member

r_j Distance between centroids of tension and compression in RC portion under flexural

$r\alpha$ Coefficient related to shear span ratio of RC portion

f_s Shear stress of concrete

ρ_w Ratio of transverse reinforcement

F_{yh} Yield stress of transverse reinforcement

n_{tf} layers' number of (FRP sheet/strip)

A_{fv} FRP's Area

d_{fv} FRP's Effective-depth

α FRP inclination-angle

w_f FRP width

S_f Space c/c sheet

f_{fe} Stress in FRP

ϵ_{fe} FRP strain

E_f Modulus-of-elasticity of FRP

V_{1F} (FRP) shear strength participation concerning to bonding shear-failures

V_{2F} (FRP) shear-strength participation corresponding to maximum (FRP)

strain

d_b bar's diameter

τ_b average bond strength

L_{tot} sum of effective-lengths of whole bars those crossed by crack

E_b bar's Modulus of elasticity

d_{net} Reduced length of (FRP rods)

d_r height of shear-strengthened part of cross-section

c concrete's cover

f_r Modulus of rupture

CHAPTER ONE: INTRODUCTION

1.1 Introduction

Many pipes and ducts are required in the construction of modern buildings to accommodate important services such as air conditioning, electricity, telephone, and computer network. Web openings in concrete beams enable the installation of these services. Transverse openings in beams are source of potential weakness. So, the presence of opening in web of reinforced concrete beam result in many problems in the beam behavior including a reduction in beam stiffness, excessive cracking, and deflection and reduction in beam capacity[1]–[14]. Additionally, including openings cause high concentration of stress around the openings, particularly at the corners. The simple beam behavior is changed to a more complex one when the total cross-sectional dimension of the beam is reduced[15], [16]. There are many shapes and sizes of openings available.



Figure 1.1 Examples illustrating beams with openings.

1.2 The shape of opening

One of the things that affect the shear strength of beam is opening's shape. It has been discovered that utilizing a circular opening provides advantages over using a square opening. This is caused to the circular openings' absence of sharp

corners, which results in a decrease in stress concentration around the openings[17],[18].

1.3 The opening's location

The load is heavily influenced by the location of openings. The ultimate load is reduced by positioning of the openings in the load path. As a result, the beam's behavior is mostly determined by the degree of interruption of the opening with a loading path[19].

1.4 Composite beam

Composite member is structural member that is made up of two materials: structural steel (rolled or built-up) and reinforced concrete. Composite beams can take numerous forms, one of which is concrete-encased beams. Composite member has become common construction technique for bridges and commercial buildings in recent years. The system of composite member allows for; a quicker construction process and thinner floor depths, reducing height of building and provide well corrosion protection. In this context, composite beams with openings are a useful tool that can be used to decrease the height of the floor by resolving problems of duct passage. However, if openings must be provided in beams especially in the shear zone. To ensure the structure's safety and serviceability so adequate handling and care are needed. Because shear failure in concrete structures is generally disastrous, due to the brittle nature and the no warning before the failure[20].

For the reason floor height in most high-rise buildings is limited, it is necessary to pass service pipes, cooling ducts, and systems of heating through transverse openings in the floor beams. Beam with web opening can have several

disadvantages, including a reduction in the beam's strength and stiffness, excessive cracking, and deflection due to high-stress concentration at the opening's corners. The openings must be strengthened to overcome the above problems. Openings take many shapes such as circular, square, and rectangular etc.[21]

1.5 Composite encased steel-concrete beams

Steel-concrete composite structures offer a higher rigidity, smaller cross-sections, and a quicker construction process than individual steel and concrete structures. Concrete encased steel beams (CESB) are one composite member in which steel beam that is partially or completely encased in concrete. Lower floor depths, high fire resistance, less maintenance and better corrosion protection for the steel beam are several reasons urge the CESB should be used in construction [22]–[27]. Openings in structural members are commonly used in current buildings and bridges to pass large ducts, air conditioning pipes, and drainage pipes, hence reducing construction depth. On the negative side, depending on the shapes, dimensions, numbers, and locations of the openings, web openings can cause problems with the load-carrying capacity of beams. The stiffness is also decreased by reducing both the gross moment of inertia at the opening and the cross-sectional area available for carrying stresses. As a result, strengthening those openings using traditional materials like steel plates or modern materials like Fiber-Reinforced Polymer (FRP) composites becomes vital[28].

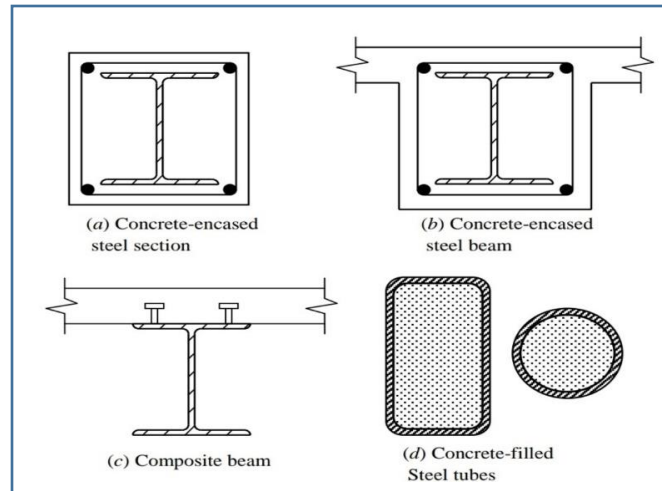


Figure 1.2 Composite Sections[28].

1.6 Strengthening process

The process of strengthening is carried out when a great performance level needed to reach, which include criteria like load carrying capacity[29]. Maintenance is a general term that encompasses both strengthening and repairing. It has become a common successful solution for keeping critical structures in service, especially when removing or replacing infrastructures is not cost-effective[30].

1.7 Techniques of strengthening

Strengthening methods such as internal steel reinforcement (I.S.R.) and near-surface mounted using FRP laminate (N.S.M.) or external bonding strengthening (E.B.) such as externally bonded FRP laminates are used as strengthening methods for the RC beams with web opening. Because of their superior properties such as high stiffness and strength, ease of installation, the ability to apply without disturbing the structure's existing functionality, non-corrosive and nonmagnetic nature of the materials, and chemical resistance. So FRP composite materials are an excellent option for external reinforcement. In

addition, it has been well demonstrated that increasing shear capacity and ductility of RC beams with web opening[31]–[36].

1.8 Fiber reinforced polymer (FRP)

Carbon, glass, and aramid fibers encapsulated in a polymer matrix in the form of wires, bars, strands, or grids are some of the most common types of high-strength non-metallic fibers, also known as fiber-reinforced polymer (FRP). FRP has shown great potential and functionality in concrete reinforcement, particularly where durability is of main concern. Nowadays, FRP has been used as a structural reinforcing material. As well as for bridge construction materials such as bridge decks. FRP can be used to strengthen and retrofit existing structures that have degraded or have strength deficiency. With its lightweight, high strength, and corrosion resistance, FRP is an attractive material for structural rehabilitation. Furthermore, because FRP is made up of thin sheets it makes very few changes to the dimensions of the existing structural member. These materials were applied to the external surfaces of the beams in various configurations and layouts by bonding each other. The use of FRPs to repair and rehabilitate damaged steel and concrete structures has gained increasingly attractive. Due to its well-known mechanical properties, particularly its high strength-to-weight ratio and low weight[10], [28], [37].



Figure 1.3 The application of FRP composites.

1.9 Near-surface mounted technique (NSM)

NSM (Near Surface Mounted) is a new technique that involves cutting grooves in the concrete cover and inserting bar into it with a special groove filler (epoxy or cement mortar). However, this procedure did not result in improved bond strength, and in some cases, casting concrete around the whole strengthened members is not practical. In the early 1960s, the epoxy industry implemented structural filled and progressed NSM technique step further by employing resins as groove fillers[38]. With the expansion of NSM as an effective strengthening system. Steel bar corrosion has led to the usage of FRP products such as carbon fiber reinforced polymer bars[38], [39].



Figure 1.4 NSM FRP bars.

1.10 CFRP technique

As structures deteriorate with time, strengthening and repairing concrete elements is widely common. Cost and time are two factors that influence whether or not a strengthening technique is used. Strengthening with FRP is currently the most common technique. FRP has many advantageous such as lightweight, corrosion resistance, high strength, and easy yet efficient application on concrete. CFRP, GFRP, and Aramid Fiber Reinforced Polymer (AFRP) fibers were used for shear repair. CFRP being extensively used as an external reinforcement to resolve the strength requirements in structural systems where has become a solution to this issue[40]–[42].

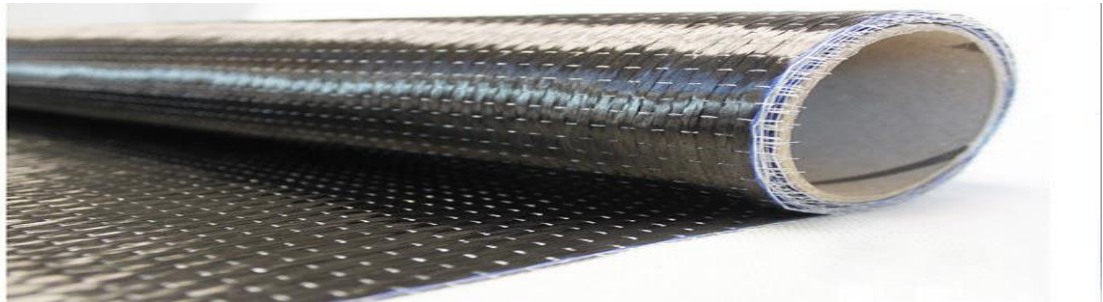


Figure 1.5 CFRP sheets.

1.11 Research objectives

The main aims of this research are:

- 1-Studying existing transverse square opening in the shear zone and effect this opening on the behavior of composite encased steel-concrete beam.
- 2-Studying effect of opening size on shear resistance of the composite encased steel-concrete beam.
- 3-Studying the strengthening techniques of composite encased steel-concrete beams with square web opening in the shear zone.

1.12 Outline of Thesis

The current research consists of five chapters:

Chapter one explains a general introduction to the present research.

Chapter two contains historical background and literature reviews number of scientific studies and researches on current research topics published by accredited scholars and researchers.

Chapter three covers the experimental works in all its aspects in terms of the characteristics of the materials used, the geometry details of the parameters studied for composite encased steel-concrete beams, casting, and the procedure of the testing.

Chapter four includes the results of the experimental testing and provides all the readings recorded during the testing in terms of deflections, cracks, etc. Presents the discussion of the results.

Chapter five the conclusions obtained from the current research and make several suggestions and recommendations for future studies to avoid the negatives that have been recorded and to develop these new types of composite encased elements more broadly.

CHAPTER TWO: LITERATURE REVIEW

2.1 Size of opening

Many researchers use the term small and large to describe the size of openings without providing a definition or a clear demarcation line.

Large openings and small openings are two types of openings. When the depth (or diameter) of the circular, square, or nearly square opening is less than 40% of the overall beam depth, it is considered a small opening. Otherwise, openings are considered large openings[43], [44].

An opening is small if its depth (d) or diameter (D) is less than or equal to 0.25 times the depth of the beam h and its length is less than or equal to its depth d , according to Some and Corley[45], [46]. As shown in Figure (2.1).

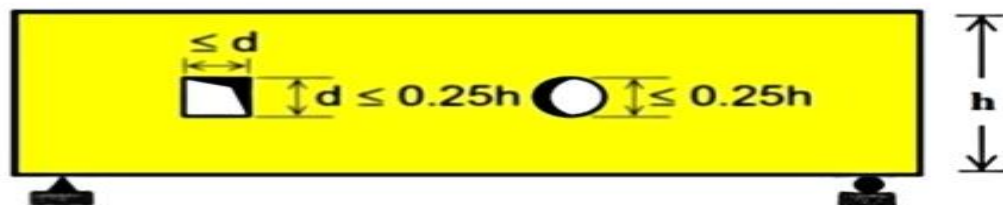


Figure 2.1 Definition of small openings according to Some and Corley.

According to Some and Corley, an opening is considered large if its depth (d) or diameter (D) is $> 0.25h$, and its length $L > d$ depth. As shown in Figure (2.2).

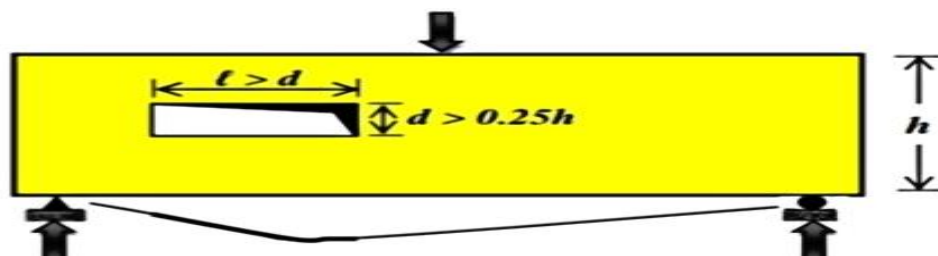


Figure 2.2 Definition of large openings according to Some and Corley.

If $L_o \leq h_c$, where L_o is length of opening and h_c is the largest of depth of bottom chord (h_b) and depth of top chord (h_t), the opening is classified as small. $L_o > h_c$ for large opening[47]. As shown in Figure (2.3).

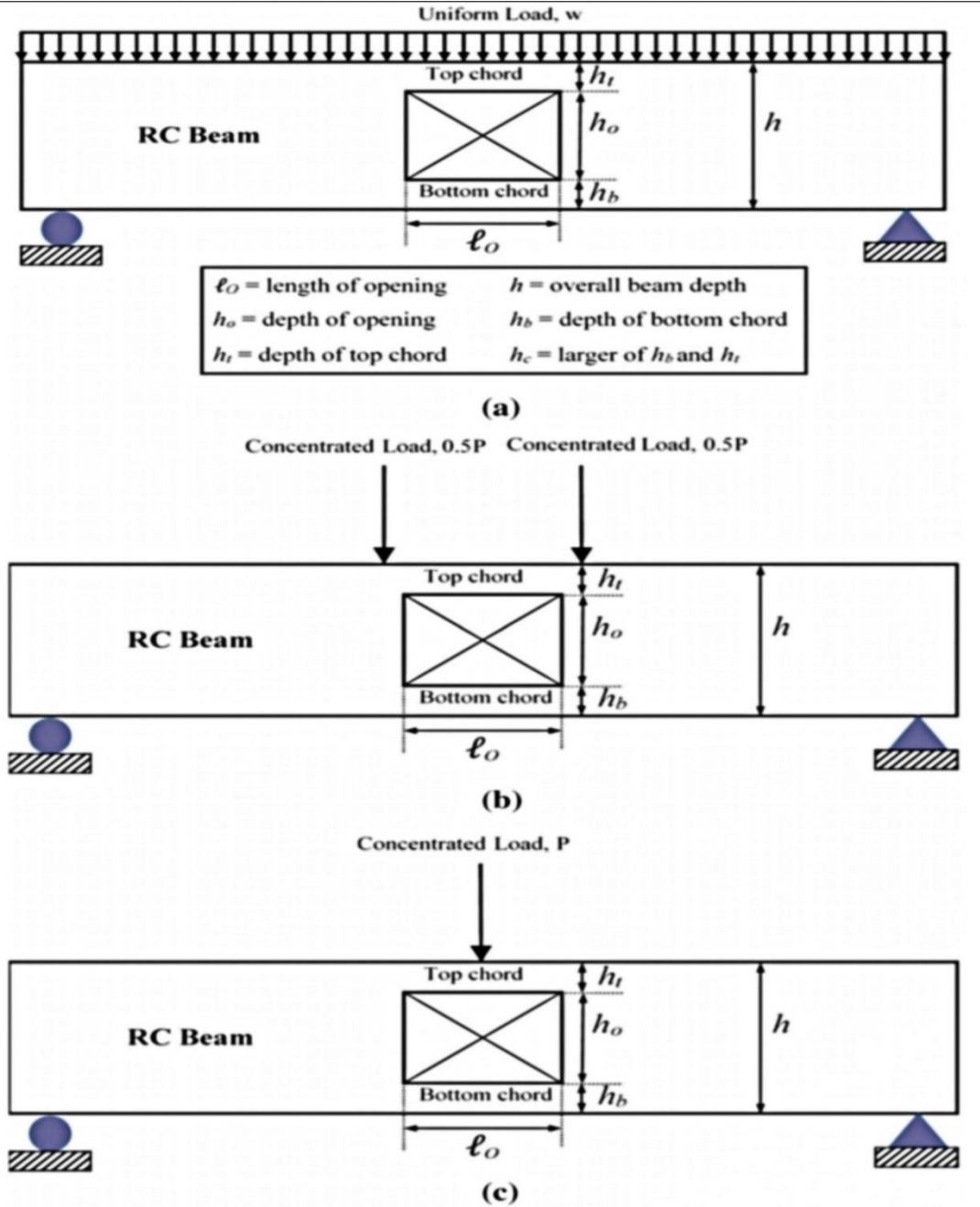


Figure 2.3 Rectangular web opening in flexural zone of a simply supported RC beam[47].

2.2 Shear failure mechanism

composite steel and reinforced concrete structural system can form a building carrying the merits of each material. One of the major concerns when designing composite structural member is preventing shear failure. Concrete-encased composite member generally shear failure occurs in one of two possible modes of failure: 1- diagonal shear failure, which is similar to shear failure in an ordinary reinforced concrete structural member.

2- shear bond failure as shown in Figure (2.4), results from cracks along with the steel flange interface and concrete. The shear bond failure in composite can be critical when the steel flange width is large and approaching the overall width of the composite section[48].

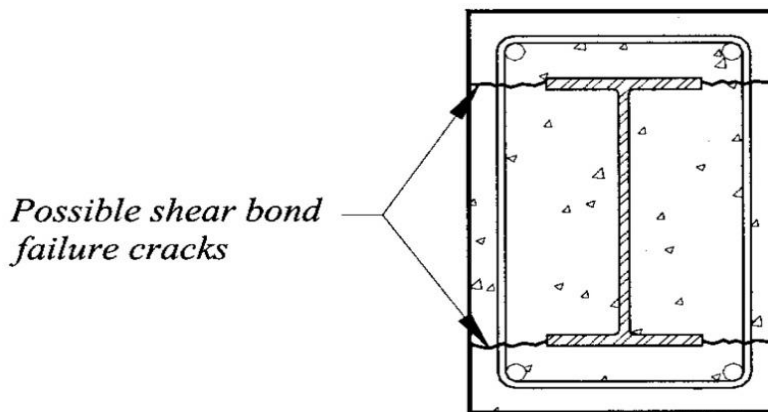


Figure 2.4 Shear bond failure Interface[48].

2.2.1 Shear design of the composite encased steel-concrete beams

Shear design has major importance in all types of concrete structures. Approaches to shear design for concrete-encased composite members have been developed. Among the shear design approaches developed for concrete-encased composite members, the design provisions suggested by American building specifications and the Japanese building codes are two widely employed

approaches. In the United States, the design provisions of composite members can be found in the American Concrete Institute ACI (1999) building code. On the other hand in Japan the concept of superposition for the shear design of composite members is adopted in the Architectural Institute of Japan AIJ Steel Reinforced Concrete (SRC) building code AIJ 1987[48].

2.2.1.1 ACI building code (ACI 1999)

There is no clear guideline available for the shear design of concrete-encased composite members in the ACI building code. It is also noted that there is no specific provision is included regarding the prevention of the shear bond failure of concrete-encased composite members. However, there are valuable provisions for the shear design of ordinary RC structural members. The diagonal shear failure mode is usually a major concern in the shear design of RC member[48], [49]. The shear capacity of an RC member that fails in diagonal shear can be calculated using the equations below in the ACI code:

$$(V_n)_{rc} = V_r + V_c \quad 2.1$$

With

$$V_r = (A_v \times F_{yh} \times d) / S \quad 2.2$$

And members subjected to shear and bending

$$V_c = 0.17 \sqrt{f_c'} bd \quad 2.3$$

Members subjected to shear, bending, and axial compression

$$V_c = 0.17 (1 + 0.073 N_u / A_g) \sqrt{f_c'} bd \quad 2.4$$

And members subjected to shear, bending and axial tension

$$V_c = 0.17 (1 + 0.29 N_u / A_g) \sqrt{f_c'} bd \quad 2.5$$

Where $(V_n)_{rc}$ = shear capacity of RC member, V_r = shear contribution of the transverse reinforcement, V_c = shear contribution of the concrete portion, A_v = area of transverse reinforcement within distance S , d = distance from extreme compression fiber to centroid of longitudinal tension reinforcements, S = spacing of transverse reinforcement, f_c' = concrete compressive strength, b = gross width of RC member, N_u = required axial compression or tension computed at factored loads, and A_g = gross area of RC member.

2.2.1.2 AIJ-SRC code (AIJ 1987)

According to the Architectural Institute of Japan (AIJ) Steel Reinforced Concrete (SRC) building code (AIJ 1987). The shear capacity of composite member is evaluated based on the method of superposition. That is

$$(V_n)_{comp} = sV_u + rV_u \quad 2.6$$

where $(V_n)_{comp}$ = shear capacity of the concrete-encased composite member. sV_u = shear capacity of steel portion, and rV_u = shear capacity of reinforced concrete (RC) portion. According to the commentary on the AIJ-SRC code, the bond between the steel shape and the concrete can be neglected in the ultimate state. Thus, the shear capacity of a concrete-encased composite member is determined in such a way that the steel and RC portions resist the shear separately without a bond between them. To determine sV_u and rV_u it is suggested that

$$sV_u = \min(\sum sM_u / l', t_w \cdot d_w \cdot F_{ys} / \sqrt{3}) \quad 2.7$$

$$rV_u = \min(\sum rM_u / l', rV_{su}) \quad 2.8$$

where sM_u = flexural capacity of the steel portion; l' = clear span length of the composite member; t_w = steel web thickness; d_w = depth of the steel web; F_{ys} =

yield stress of steel; rM_u = flexural capacity of RC portion; and rV_{su} = shear capacity in rV_u controlled by the shear failure of RC portion. To determine rV_{su} in (2.9), the following formula is suggested:

$$rV_{su} = \min (rV_{su1}, rV_{su2}) \quad 2.9$$

$$rV_{su1} = B \cdot r_j \cdot (0.5 \cdot r\alpha \cdot f_s + 0.5 \cdot \rho_w \cdot F_{yh}) \quad 2.10$$

$$rV_{su2} = B \cdot r_j \cdot (b'/B \cdot f_s + \rho_w \cdot F_{yh}) \quad 2.11$$

where: rV_{su1} = shear capacity in rV_{su} due to diagonal shear failure of RC portion. rV_{su2} = shear capacity in rV_{su} due to shear bond failure of RC portion; B = gross width of composite member; r_j = distance between centroids of tension and compression in RC portion under flexural; $r\alpha$ = coefficient related to shear span ratio of RC portion, conservatively taken to equal 1.0; f_s = shear stress of concrete. ρ_w = ratio of transverse reinforcement; F_{yh} = yield stress of transverse reinforcement; and b' = effective width of concrete.

2.2.1.3 AISC-LRFD SPECIFICATION (AISC 1993)

For concrete-encased composite beams. AISC-LRFD specification states that the shear capacity should be determined by the properties of the steel section alone. The shear capacity contribution of the RC portion is conservatively neglected.

2.3 Shear Capacity of Composite Member

In the proposed approach. The shear capacity of a concrete encased composite member can be determined as follows:

$$(V_n)_{comp} = (V_n)_s + (V_n)_{rc} \quad 2.12$$

with

$$(V_n)_s = 0.6F_{ys} A_{ws} \quad 2.13$$

$$(V_n)_{rc} = \min[(V_n)_{rc1}, (V_n)_{rc2}] \quad 2.14$$

Where $(V_n)_s$ represents the shear capacity of steel shape in the composite member; $(V_n)_{rc}$ denotes the shear capacity of the RC portion in the composite member; A_{ws} = area of steel web; $(V_n)_{rc1}$ and $(V_n)_{rc2}$ = shear capacities of the RC portion in the composite member controlled by diagonal shear failure and shear bond failure, respectively. As indicated in (2.14), the shear capacity of the RC portion $(V_n)_{rc}$ is determined as the smaller value of the diagonal shear capacity $(V_n)_{rc1}$ and the shear bond capacity $(V_n)_{rc2}$.

2.4 Shear capacity and (CFRP bars/sheets)

Banding a steel plate to the tension zone of a concrete member by adhesive resin was a workable technique for increasing the beam's shear and flexural strength. Several bridges and buildings were strengthened by (FRP) technique; because the steel plate could corrode, causing its bond to the concrete substrate to degrade; and because of their installation's onerousness, which requires utilize of heavy equipment. Researchers have started using (FRP materials) as a substitute for steel plate, external post-tensioning, and section enlargement (e.g. concrete-column jacketing) (ACI 440.2R-08)[50], [51]. Considerable research studies in shear and flexural strengthening of structures have been conducted, mostly in the United States, Europe, and Japan (ACI 440.2R-08)[50].

Table (2.1) represent comparison between steel-reinforcement and (CFRP types)[52].

Table 2.1 Comparison between steel-reinforcement and (CFRP types).

	Steel	GFRP	CFRP	AFRP
Nominal yield stress, (MPa)	(276 to 517)	N/A	N/A	N/A
Tensile strength, (MPa)	(483 to 690)	(483 to 1600)	(600 to 3690)	(1720 to 2540)
Elastic modulus, x10 ³ (GPa)	(200.1)	(35.0 to 51.0)	(120.0 to 580.0)	(41.0 to 125.0)
Rupture strain, %	6.0 to 12.0	1.2 to 3.1	0.5 to 1.7	1.9 to 4.4
Typical densities (g/cm ³)	(7.9)	(1.2 to 2.1)	(1.5 to 1.6)	(1.2 to 1.5)

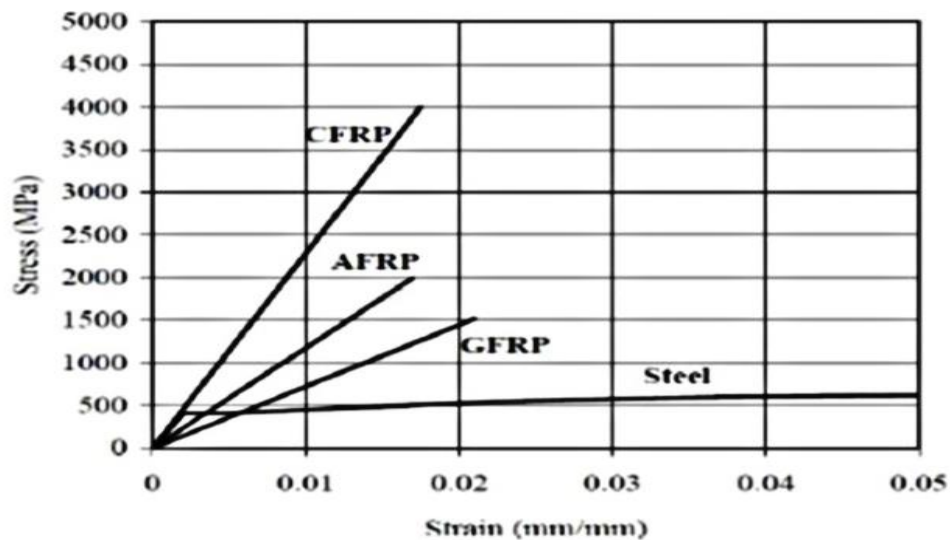


Figure 2.5 Comparison among (CFRP,GFRP,AFRP, and steel bars) in term of stress-strain relationship ALNATIT 2011.

The shear-failure mode of the (RC) beam must be avoided because it is unpredictable and brittle. On (RC) structures-rehabilitation, (CFRP) material is being used as a competitive alternative. There are two main techniques for (CFRP's) applied as the pursues shear strengthening :-

2.4.1 Externally bonded reinforcement (EBR) strips/sheets

Widespread shear strengthening-configuration of this technicality comprise [50]:-

- . 2 sides
- . 3-sided "U-wrap"
- . Completely wrapped

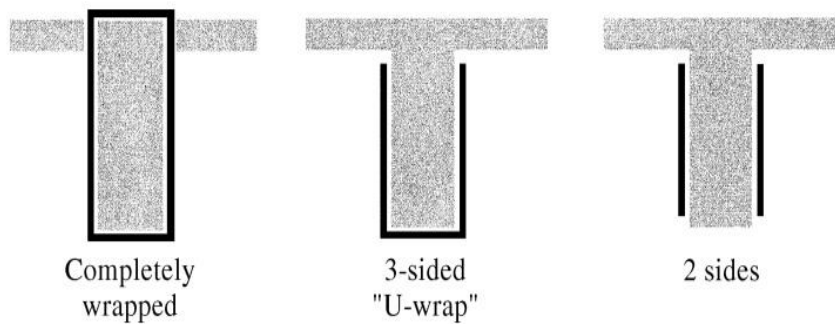


Figure 2.6 Typical wrapping schemes for shear strengthening using FRP laminates[50].

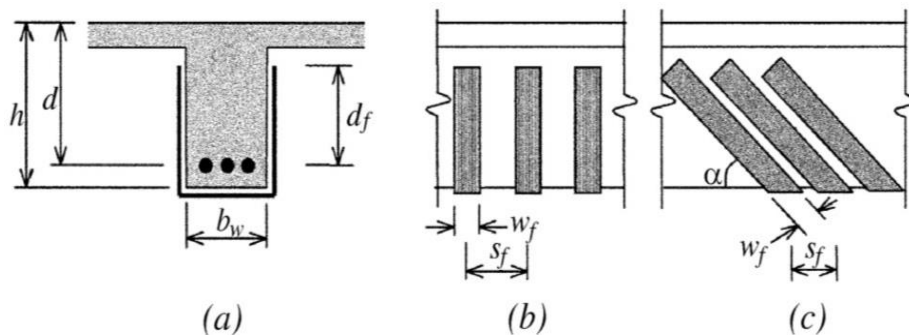


Figure 2.7 Illustration of the dimensional variables used in shear-strengthened calculations for repair, retrofit, or strengthening using FRP laminates[50].

2.4.2 Near-surface (NS)

It's one of the more favorable concrete structure strengthening techniques. Although research on this topic only a few years ago, it has attracted worldwide attention. There is no need for highly-skilled and experienced workers in FRP installation. Design is dictated by (ACI 440.2R)[50].

The effectiveness of the NSM-technique with (CFRP-laminates) for shear-strengthening of T-beams was the aim of (Dias & Barros, 2010)[53]. Fifteen T-beams were cast, with three inclinations of laminates (45, 60, and 90), and three different stirrups & FRP ratios, and found that (NSM) was more efficient than (EBR) in terms of increasing load-capacity after shear-cracks formulation. After cutting and cleaning thin slots, the strengthening procedure is resumed for CFRP laminates installation.

The effectiveness of NSM with CFRP laminates for shear strengthening of T-beams [54]. An experimental program was consisted of (nine T-beams), five of which served as reference beams and the other with NS CFRP shear strengthening T-beams, and their variables were the number of stirrups in the shear span zone (a) and the number and angle of the CFRP. Three-point loads are used to evaluate all beams. They're deduced that NSM shear strengthening with CFRP-laminate is extremely effective in beams for ensuring increased CFRP's tensile capacity.

2.4.3 CFRP's Contribution in shear capacity

The FRP sheet/strip shear capacity count on numerous factors. Modulus of elasticity FRP, FRP's thickness that applied on concrete's surface, FRP's orientation, concrete's compressive strength. FRP's application technique predicting shear strengthen contribution, and understanding shear failure mechanisms of FRP had been the research study to many types[55]. Some existent models are presented in the following:-

2.4.3.1 CFRP sheet's contribution in shear capacity

- ACI 440 Model

The shear strength participation proposed in [41], [50] and [56] as following:-

$$\phi V_n = \phi (V_c + V_s + \psi_f V_f) \quad 2.15$$

$$V_f = [A_{fv} \times f_{fe} \times (\sin \alpha + \cos \alpha) \times d_{fv}] / S_f \quad 2.16$$

$$A_{fv} = 2 \times n_{tf} \times w_f \quad 2.17$$

$$f_{fe} = \epsilon_{fe} \times E_f \quad 2.18$$

(n_{tf}) are layers' number of (FRP sheet/strip) applied. $\phi = 0.75$, (A_{fv}) FRP's Area, (d_{fv}) FRP's Effective-depth, (α) FRP inclination-angle, (w_f) FRP width. (S_f) Space c/c sheet, (f_{fe}) stress in FRP, (ϵ_{fe}) FRP strain, (E_f) modulus-of-elasticity of FRP.

$$\epsilon_{fe} = \kappa_v \epsilon_{fu} \leq 0.004 \quad [\text{for U-jacketing and (two-sides) bonding}] \quad 2.19$$

$$\epsilon_{fu} = C_E \times \epsilon_{fu} \quad 2.20$$

$$\kappa_v = (k_1 \times k_2 \times L_e / (11900 \times \epsilon_{fu})) < 0.75 \quad 2.21$$

$$L_e = 23300 / (n_{tf} \times t_f \times E_f)^{0.58} \quad 2.22$$

$$k_1 = (f_c' / 27)^{2/3} \quad 2.23$$

$$k_2 = (d_{fv} - L_e) / d_{fv} \quad [\text{for U-jacketing bond}] \quad 2.24$$

$$k_2 = (d_{fv} - 2 \times L_e) / d_{fv} \quad [\text{for (two sides) bonding}] \quad 2.25$$

$$(V_s + V_f) \leq (0.66 \sqrt{f_c'} \times b_w d) \quad (\text{shear strength limits}) \quad 2.26$$

k_1 =modification factor applied to κ_v to account for concrete strength, k_2 = modification factor applied to κ_v to account for wrapping scheme, L_e =active bond

length of FRP laminate (mm), t_f =nominal thickness of one ply of FRP reinforcement (mm), ϵ_{fu} =design rupture strain of FRP reinforcement (mm/mm), κ_v =bond-dependent coefficient for shear, V_s =nominal shear strength provided by steel stirrups.

2.4.3.2 NS CFRP bar's contribution in shear capacity

(De Lorenzis & Nanni) [57] are proposed two models to predicted (NS FRP-bars) contribution in shear capacity for beams, with reference to failure mechanisms, the first (V1F) is (FRP) shear strength participation concerning to bonding shear-failures, second (V2F) is (FRP) shear-strength participation corresponding to maximum (FRP) strain, as follows:-

$$V_{1F} = 2\pi \times d_b \times \tau_b \times L_{tot} \quad 2.27$$

$$\tau_b = 0.001 \times (d_b \times E_b) / L_i \quad 2.28$$

$$L_{tot} = d_{net} - S \rightarrow \text{if } (d_{net}/3) \leq S \leq d_{net} \quad 2.29$$

$$L_{tot} = 2 \times d_{net} - 4 \times S \rightarrow \text{if } (d_{net}/4) \leq S \leq d_{net}/3 \quad 2.30$$

$$d_{net} = d_r - 2 \times c \quad 2.31$$

Where; (db) bar's diameter, (τ_b) average bond strength, (L_{tot}) sum of effective-lengths of whole bars those crossed by crack, (E_b) bar's Modulus of elasticity, (L_i) rod's Effective-length crossed by crack corresponding to tensile-strain, (d_{net}) Reduced length of (FRP rods), (S) NS CFRP bar's Spacing, (d_r) height of shear-strengthened part of cross-section, (c) concrete's cover.

$$V_{2F} = 2 p db \tau_b L_i \quad (d_{net}/4) \leq S \leq (d_{net}/3), \quad V_{2F} \text{ controls if } L_i > S. \text{ If } L_i < S \text{ } V_{2F} \text{ controls with the value} \quad 2.32$$

$$V_{2F} = 2\pi \times db \times \tau_b \times (L_i + d_{net} - 2S) \quad 2.33$$

$$\text{If } (d_{net} - 2S) \leq L_i \leq S \quad 2.34$$

$$V_{2F} = 4\pi db \tau_b L_i \quad \text{if } L_i < d_{net} - 2S \quad 2.35$$

$$(d_{net}/4) < S < (d_{net}/3) \quad V_{1F} \text{ controls if } L_i > d_{net} - 2S \quad 2.36$$

If $L_i < d_{net} - 2S$, V_{2F} controls with the value

$$V_{2F} = 2\pi \times db \times \tau_b \times (L_i + d_{net} - 2S) \quad \text{if} \quad 2.37$$

$$S < L_i < d_{net} - 2S$$

$$V_{2F} = 2\pi \times db \times \tau_b \times (2L_i + d_{net} - 3S) \quad \text{if} \quad 2.38$$

$$d_{net} - 3S < L_i < S$$

$$V_{2F} = 6\pi \times db \times \tau_b \times L_i \quad \text{if} \quad 2.39$$

$$L_i \leq d_{net} - 3S$$

Also, to estimate the NSM FRP bar contribution to the shear resistance of an RC beam V_f . An equation was first proposed by De Lorenzis and Nanni (2001) and adopted by Dias and Barros (2010) [53],[57] and [58], V_f can be given by:

$$V_f = [2\pi db L_{tot} - \min \tau_{bond}] \sin \theta \quad 2.40$$

Where the term in the square brackets is the tensile force that can be developed in the NSM bar. db =the diameter of the bar, θ =the angle of inclination of

the NSM bars, τ_{bond} =the tensile stress in the NSM bar and $L_{\text{tot-min}}$ =the minimum total length of the FRP bars intercepted by the shear crack.

2.5 Shear connectors

Shear connectors are usually used in composite beams. To transfer longitudinal shear forces through the steel-concrete border, also to prevent or reduce relative displacement of concrete and steel sections which happens due to composite action in a composite beam. There are many types of shear connectors, such as headed stud shear connector, channel shear connector, and angle shear connector etc. Using angles is cheaper than studs and channels[59]–[63].

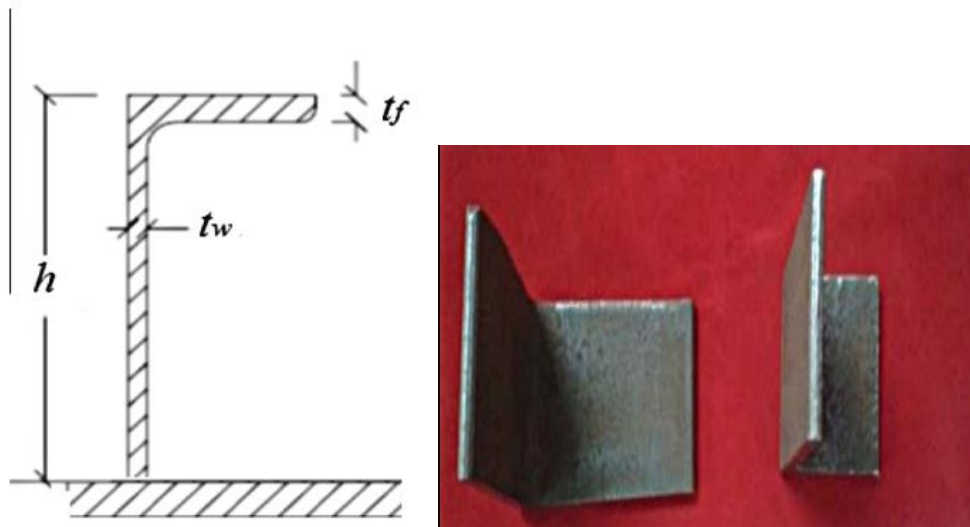


Figure 2.8 Angle shear connector[62], [63].

2.6 Literature review

It has been found that concrete-encased steel beams CESBs have become one of the most important composite members used in the construction in recent years. Openings in structural members are given the impression to pass big ducts, air conditioning pipes, and drainage pipes. It also illustrated that, relying on the shapes, locations, numbers, and dimensions of the openings[22].

2.6.1 Composite beam with web opening

Tiago Miguel [64], in this research studied design resistance calculation for composite beams with large web openings. It was done to esteem the structural perforated beams behavior. In addition to influence of web openings in load carrying capacity, a numerical model was developed. The concrete's and steel's non-linear behavior has been occupied into account. So the concrete was modeled using finite element software's concrete damaged plasticity CDP. A design model is presented that describes the performance of beams with large web openings. As a results, composite beams' load capacity reduced by the presence of openings.



Figure 2.9 Rectangular web openings in composite beams[64].

Yokesh N et al. [65], the flexural behavior of a concrete-encased cold-formed steel composite beam with M20 rank concrete was inspected by an experimental study. Totally four beam specimens with and without web opening were tested with different percentages of steel thickness (2mm, 2.5mm, and 3mm). To evade slip and to transfer horizontal shear between cold-formed steel and concrete, shear connectors were provided for the beam without web opening. Beam encased concrete with web opening performed better than the beam without web opening, and the beam with the lowest percentage of steel showed minimum deflection when compared to the other beams.

Boshra El-Taly et al. [66], Eleven fully CESB beams with and without web opening were studied under static loading using four-point loading system. The effects of the existence of web opening were studied in two stages. Considering the impact of three diverse strengthening materials on the flexure or shear zones of the beams on the CESB's behavior. As on the exterior bonded reinforcement strengthening materials, steel plates, carbon fiber-reinforced polymer wraps, and glass fiber-reinforced polymer wraps were used. A Finite-Element Analysis (FEA) was completed using the ANSYS release 19.0 program. Due to the effect of the web opening, the ultimate load and its corresponding deflection decreased by about 58.28 % and 80.17 %, respectively. Furthermore, CESB shear strengthening with web opening in the shear zone was more active than flexural strengthening with the three different strengthening materials. Also, on the performance of the tested beams, using a steel plate was more effective than using carbon fiber wraps or glass fiber wraps. High similarity between FE and experimental results based on FEA was achieved.

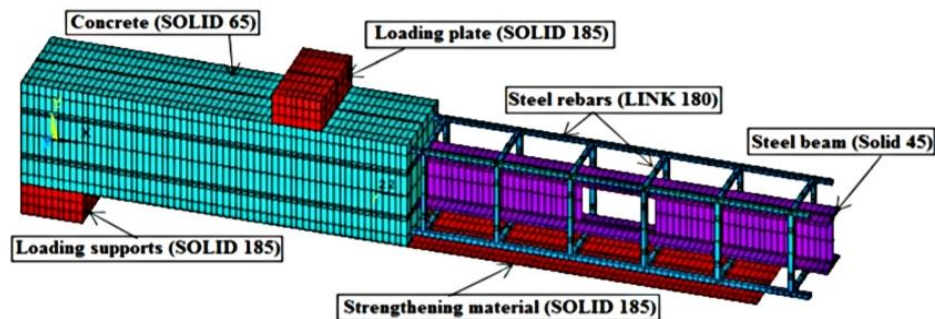


Figure 2.10 FM model used[66].

2.6.2 Strengthening and location of transverse openings in shear zone

Kirijaa Ratanarajah [67], the research was conducted to investigate CFRP strips might be used to strengthen beams with large openings. The study was focused on the results of circular and square-shaped openings. Based on the failure behavior of strength beams corresponding without strengthening. The amount and configuration of CFRP strips were determined. The circular opening was lost about 76 % of its capacity, while the square opening was lost about 74 %. The capacity of beam with square opening after using CFRP was regained by 46.22 % when compared to solid beam. On other hand as compared to solid beam the beam with the circular opening regained of its capacity by 45.35 %.

Waleed A. Jasim et al. [68], The experimental study was conducted on ten of deep beams. Two of which were control specimens without openings and eight of which had large web openings in the shear spans. Variables have been used as shear span to overall depth of the member cross-section ratio, as well as the location and dimensions of the opening. The load-carrying capacity of deep beams with openings compared to the control deep beams in test results showed decreased. This reduction was reached 66 %. The position of the opening in the shear span has less of an effect on the performance of structural concrete deep beams at different stages of serviceability. Because the load path is less discontinuous, specimens with openings adjacent to the interior edges of shear spans observed only an 11% increase in load capacity at failure compared to specimens with openings in the center of shear spans. It is feasible to recommend the creation of openings at the interior edges of shear spans of structural concrete deep beams if they are required.

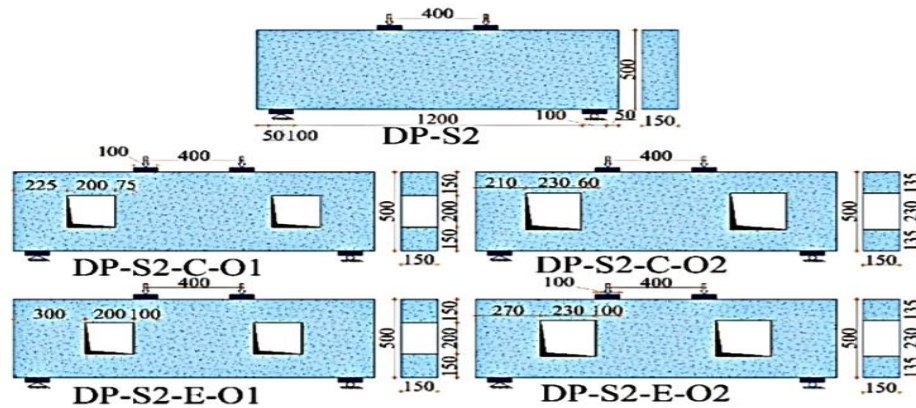


Figure 2.11 Configuration of experimental specimens[68].

2.6.3 Strengthening techniques for web openings

Alaa M. Morsy et al. [69], the performance of R.C. beams with either strengthened or un-strengthened openings was investigated. An extensive experimental program was carried out. A total of 24 specimens were tested in two series to examine openings affect the behavior of RC beams depending on the shape, aspect ratio, and orientation of the opening in the shear and flexural zones. Also investigated the effect of various opening strengthening methods on the behavior of RC beams. Including internal steel reinforcement (I.S.R.), internally embedded fiber-reinforced bars, and near-surface mounted using FRP laminate (N.S.M.). Or using external bonding strengthening (E.B.) such as externally bonded FRP laminates and steel boxes. All specimens were tested under three-point loading with 1500 mm effective span of beams, and all specimens were designed to govern flexure failure before shear failure. The circular openings showed the least reduction in the beam's load capacity in the first series when compared to square and rectangular openings. The second series showed the effect

of strengthening openings on beam behavior; the usage of CFRP externally bonded improved both beam strength and ductility.

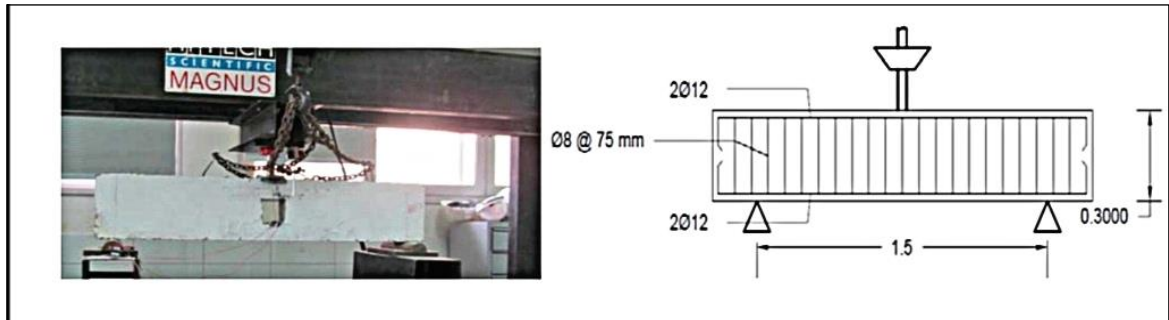


Figure 2.12 The beam test setup and the steel reinforcement configuration[69].

Hayder H. Kamonna [70], The experimental work included testing of thirteen simply supported reinforced concrete deep beams under two-point load. Control specimens included four specimens. One of the specimens without openings, while the other three specimens had two symmetrical openings at each shear span. The other nine specimens were strengthened by using NSM steel bars around the openings in three different configurations. All of the specimens had cross-section of 200 mm x 400 mm and total length of 1500 mm. The presence of openings in the beam resulted reduction in the ultimate load of about 49%, 56%, and 70% for specimens with square openings near loading points, square openings at the load path, and rectangular openings; respectively. The test results also showed that specimens strengthened by vertical bars has improved their ultimate load by up to 14%. The ultimate load of specimens strengthened by both vertical and horizontal bars has improved by up to 40%. While a diamond strengthening scheme has increased the ultimate load by up to 34%.

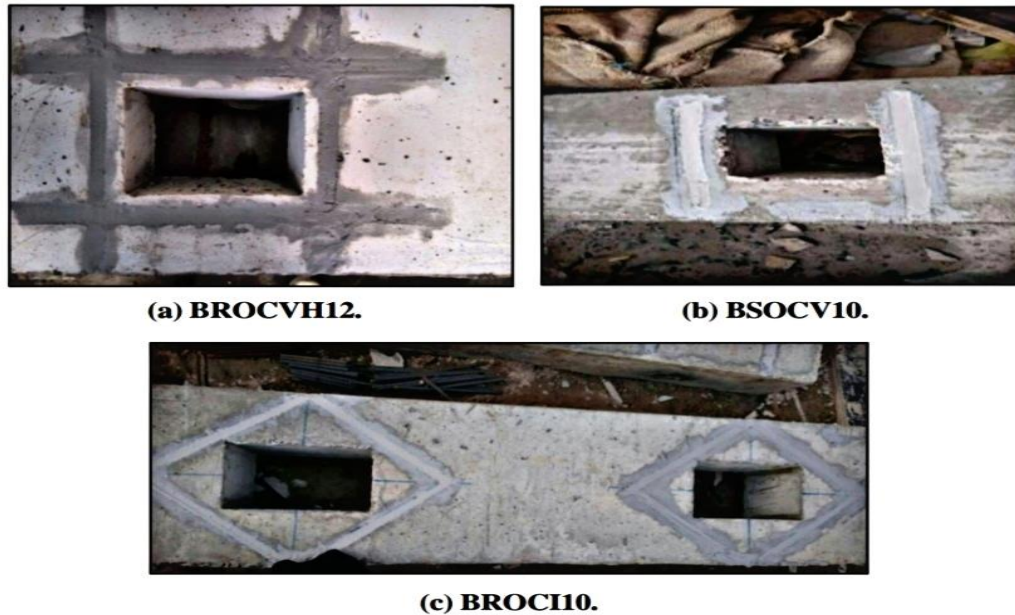


Figure 2.13 The embedding of NSM steel bars into the grooves by epoxy paste[70].

2.6.4 Longitudinal openings of composite beam

Yaarub Gatia et al. [71], The behavior of eight reinforced concrete (RC) beams were examined in this study. These beams were involved in two groups. Dimensions, reinforcement, concrete type, and hole dimensions were all the same on all beams. The method for selecting the optimum hollow core section, as well as the effect of web openings with a fixed hollow core section. When comparing to solid section, due to recorded load capacity a reduction was produced by hollow-core position at mid and bottom section by about (2 % -14 %). As a result, the optimum hollow core section was in the mid-beam section, which used to unify the beam with longitudinal and transverse opening BLTO sections. According to the position of the web opening different BLTO types indicated different loading data. When compared to a hollow beam (without transverse opening) and a solid beam the opening provision was reduced by about 20.4 % and 22 %; respectively.

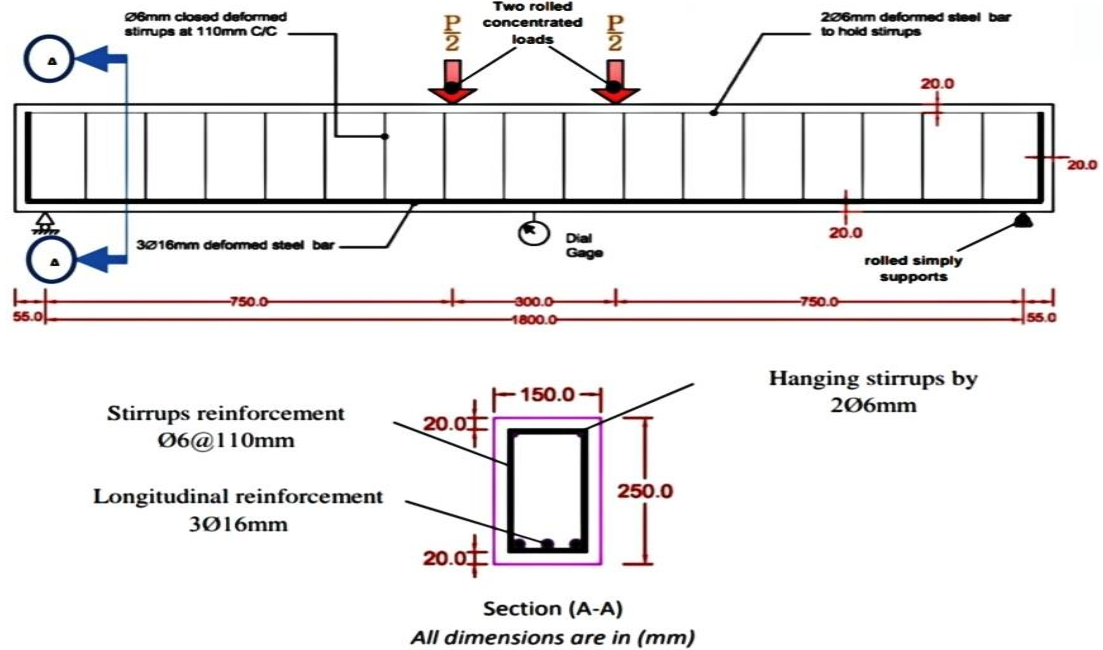


Figure 2.14 Setup of beams with reinforcement arrangement[71].

Ahmed Ismail et al. [72], The shear behavior of nine reinforced high-strength self-compacted concrete (RHSSCC) deep beams with longitudinal openings of different shapes, sizes, and locations were investigated. Two shapes (square and circular) were chosen. As well as two opening positions (compression and tension zone). The load capacity, deflection, absorbed energy, and pattern of cracks were all recorded and discussed. The experimental program showed that longitudinal openings reduce the loading capacity of RHSSCC deep beams. So that increasing opening size decreases capacity load also changing longitudinal opening shape has a slight effect. Longitudinal openings in the compression zone have a more reduction than longitudinal openings in the tension zone.



Figure 2.15 Casting beams with the longitudinal opening[72].

Ahmed Abbas et al. [73], This study was investigated using the longitudinal and transverse opening in beams (BLTO). As one of the best solutions for minimizing problems and solving pipes and other services. Performed experimentally by a researcher and implemented High strength concrete (HSC) beam that using the finite element method in this study. The experimental results were validated using ANSYS software, which was used to compare the force-displacement relationship, ultimate load capacity, maximum displacement, and crack pattern using the same properties, geometry, materials, and conditions. The verification process between the experimental and theoretical programs demonstrated that the obtained results are very similar. This research also examined the behavior of (RC) beams with longitudinal and transverse openings. Despite the presence of shear cracks the registered failure mode of the beam was a flexural failure, and the flexural cracks were the controller in the behavior.



Figure 2.16 Beams with openings[73].

Dinesh KannaM et al. [74], The behavior of steel beams, composite beams, and pre-stressed beams having transverse openings was studied. In the area of RC beams having longitudinal and transverse openings, a great deal of study has been done. The majority of the work focused on the strength and behavior of beams with openings in terms of flexure, shear, flexure-shear, pre-cracking, and post-cracking deflection, crack width, external and internal strengthening, and various loading conditions. The effect of opening, as well as the optimum shape, size, and position of the opening in reinforced concrete shallow beams without strengthening. Various strengthening techniques were preferred by different authors.

2.7 Summary

All used of reinforced concrete (RC) and composite beam with web opening that presented by previous studies and reviewed are subjected to a set of variables; including shape of opening, size of opening, location of opening, strengthening techniques and method of use. The results of the researches varied according to these variables, but can summarize the conclusions that most research participated in each of the four areas as follow :-

1-Researchers proved that openings in beam resulted reduction in the ultimate load of beam unless used special reinforcement is provided in sufficient quantity with proper detailing around openings.

2-The researchers used many strengthening techniques around opening, but the most successful technique was usage of CFRP externally bonded improved both beam strength and ductility.

3-With respect to shape of opening, the most of researchers approved that circular opening advantages over using a square opening.

4- The position of the opening in the shear span has less of an effect on the performance of structural concrete deep beams at different stages of serviceability. Because the load path is less discontinuous, specimens with openings adjacent to the interior edges of shear spans observed only an 11% increase in load capacity at failure compared to specimens with openings in the center of shear spans.

CHAPTER THREE: EXPERIMENTAL WORK

3.1 General

This chapter shows experimental steps for techniques of strengthening composite encased steel-concrete beams with transverse web openings in shear zone. In the experimental program, a total of fifteen composites encased steel-concrete beams were tested up to failure by two-point loading to investigate the structural behavior of beams, crack patterns, shear mode, ultimate load, and load-deflection relationship. The opening region was strengthened by many strengthening techniques such as the Near Surface Mounted method (NSM), CFRP strips method, Reinforcement arrangement, and extruded encasing transversely to reduce the loss of shear capacity due to existing openings in shear zone. Where transverse openings were made using cork material, and longitudinal opening was made by using steel box section (built-up section) which has dimension width 50mm, height 140mm and thickness 2mm.

3.2 Descriptions of specimens

Fifteen simply supported composite encased steel-concrete beams with square openings in the shear zone, three of them control specimens, and others are strengthened with different strengthening techniques. The total span of a typical specimen is (2100 mm), with a c/c span of (1800 mm) and a cross-section (300mm) height and (200 mm) width. The description details of the tested beams are shown in Table 3.1-:

Table 3.1 Details of the Tested composite encased steel-concrete beams

Group No.	Beam name	Transverse opening	Strengthening type
GR.1	CB	---	---
	BW1	(50×50) mm	---
	BW2	(136×136) mm	---
GR.2	CIS1	(50×50) mm	extruded encasing transversely
	CIS2	(136×136) mm	extruded encasing transversely
GR.3	RIS1	(50×50) mm	Reinforcement arrangement
	RIS2	(136×136) mm	Reinforcement arrangement
GR. 4	ECW1	(50×50) mm	CFRP fully wrapping sheets
	ECW2	(136×136) mm	CFRP fully wrapping sheets
	ECS1	(50×50) mm	CFRP diagonal sheets
	ECS2	(136×136) mm	CFRP diagonal sheets
GR.5	ECR1	(50×50) mm	CFRP diagonal bars
	ECR2	(136×136) mm	CFRP diagonal bars
	ECR3	(50×50) mm	CFRP bars rhombus shape
	ECR4	(136×136) mm	CFRP bars rhombus shape

All beams have the same width, depth, a/d, and main reinforcement.

All beams have diagonal reinforcement $\varnothing 6$ mm except solid beam doesn't have diagonal reinforcement.

3.3 Material characteristics

The materials used in the concrete mixture were ordinary Portland cement (OPC), sand, and coarse aggregate with a maximum size of 10 mm. Concrete compressive strength (f_c') = 23.53MPa at the age 28-day. The mix design proportional of cement, fine aggregate, and coarse aggregate were (1:1.5:3). The water-cement ratio by weight was 0.45. At the same time were cast six cylinders 150×300 mm, three prisms 100×100×500 mm and cured alongside the specimens.

3.3.1 Material Properties

Full description of materials were used in this the research are present in the following subsection.

3.3.1.1 Cement

Ordinary Portland cement (OPC) was used in this study. The product name of the cement was Baziani, which is commonly available in the local markets. For using cement the physical and chemical properties are given in Tables (3.2), (3.3) respectively; conform with [ASTM C150, and Iraqi-specifications standard (IQ.S No. 5/2017).

Table 3.2 Physical properties of cement

Test	Iraqi specification standard (IQS No.5)	Results
Fineness test (cm^2/gm)	2300 min	2390
Initial setting time (minutes)	45 min	53
Final (minutes)	600 max	530
Soundness autoclave expansion %	0.80 max	0.62
Compressive strength (MPa) 3 day	15 min	16.70
7 day	23 min	26.29

Table 3.3 Chemical properties of cement

Test	Iraqi specification standard (IQS No.5)	Results %
SiO ₂	--	--
Al ₂ O ₃	--	--
Fe ₂ O ₃	--	--
Lime Saturation	1.02-0.66	0.79
MgO	Max 5	3.50
SO ₃ not more than when C ₃ A less than 5% more than 5%	2.5 2.8	2.30
Loss when burning	4 Max	3.10
Non-soluble substance	1.5 Max	1.10
C ₃ S	--	--
C ₂ S	--	--
C ₃ A	--	--
Fe ₂ O ₃ /AL ₂ O ₃	--	--



Figure 3.1 Cement used in the present work.

3.3.1.2 Fine Aggregate

Natural sand from (Jabal Al Salam/ Basra) region was used in this work as fine aggregate. The fine aggregate used has gradation that lies within the upper and lower limits of the ASTM C33/C33M specification and Iraqi specification (IQ.S 45/2017) zone (2) as shown in table (3.4).

Table 3.4 Grading of fine aggregate

Sieve size (mm)	Passing %		
	Fine aggregate	IQ.S No. 45 zone (2)	ASTM C33/C 33M
9.5	100	100	100
4.75	100	90 - 100	90 - 100
2.36	82.17	75 - 100	80 - 100
1.18	60.37	55 - 90	50 - 85
0.60	39.64	35 - 59	25 - 60
0.30	19.50	8 - 30	5 - 30
0.15	6.38	0 - 10	0 - 10

3.3.1.3 Coarse Aggregate

Coarse aggregate was used in this work with a maximum size of aggregate 10mm. The coarse aggregate was cleaned and was washed by tap water, then dried before use. The sieve analysis of coarse aggregate lies within the lower and upper limits of the Iraqi specification (IQ.S No.45/2017) as shown in table (3.5).

Table 3.5 Grading of coarse aggregate

Sieve size (mm)	Passing %	
	Coarse aggregate	IQ.S No.45/2017
20	100	100
14	100	100
10	100	85 - 100
4.75	5	0 - 30
2.36	0	0 - 10

3.3.1.4 Water

Clear water should be used in mixing concrete. So using the drinking water produced by (Reverse-Osmosis). RO- water was used during the casting and curing process. The water was brought to the laboratory by tanker from the nearest RO water station.

3.4 Geometry of the tested beams

In the present experimental program, all of the fifteen simply supported beams were in the overall dimensions 2100 mm, 200 mm, 300 mm in length, width, and depth respectively; as shown in Figure (3.2), the overhanging length was 150 mm while the shear span was 630 mm. All of the beams specimens were

tested under four-point loads. The distance between loads was 540 mm. To stay away from the requirements of the deep beam principle, the specimen dimensions were selected to meet ACI318M-19[75] requirements to overcome the two requirements of the deep beam, because the deep beam gets if one of the following cases occur:

- If $L_n/h \leq 4$ (deep beam) → to avoid that should > 4 (shallow beam)
- If $a/h \leq 2$ (deep beam) → to avoid that should > 2 (shallow beam)

In the present research, the clear span (L_n) is taken 1800 mm, and overall depth 300 mm so that the aspect ratio (L_n/h) will be 6 so, the beam specimen is far from falling in the deep beams' principle.

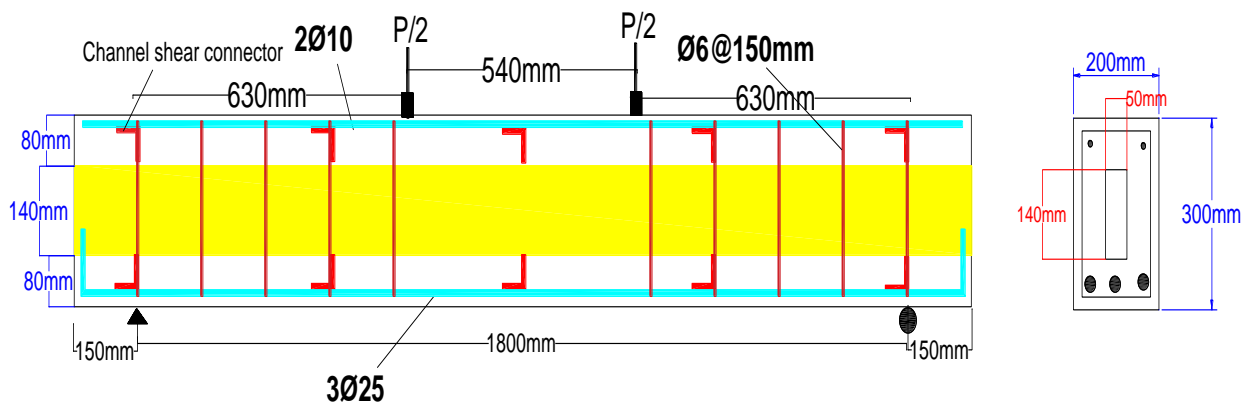


Figure 3.2 Geometry for control beam.

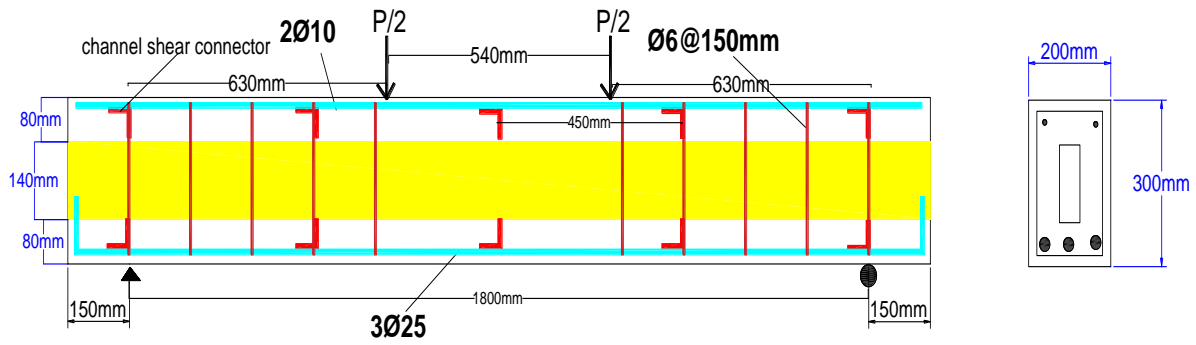
The design calculations for the reference composite encased steel-concrete beam dependent on equilibrium equation between compressive forces (which included participate concrete part and steel box part) and tensile forces (which included participate steel bar and steel box part). With respect to shear strength which included participate; shear strength of steel box according to AISC code, shear strength for stirrups, shear strength of concrete.

Because the present study focus on shear behavior, so all the specimens are designed with enough steel reinforcement ($\varnothing 25$ mm) to avoid flexural failure. For all beams used $2\varnothing 10$ mm steel bars to hold the stirrups in their zone. All the composite encased steel-concrete beams were connected fully bond between the concrete and the steel box section by using enough shear connectors (angles). Twenty (20 angles) were used in each composite encased steel-concrete beam, 5 angles for each plate of the four plates of the steel box. Spacing between angle to angle was (450mm), and dimension of angle where length of angle shear connector was 50mm, thickness of the web of an angle (t_w) 3mm.

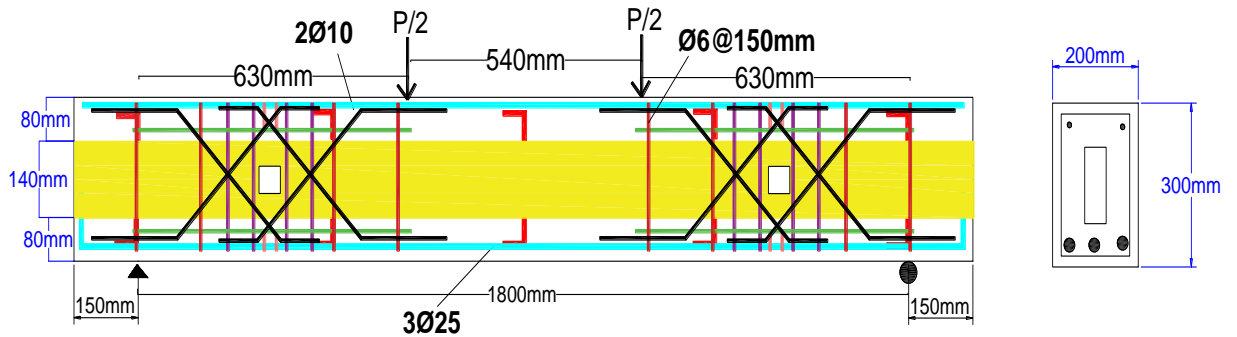
3.5 The specimens variables in the present study

The main parameters studied in this research are the size of the opening and methods of strengthening. The specimens were divided into five groups to make comparisons between these specimens in terms of the type of failure, maximum load failure, deflections, and cracks.

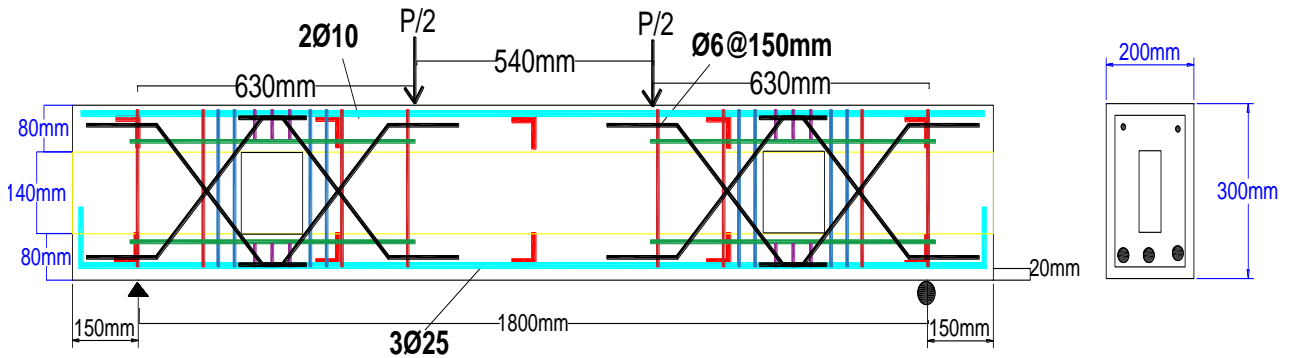
The first group consisted three beams of composite encased steel-concrete one of them solid beam and two other with square transverse web openings that were fabricated in steel section in the shear zone by embedded cork material. To make comparison between the solid beam (CB), composite encased steel-concrete beam with small (50×50 mm) square openings (BW1) at center of shear zone, and encased steel-concrete beam with large (136×136) square openings (BW2) at center of shear zone, as shown in Figure (3.3).



a-Control beam (CB).



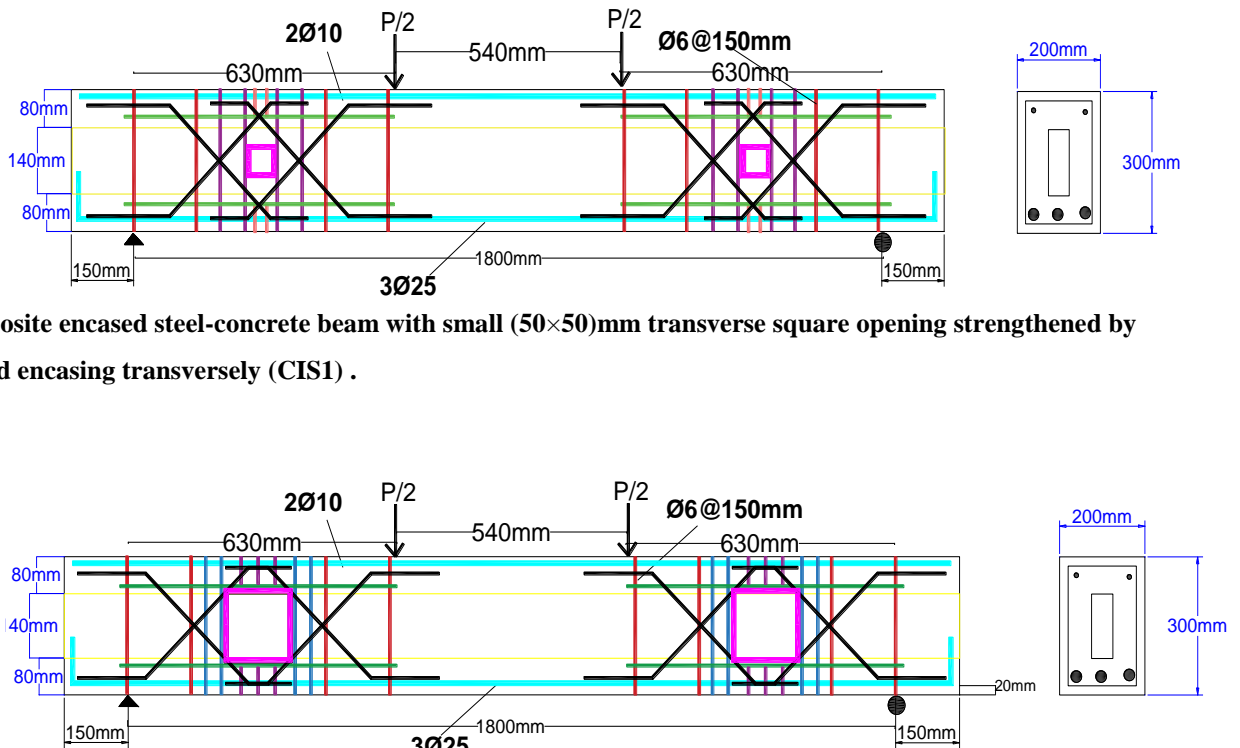
b-Composite encased steel-concrete beam with small (50×50)mm transverse square opening (BW1).



c-Composite encased steel-concrete beam with large (136×136)mm transverse square opening (BW2).

Figure 3.3 Details of first-group.

The second group investigates the effect of the strengthening technique by using the extruded encasing transversely (EET) which consisted steel section has thickness (2mm) welded around square opening, dimensions of steel section welded depends on dimensions of transverse square opening with respect to small opening dimension of welded steel section are (50×50)mm and extends to the end of beam width (70)mm. On the other hand with respect to large opening dimension of welded steel section are (136×136)mm and extends to the end of beam width (70)mm. Study effecting of this method to increasing load-carrying capacity of composite encased steel-concrete beam with square openings strengthened by this method and comparison the result with control beam with small square openings (50×50) mm and control beam with large square openings (136×136) mm, as shown in Figure (3.4).

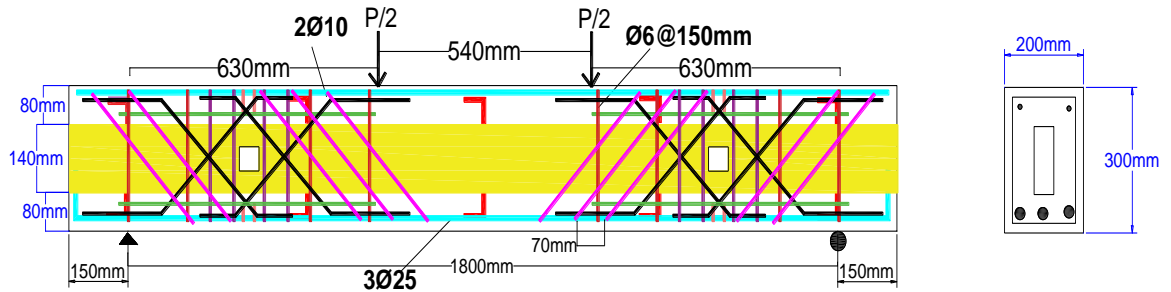


a-Composite encased steel-concrete beam with small (50×50)mm transverse square opening strengthened by extruded encasing transversely (CIS1) .

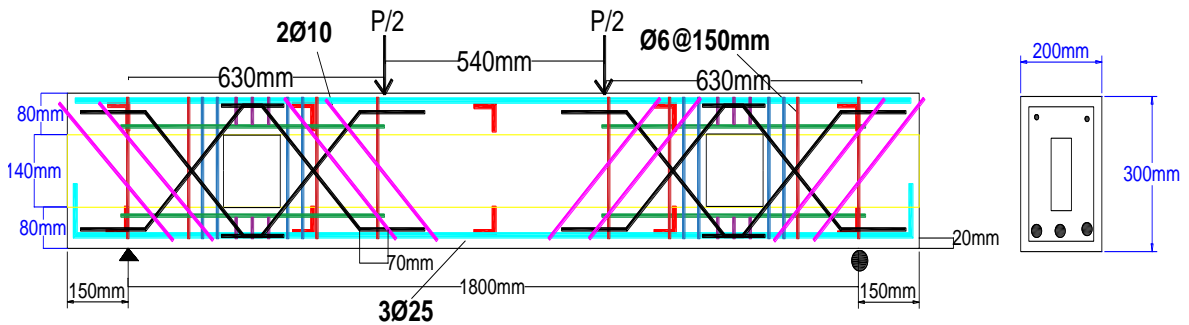
b-Composite encased steel-concrete beam with large (136×136)mm transverse square opening strengthened by extruded encasing transversely (CIS2) .

Figure 3.4 Details of second-group.

The third group studies the reinforcement arrangement strengthening method which includes add diagonal bars at each side of the web opening to increasing load-carrying capacity for composite encased steel-concrete beams with small and large square openings and results comparison between beams strengthened and control beams as shown in Figure (3.5).



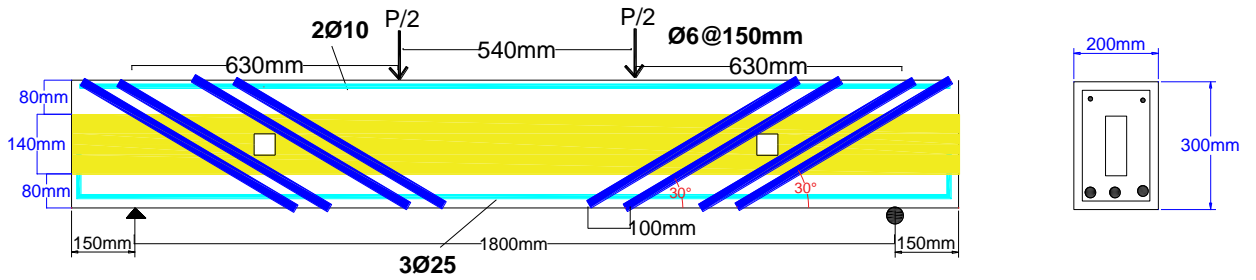
a-Composite encased steel-concrete beam with small (50×50)mm transverse square opening strengthened by reinforcement arrangement (RIS1) .



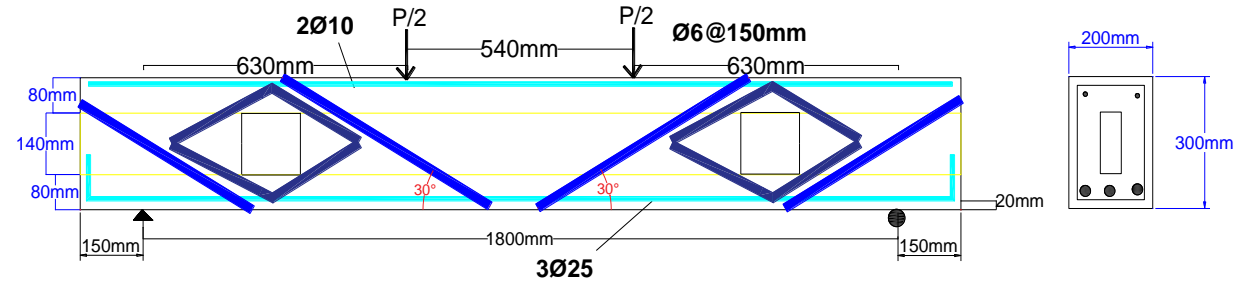
b-Composite encased steel-concrete beam with large (136×136)mm transverse square opening strengthened by reinforcement arrangement (RIS2) .

Figure 3.5 Details of third-group.

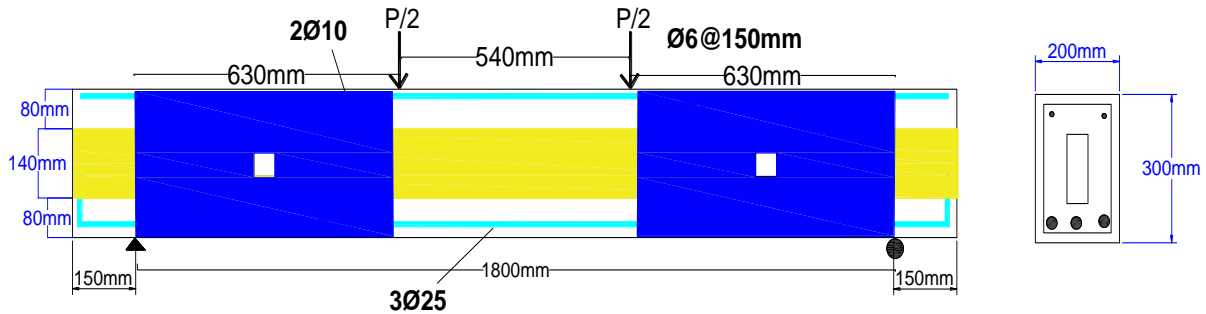
The fourth group includes using CFRP strips (the CFRP strengthening configuration was a fully wrapping system and diagonal strengthening sheets around the square openings) as a strengthening technique to study effecting of this method on increasing load-carrying capacity of composite encased steel-concrete beam with transverse openings, Figure (3.6).



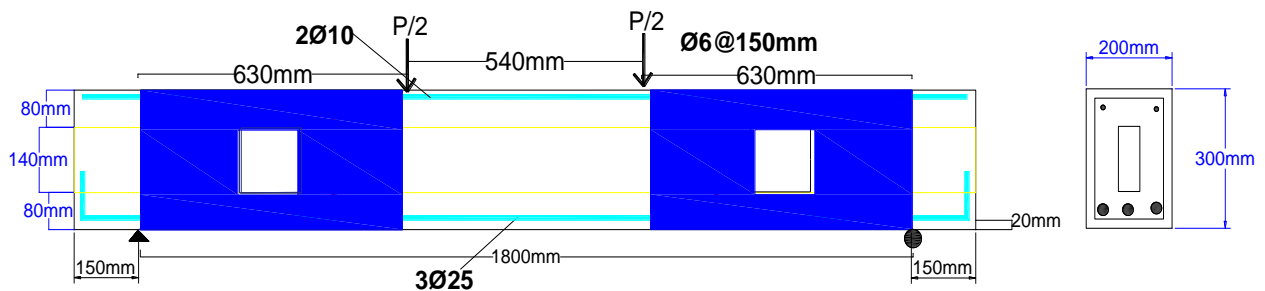
a- Transverse square opening strengthened by CFRP diagonal sheets (ECS1) .



b- Transverse square opening strengthened by CFRP diagonal sheets (ECS2) .



c- Transverse square opening strengthened by CFRP fully wrapping sheets (ECW1) .



d- Transverse square opening strengthened by CFRP fully wrapping sheets (ECW2) .

Figure 3.6 Details of fourth-group.

The fifth group involves the NSM method used as strengthening technique (using NSM CFRP bars in two different arrangements around the square openings with a rhombus shape and diagonal bars). Near-surface mounted method which includes used CFRP bar ($\varnothing 6$ mm) with epoxy is used as a bonding material, the reason for using this method is to study effecting of this method on load-carrying capacity, as shown in Figure (3.7).

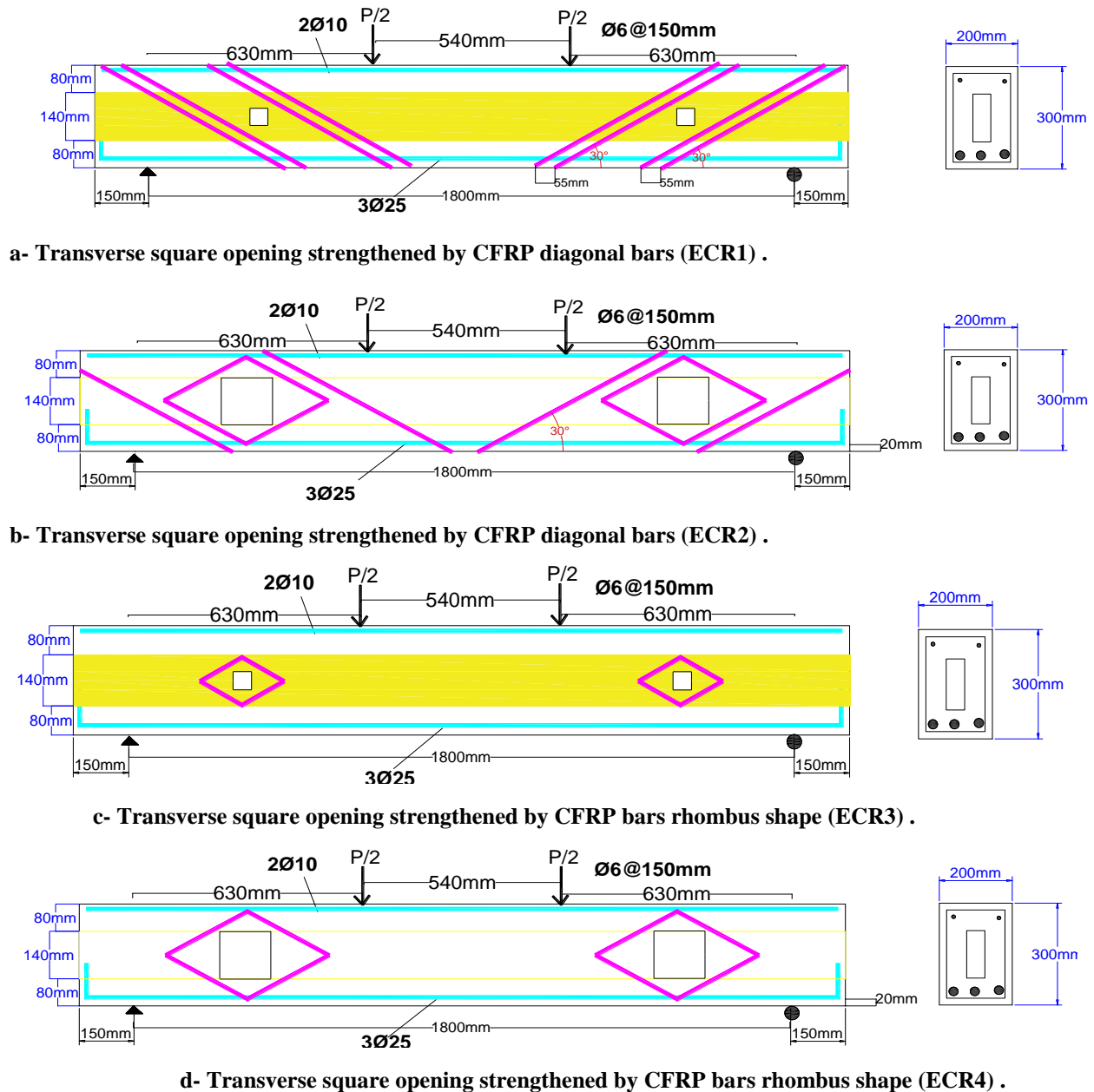


Figure 3.7 Details of fifth-group.

3.6 Steel materials used in the present work

In the present work composite encased steel-concrete beams contain many steel materials such as (steel boxes, shear connectors, and steel reinforcement). In this section, the properties of the steel materials will be mentioned below.

3.6.1 Steel box section

Steel box sections were used in the present research. All the steel box sections have the same thickness (2 mm). All steel sections were fabricated with dimensions 50 mm width and height 140 mm, by local workshop. The hollow section was tested following the American specification for steel materials testing ASTM A370-10 [76].

Table 3.6 Tensile properties of the steel section.

Dimensions of steel hollow box	Average yield tensile strength (MPa)	Average ultimate tensile strength (MP)
50×140	280.97	405.39

3.6.2 Angle shear connector

The angle shear connector is one of the shear connectors. angle shear connectors is easier compared angle shear connectors to the other connectors. Since in most steel shops, commercial standard sizes for hot rolled steel profiles of C-shaped shear connectors are available. Moreover, by simple cutting in their long steel profiles, these types of connectors can be easily prepared[62]. Figure (3.9) shows angle shear connectors with steel box.

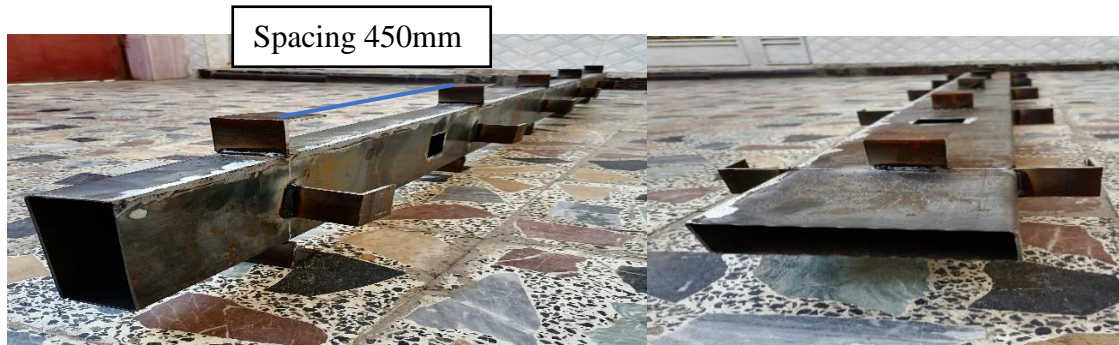


Figure 3.8 Angle shear connectors with steel box.

3.6.3 Steel reinforcement

In this research, three sizes of steel reinforcement were used ($\emptyset 6$, $\emptyset 10$ & $\emptyset 25$) mm, all beams have the same interior steel reinforcement. The longitudinal flexural tensile reinforcement is (3 $\emptyset 25$) deformed steel bars. The longitudinal compression reinforcement is (2 $\emptyset 10$) deformed steel bars. The shear reinforcement (stirrups) is designed with ($\emptyset 6 @ 150$ mm). The steel bars were Iraqi origins and can be identified through the brand stamped on the blinds as shown in the Figure (3.9).



Figure 3.9 Steel bars were used in this research.

Table 3.7 Tensile test results of steel reinforcing bars

Table 3.8 Tensile test results of steel reinforcing bars

Nominal diameter (mm)	Yield strength (MPa)	ASTM A615/A615M	Ultimate strength (MPa)	ASTM A615/A615M
6	378.57	280	424.5	420
10	416.34	420	618.567	620
25	585.89	420	693.36	620

3.6.4 Reinforcement details of opening

Long stirrups were placed on each sides of opening to avoid beam-type failure, while short stirrups were used upper and lower of opening to avoid frame-type failure. At each corner bars were placed to anchorage short stirrups. Also, bars were placed diagonally on both sides to effective crack control[16], as shown in Figure (3.10). It's worth to mention that equation to calculate shear strength of opening according to AIC code.

$$V = V_{SV} + V_{Sd} = (A_v \times f_{yv}) / S \times (d_v - d_o) + A_d \times f_{yv} \times \sin \alpha \quad 3.1$$

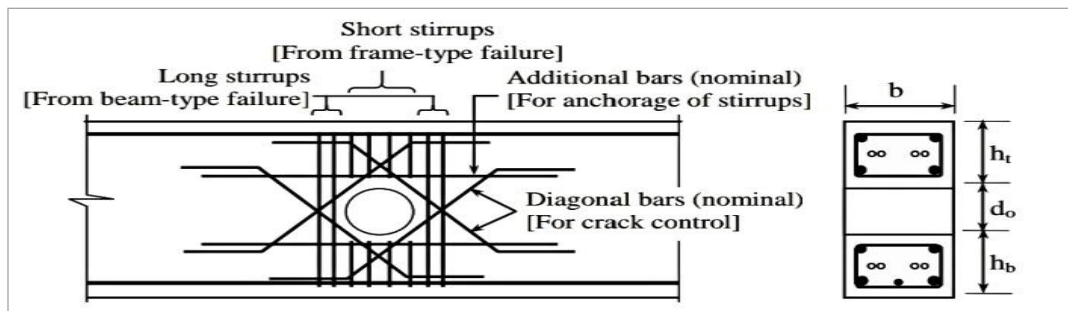


Figure 3.10 Reinforcement details around a small and large opening[16].

In this search reinforced opening as follow:

1-Put longitudinal stirrups (two stirrups) $\text{Ø}6\text{mm}$ at each sides of small and large opening to avoid beam-type failure as shown in Figure (3.11).

2-After that put short stirrups ($\text{Ø}6\text{mm}$) at top and bottom of small and large opening the number of stirrups used dependent on available distance around opening. And the aim of use short stirrups to avoid frame-type failure, as shown in Figure (3.11).

3-To anchorage short stirrups put additional bars (nominal) $\text{Ø}6\text{mm}$ at top and bottom of opening, as shown in Figure (3.11).

4-placed diagonal bars ($\text{Ø}6\text{mm}$) around opening to crack control, as shown in Figure (3.11).

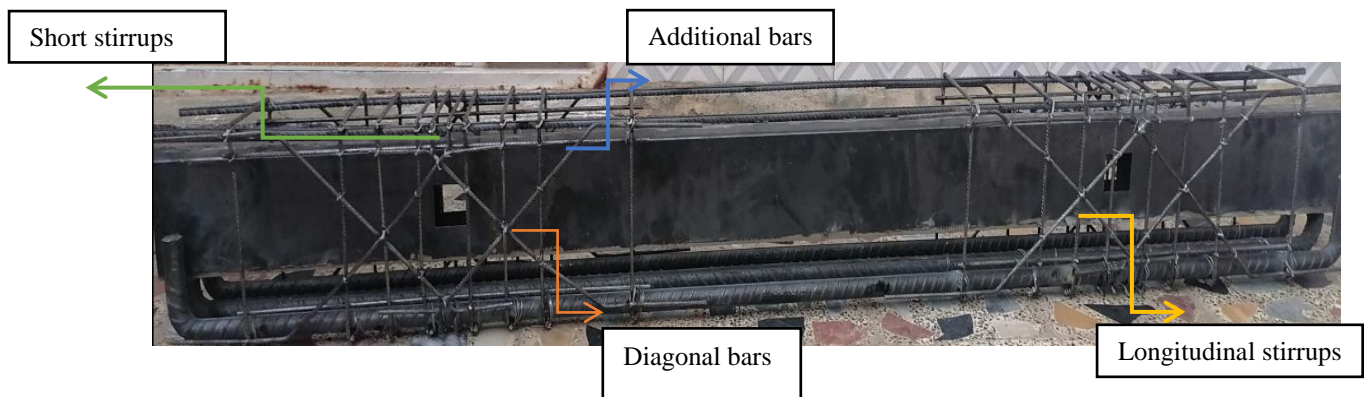


Figure 3.11 Reinforcement opening details for small and large openings.

3.7 Extruded encasing transversely (EET)

Extruded encasing transversely which consisted steel section welding around square opening, dimensions of steel section welding depend on dimensions of transverse square opening and extends to the end of beam width. Where steel section welding dimension in small opening were (50×50) mm and extends 70 mm from beam's width in both sides of the opening, as shown in Figure (3.12). In the same way steel section welding dimension's in large opening were (136×136) mm and extends 70 mm from beam's width in each sides of opening. This steel section was welded in normal welding method. The composite method is one of the new strengthening methods used in this research to study effecting presence of this welded steel section around opening on improving shear strength of beam, , as shown in Figure (3.13).



Figure 3.12 Small square transverse openings strengthening by composite method CIS1.



Figure 3.13 Large square transverse openings strengthening by composite method CIS2.

3.8 Reinforcement arrangement

This method used bars reinforcement arrangement as a strengthening technique for encased composite steel-concrete beams with transverse web openings. This method included placing the diagonal bars reinforcement ($\varnothing 6\text{mm}$) and arrange it around the openings in manner that ensures the increase in the efficiency of the beam. To avoid cracks that arise at the corners of the openings as result focus of stresses around corners of openings, so this method used. Where the inclined bars restrict the movement of the cracks that expected initiated from the corner of the opening toward load point and supports, , as shown in Figures (3.14) & (3.15).

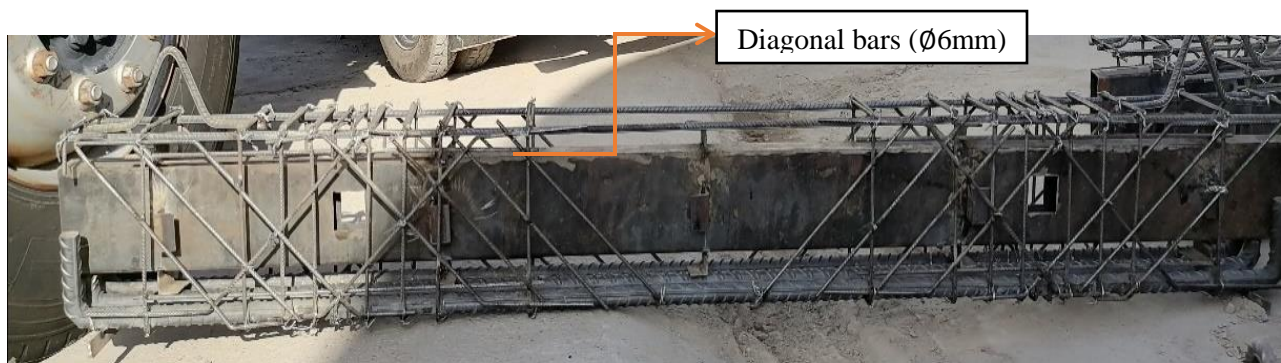


Figure 3.14 Small square transverse openings strengthening by reinforcement arrangement RIS1.



Figure 3.15 Large transverse square openings strengthening by reinforcement arrangement RIS2.

3.9 Specimens preparation

3.9.1 Molds

Fifteen wooden molds, (200x300x2100) mm dimensions, were used to pour beam specimens. The molds were manufactured with (18mm) thick plywood base and two movable sides. The sides were fixed to the base by screws. It may be noted that to ensure that it would be easy to remove the samples when the concrete hardened, the inner faces of the molds were oiled. When the mixing process was completed, the beam specimens were then cast in three layers and compacted by vibrator to shake the mix and consolidate it into the molds. The surface of the concrete (top face of beam specimens) was leveled with a trowel, as shown in Figure (3.16).



Figure 3.16 Molds.

3.9.1.1 Mold preparation

Fifteen plywood molds were prepared, and the plywood was selected with the highest thickness available in the market. The mold parts were tightly linked in a way that made it easier to separate the parts after the casting process without any effect on the concrete beam, and the single wooden mold consists of five parts:

- 1- Base mold dimensions 2100 x 200 x 18 mm.
- 2- Sidewalls with dimensions of 2100 x 300 x 18 mm and have square openings.
- 3- Small side pieces of dimensions 300 x 200 x 18 mm.

In the present work, the beams have transverse square openings and longitudinal openings. Where longitudinal opening made by steel box section and transverse square opening made by using cork material.

After completing the mold, plastic spacers were placed on the base of the mold and on the two side walls of the mold to provide a concrete cover for the reinforcement steel cage. As shown in Figure (3.17).



Figure 3.17 Preparing the molds.

3.10 Mixing procedures for the specimens

The materials of concrete were cement, sand, coarse aggregate, and water. Batching plant mixing was done to ensure consistent mixing followed by pouring the concrete into molds of size (200x300x2100) mm, also six cylinders of size (150 x300) mm and three prisms of size (100 x100 x500) mm.

Table 3.9 Concrete Mix Design

For 1m ³ of concrete	Cement (kg)	Sand (kg)	Gravel (kg)	Water (L)
	500	800	1150	205

3.11 Workability test

Measurement of slump test was taken immediately after mixing concrete before casting it into specimens molds.

3.11.1 The slump test

The slump test of concrete measures the consistency of fresh concrete before it sets. It is performed to check the workability of concrete. In this study, the slump test in the normal type of concrete was (10-40) mm, according to EN 206-1:2000.



Figure 3.18 Slump test.

3.12 Pouring of the specimens

Before starting the pouring process into the beam molds, the molds of structural beams were placed on the ground and leveled. The water used in the casting process was RO water (Reverse Osmosis, is water purification technology). After the pouring of concrete, the surface of the specimens is leveled by a steel trowel.

3.13 Curing and age of testing

After (24) hours, the beam specimens, cylinders, and prisms were stripped from the molds. cylinders and prisms cured (kept) in a water bath for (28) days. In addition to beam specimens cured by using wet burlap was used to cover

the specimens. Before (24) hours from the date of testing, they were taken out of the wet burlap and cleaned by a water-jet pump. To prepare the surfaces of specimens for paint by white-color to detect the crack pattern, and then tested.



Figure 3.19 Curing of specimens.



Figure 3.20 Cleaning of specimens by water jet pump.



Figure 3.21 Painting the specimens by white color.

3.14 Testing for mechanical properties of normal concrete

To determine the main mechanical properties of normal concrete mix, three tests were performed to determine three mechanical properties (compressive strength, splitting tensile strength, and modulus of rupture). These tests were carried out according to the specifications of the American Society for Materials Testing (ASTM). Figure (3.22) shows a simple outline for these tests. All these tests were done at the University of Misan- Faculty of Engineering Laboratory.

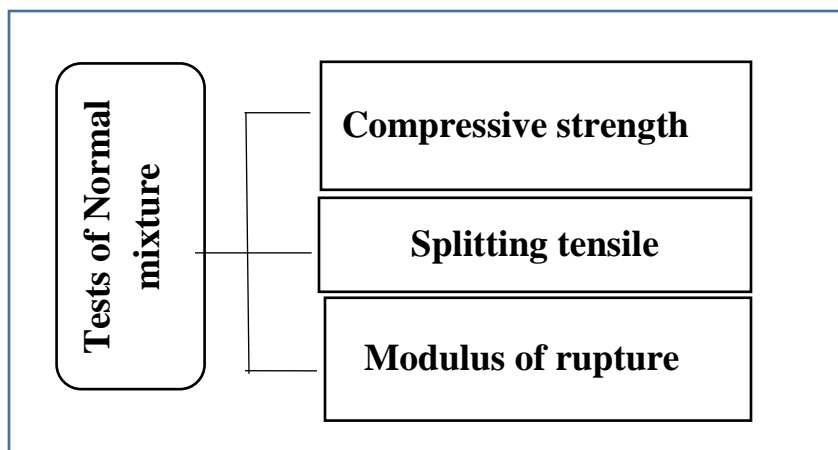


Figure 3.22 Tests of Normal mixture.

3.14.1 Compressive strength

To test the compressive strength of Normal concrete the cylinders were used with a diameter of 150 mm and a height of 300 mm. The tests were carried out in the laboratory of the Faculty of Engineering, University of Misan, by using a

universal ELE compression Machine model with a capacity of 2000 KN to test the cylinders by axial loading. By the ACI 318M-19 standard to find compressive strength, the average of three cylinders readings was taken at the age of 28 days.

Table 3.10 Experimental values of compressive strength

Cylindrical compressive-strength of (28-Days) MPa
22.9
23
24.7
Average of compressive strength (MPa)=23.53



Figure 3.23 Compressive Strength Results and failure modes.

3.14.2 Splitting tensile strength (f_{ct})

The Brazilian method which is an indirect tensile strength test conforming to ASTM C496-04 specification was used. Three cylinders with a diameter of 150

mm and a height of 300 mm were placed horizontally in the universal ELE Machine with a capacity of 2000 KN to apply the load vertically along the length of the cylinders. The results of the tests are shown in the Figure (3.24).

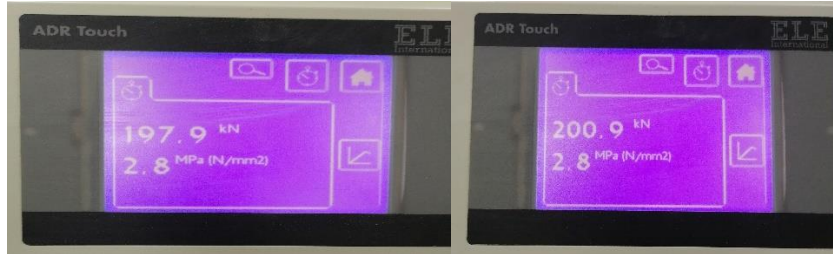


Figure 3.24 Test results of splitting tensile strength.

The results of the test-machine based on the following formal:

$$\text{Split Tensile Strength } (f_{ct} = 2P/\pi \cdot D \cdot L)$$

Table 3.11 Experimental values for the splitting tensile strength

Load (KN)	Splitting Tensile Strength (MPa)
200.9	2.8
197.9	2.8
192	2.7

3.14.3 Modulus of rupture (f_r)

To test flexural strength of concrete according to the ASTM C78-84 standard. The test was performed by using three points of loading by a machine with 63 KN capacity, which was manufactured by Central Organization for Standardization and Quality Control (COSQC). Three prisms having dimensions (100*100*500) mm were cast for this test. The results of tests were calculated by the mathematical formula below. The results obtained in the present work shown in the Figure (3.25).

$$(1 \text{ kg}) = (9.8066 \text{ N})$$

$$f_r = 3PL/2bd^2 \quad 3.2$$

where:

f_r = Modulus of rupture (MPa).

P= Ultimate failure load (N)

L= Span length between the supports, (center to center) (mm).

b= prism cross section width (mm).

d= prism cross section depth (mm).

Table 3.12 Flexural test results

Prisms Test		Specimens' values		
	Test load (kg)	497	543	539.5
Rupture test	Test load (N)	4873.88	5324.98	5290.66
	Stress (MPa)	3.29	3.59	3.57
	Average stress	3.48		



Figure 3.25 Test results and failure modes of modulus of rupture for prisms.

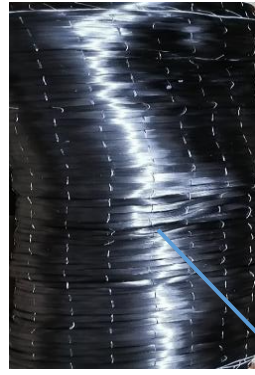
3.15 Carbon fiber reinforced polymer (CFRP)

The carbon-fibers-materials are one technique that improves the performance by increasing the ultimate capacity Composite encased steel-concrete beams. So our thesis will investigate shear behavior, and the shear-behavior performance of [(Normal concrete) Composite encased steel-concrete beams] strengthened by [CFRP (bars and sheets)].

3.15.1 CFRP sheets

The use of FRP as external reinforcement to strengthen RC beams has received research interest. Carbon, aramid, or glass fibers are the most common types of FRP in the concrete industry. FRPs are usually found as sheets, strips, wraps, or laminates. These materials were applied to the external surfaces of the beams in various configurations and layouts by bonding each other. Because FRPs are well-known for providing good mechanical properties. Using them to repair and rehabilitate damaged steel and concrete structures has become increasingly appealing, particularly with their high strength and low weight. Thus, in an existing

beam external strengthening materials such as steel plates or Fiber Reinforced Polymer (FRP) materials are crucial to strengthen the area around the opening. The experimental test results show that the CFRP system's strengthening technique is effective in improving the strength capacity of composite beams[77].



CFRP sheets

The table (3.14) below shown property of CFRP sheets.

Table 3.13 Properties of CFRP sheets.

Property	CFRP sheets
Modulus of Elasticity (MPa)	175000
Rupture strain	0.015
Ultimate tensile strength (MPa)	3500

3.15.2 Adhesive material (epoxy)

The process of externally covering concrete members with polymer fibers requires the presence of binders, which works to adhere the polymer fibers to the concrete surface tightly. In this study, a medium-viscosity epoxy called (Sikadur 330 C) was used, which is made up of two main parts: the resin (Resin (A)) and the hardener (Hardener (B)), as shown in the Figure (3.26). The resin (A) is mixed with the hardener (B) in a proportion by weight (4:1), as shown in the Figure

(3.27). As recommended by the company producing this material. (Appendix A). To form an epoxy mixture which is used in the process of gluing the fibers on the concrete surface.



Figure 3.26 Component A and Component B of Sikadur®-330.



Figure 3.27 Light gray paste of Sikadur®-330 components (A+B) mixing.

3.16 Strengthening procedure of CFRP sheets

The external strengthening (Carbon Fiber Reinforced Polymer and epoxy adhesives) was performed as follows:

- 1- Shear zones surfaces were scraped with electrical abrasive paper and then cleaned with a brush to achieve good bonding between the composite encased steel-concrete beams and the CFRP sheets.
- 2- Scissor was used to cut the CFRP sheets to the proper dimensions.
- 3- For at least 3 minutes, the epoxy resin parts A (Resin (A)) and B (Hardener (B)) were mixed in a 4:1 ratio.

4- At the specified regions (prepared surfaces) the mixed resin was applied to surface of composite encased steel-concrete beams and CFRP sheets, then the strips were installed to composite encased steel-concrete beam surface with a small pressure to force air bubbles and excess epoxy to out.

The strengthened specimens were tested at least 7 days after CFRP installation.



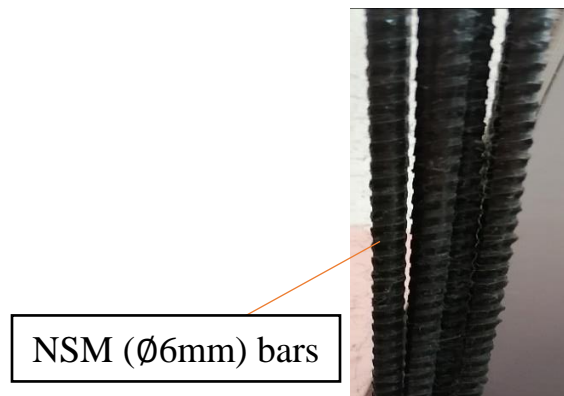
Figure 3.28 Electrical abrasive-paper.



Figure 3.29 Composite encased steel-concrete beams with square openings strengthened by CFRP strips.

3.17 Strengthening by using NSM CFRP bars

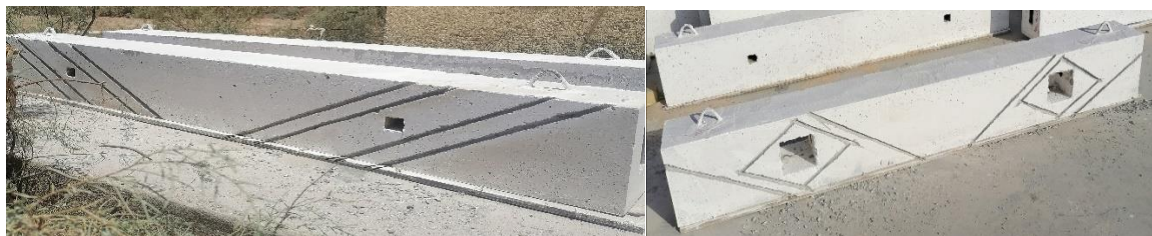
To achieve the process of NSM strengthening, the following steps were followed: The boundaries of the desired grooves which were needed for embedding the strengthening bars ($\varnothing 6\text{mm}$) were first fixed by a sketch. The sketch was made to ensure that the grooves were drilled with the correct shapes and dimensions. Ensuring that the strengthening bars were kept at a distance of at least 20 mm from the opening edges. The grooves were drilled in depth and width of about $1.5d_b$ (d_b is the diameter of the bar). Using a special concrete saw with a diamond blade the grooves were made in the concrete with the required predetermined size. They were cleaned with water and then dried by air to remove dust. The epoxy paste layer that was added was half the depth of the groove. The strengthening bar was placed gently and then slightly pressed into the groove. Allowing the epoxy paste to flow around it and fill the space between the bar and the groove's sides. The second layer of epoxy paste was added, and the surface was leveled, such that the bar was completely hidden. The specimens were left for seven days to let the epoxy paste reach the desired strength[58],[78].



The table (3.15) below shown property of CFRP bars.

Table 3.14 Properties of CFRP bars.

Property	CFRP bars
Modulus of Elasticity (MPa)	175000
Nominal bar diameter (mm)	6
Tensile stress in the CFRP bar (MPa)	2.05



(a) ECR1

(b) ECR2



(c) ECR3

(d) ECR4

Figure 3.30 Grooves installation.



(a) ECR2

(b) ECR4



(c) ECR1 & (d) ECR3

Figure 3.31 NSM Installation.

3.18 Test Procedure

After the curing of the specimens was completed, the specimens were extracted from the treatment tank at the age of 28 days. Beams were coated in white color so that the cracks can be easily observed that are appearing during the loading process. Beam specimens were sited on the testing machine and attuned so that centerline, supports, point load, and LVDT were in their correct positions. Each beam was tested individually and placed inside the frame of the testing machine for testing on a supported where beams length was 2100 mm, while a clear span becomes 1800 mm centerline of supports. Beam specimens were tested up to failure under four-point loading with static load using a Universal Testing Machine (UTM) of 600 KN. Loading rate was applied as 5kN/min. A spreader beam was used to transference the load to test specimen over two loading points at 540 mm at a distance. At the end of each load raise, notes and measurements were recorded for the mid-span deflection and crack development and propagation on the beam surface. Beam deflection was observed by a number of linear variable displacement transducers (LVDTs) sited at the bottom soffit of the beam. Crack progress and propagation were marked and failure mode was verified.



Figure 3.32 Universal Testing Machine.

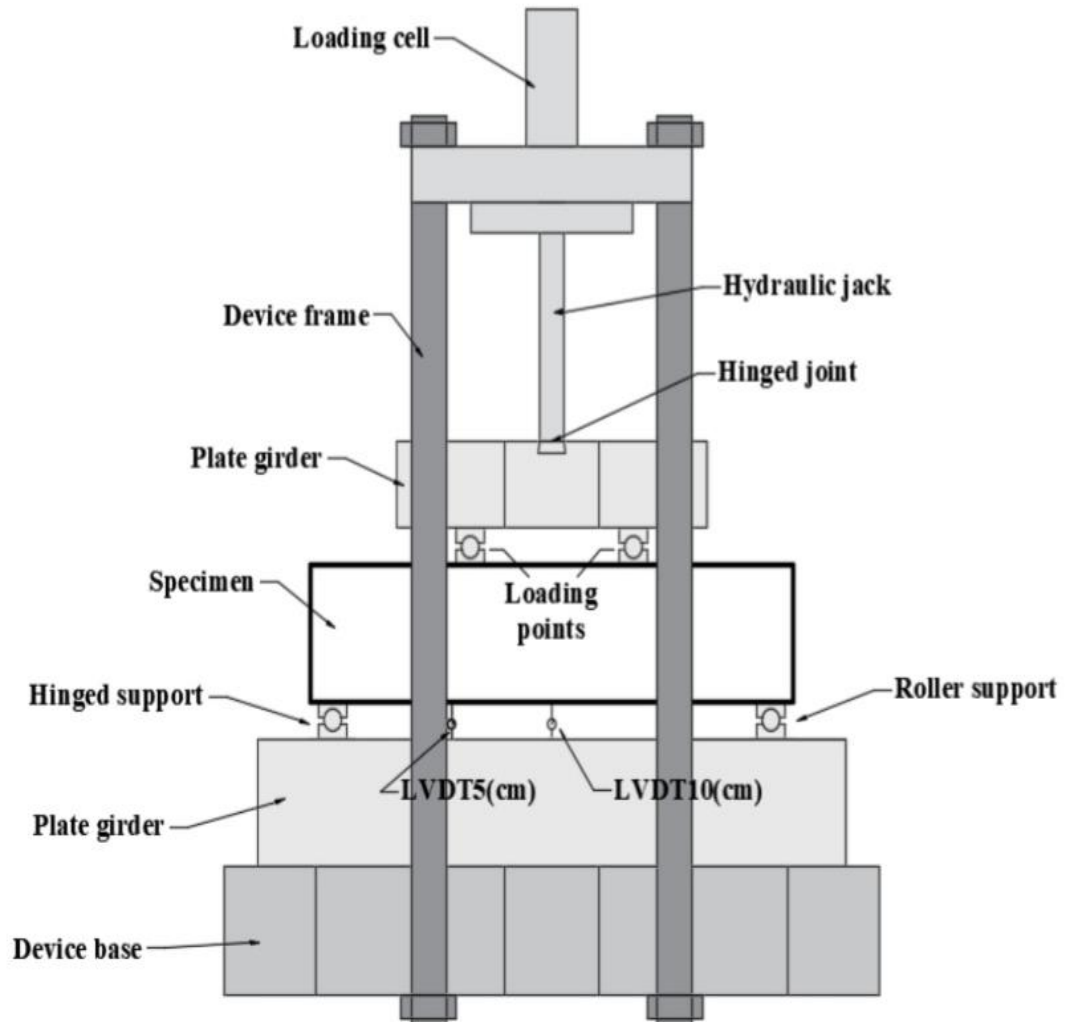


Figure 3.33 Schematic Testing Setup.

CHAPTER FOUR: EXPERIMENTAL RESULTS AND DISCUSSION

4.1 Introduction

The main purpose of this work was to investigate the structural behavior of composite encased steel-concrete beams, which including (15) beams; control beam (solid beam) (CB), composite encased steel-concrete beam with small square openings (BW1), composite encased steel-concrete beam with large square openings (BW2). As well as, other of composite encased steel-concrete beams were strengthened with different strengthening techniques. All the presented beams have the same dimensions, properties, reinforcement, and the same concrete type (Normal Concrete). This chapter will show all the results recorded after the shear test of the fifteen beams tested under two-point loads. Results were collected and discussed. All the load-carrying capacity and deflections were recorded. The records included ultimate loads, first cracks, and crack patterns in which applied load occurs. The stiffness, ductility and toughness are also presented and discussed in this chapter.

4.2 General structural behavior of beams during the testing

The recorded test results have shown in Table (4-1). The table consists of fifteenth specimens of simply supported beams subjected to two-point loads. During the testing, each beam showed a different behavior when reaching the ultimate load, but in the initial phase of loading, all the beams have shown an elastic behavior and the deflections were very small. During this phase of loading, it was observed that the cross-section was fully effective in resisting the loads. By increasing the loads. The first crack was observed in the lower part of the beams in

the shear zone (near support) between the point load and support. After increasing the loads, non-linear behavior began which is an indicator that tested beams reach their plastic phase. At the end of loading, the existing cracks began to grow and extended rapidly to the loading point and support. Table (4.1) shows the details of the results recorded during the testing.

Table 4.1 Tests results of tested beams

Beam Designation	The load capacity of shear (KN)		Max. Deflection (mm)	Failure mode
	Frist Crack	Ultimate load		
CB	60	295.4	14.734	Diagonal shear
BW1	45	320	15.779	Diagonal shear
BW2	18	153.9	15.98	Diagonal shear
CIS1	30	307	16.57	Diagonal shear
CIS2	45	127	16.36	Diagonal shear
RIS1	65	367	13.709	Diagonal shear
RIS2	35	143.4	16.27	Diagonal shear
ECW1	35	346	14.23	De-bonding failure
ECW2	35	176	11.27	De-bonding failure
ECS1	55	302.7	16.24	De-bonding failure
ECS2	15	154.1	15.03	De-bonding failure
ECR1	30	308.7	18.698	Diagonal shear
ECR2	25	155.7	15.9	Diagonal shear
ECR3	35	315	16.5	Diagonal shear
ECR4	25	135.2	16.7	Diagonal shear

4.3 General failure modes in the composite encased steel-concrete beams

The main focus in this work has been to study the structural behavior and the shear failure mode of the new type of structural elements (composite encased steel-concrete beams). These beams consisted of a hollow steel box section encased (embedded) in the concrete section beam (fully encased). In general, in all specimens, the failure mode that occurred in these new elements has been the diagonal shear failure. Diagonal cracks have initiated from the top corner of the opening toward the point load and the bottom corner of the opening toward the support.

4.4 Load-deflection behavior and crack patterns for tested beams

After the curing process of beams has finished, the beams have painted in white color and have transferred to the testing machine, and the load has applied in the center of the beam specimens by increasing the pressure of the hydraulic jack. Deflections have recorded during the test. The general experimental behavior of the composite encased steel-concrete beams has noticed during the test can be summarized as follows; when increased the applied load the first crack occurs in the tension zone and give us an indication that the concrete loses its tensile strength. The increase in applied loads led to concentrate diagonal cracks at corners of openings. Finally, with increasing the load's diagonal cracks (shear cracks) extended from corners of opening toward support and point of concentrate load.

The main final cracks were in the shear zone between applied load and support for all tested beams, including the control beam (solid beam), and has showed an indication that all the tested beam fails in shear failure without splitting failure between concrete and hollow steel box.

The data for (control beam in group No.1) solid beam specimen (CB) are shown in Figure (4.1), the first crack was observed at load of 60 KN in the tensile tension zone of the specimen which indicate that the concrete start to lose its tensile strength after the first crack occurs. As the load increases, the final failure of the concrete is achieved at an ultimate load $P_u = 295.4$ KN. the results of load-deflection for (CB) are shown in Figure (4.1).

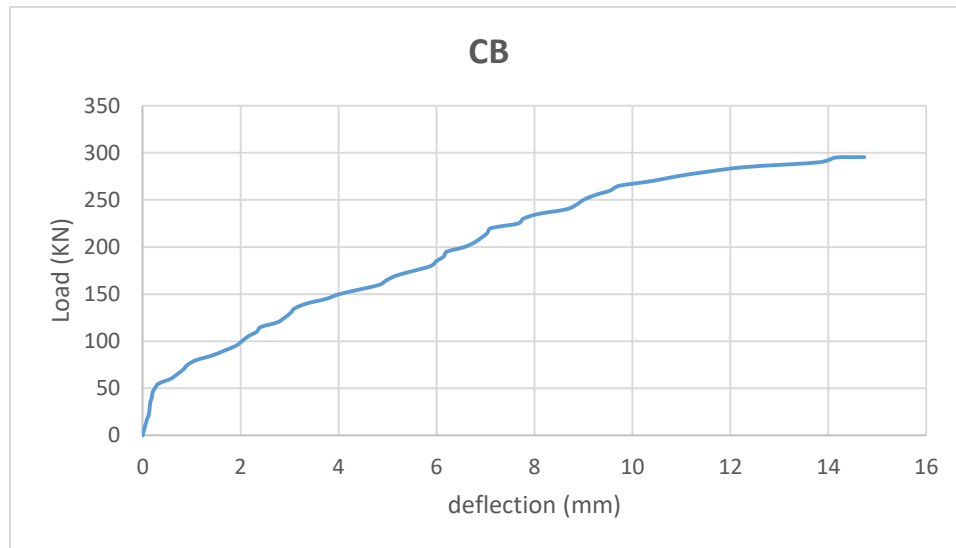


Figure 4.1 Load-deflection behavior and crack patterns for CB.

The data and load-deflection values for different stages for the composite encased steel-concrete beam with small square openings (BW1) are shown in Figure (4.2). From the Figure, it is noted that (BW1) cracking at load of 45 KN, after the first crack with increasing the load the concrete crushing at $P_u = 320$ KN.

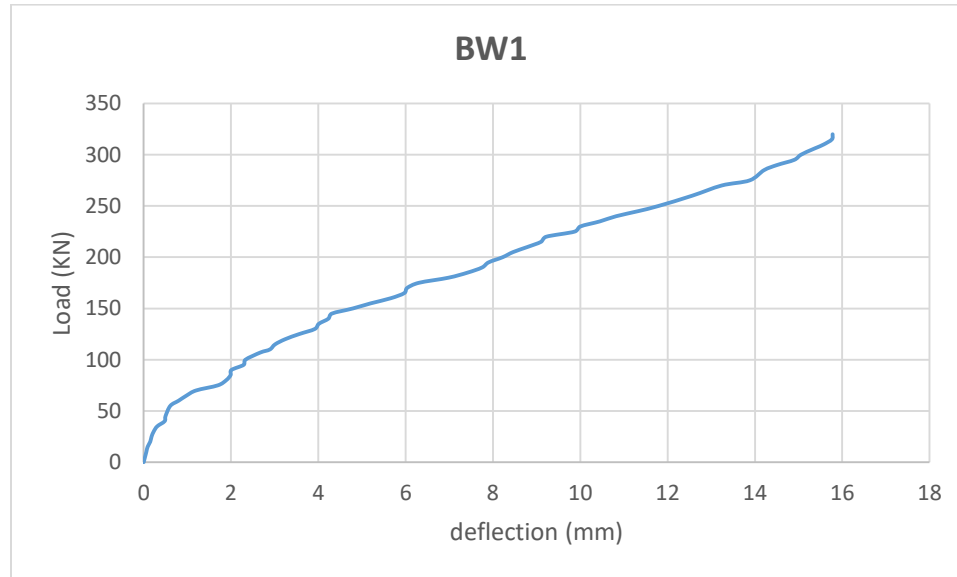


Figure 4.2 Load-deflection behavior and crack patterns for BW1.

The data for the control beam for the composite encased steel-concrete beam with large square openings (BW2) are shown in Figure (4.3). It is indicated that the first crack was recorded at load of 18 KN, and concrete lost its tensile strength after the first crack occurs. The loading continued, with increase the load the concrete crushing at $P_u = 153.9$ KN. The result of load-deflection for (BW2) shown in Figure (4.3).

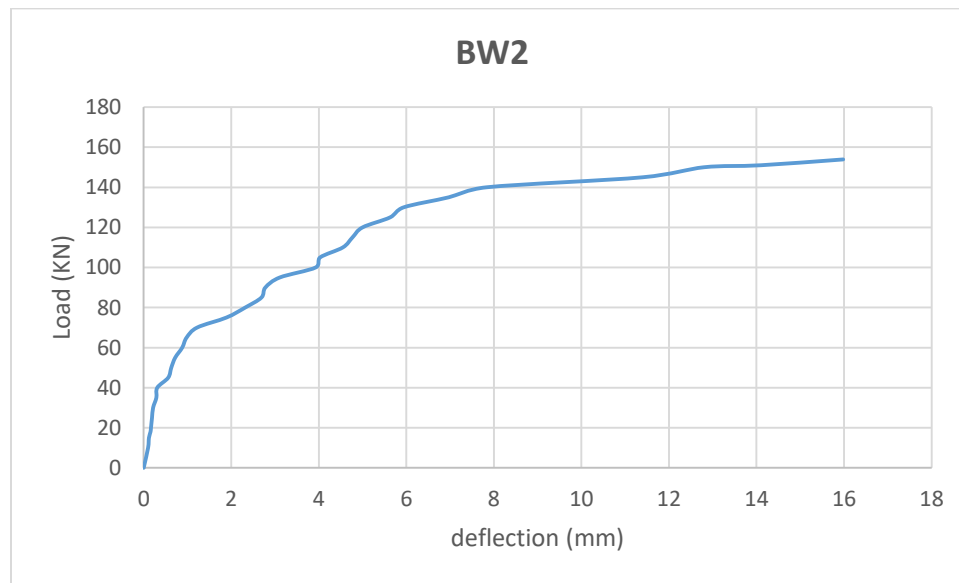


Figure 4.3 Load-deflection behavior and crack patterns for BW2.

The results of load-deflections behavior and crack patterns for different stages for all the tested beams are shown in Figs. (4.4 to 4.15).

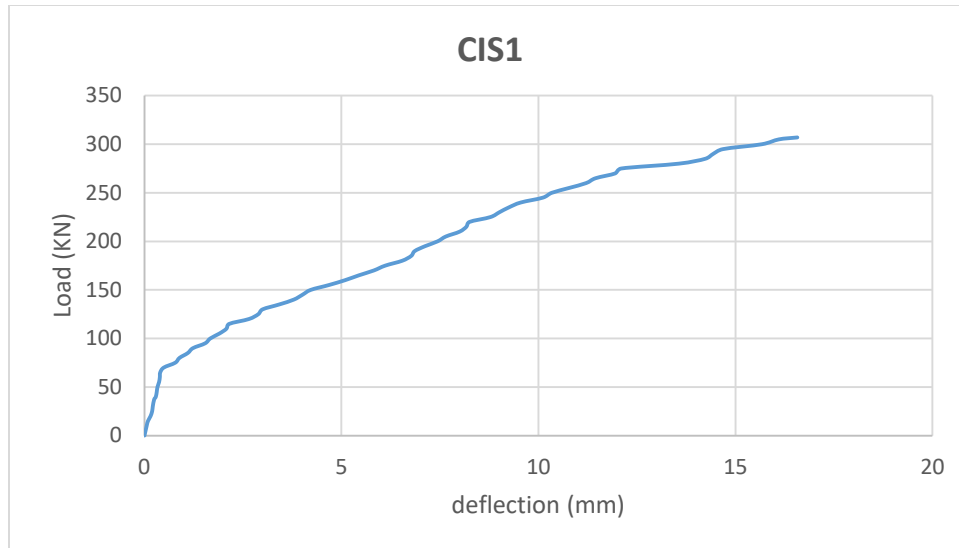


Figure 4.4 Load-deflection behavior and crack patterns for CIS1.

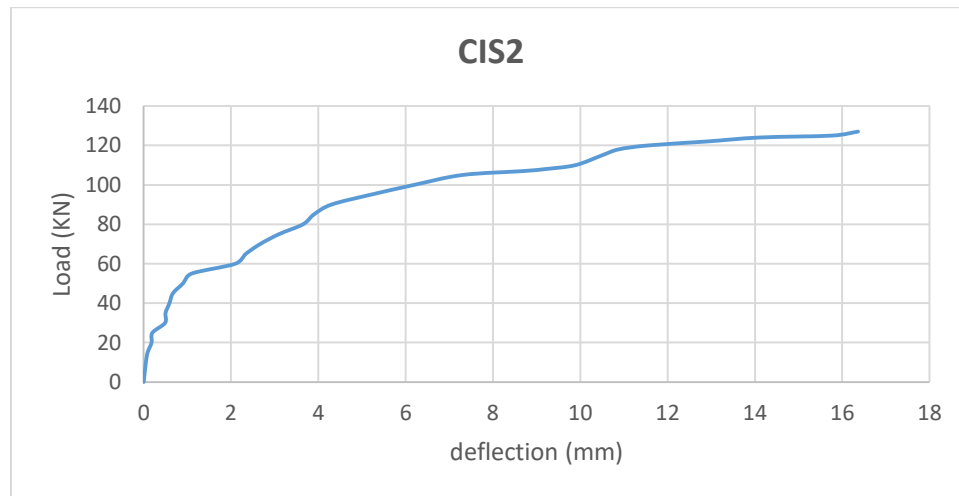


Figure 4.5 Load-deflection behavior and crack patterns for CIS2.

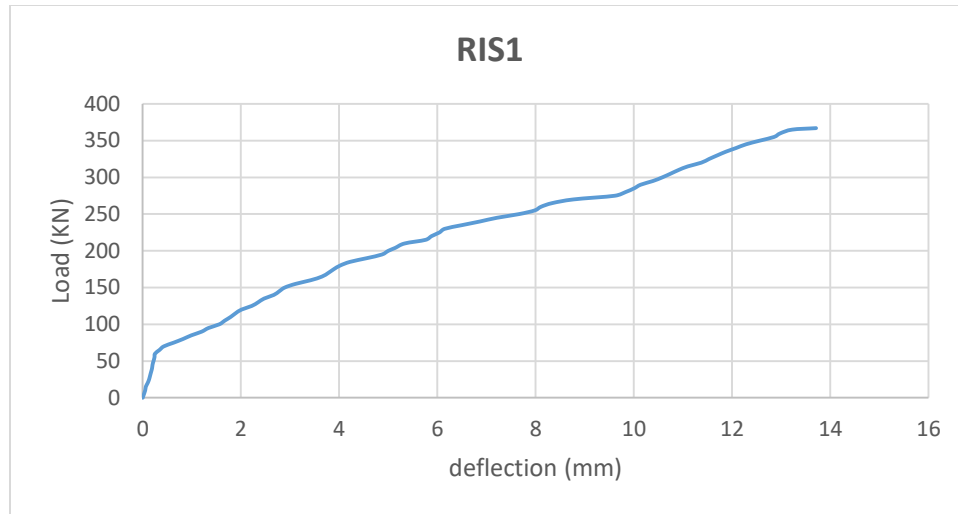


Figure 4.6 Load-deflection behavior and crack patterns for RIS1.

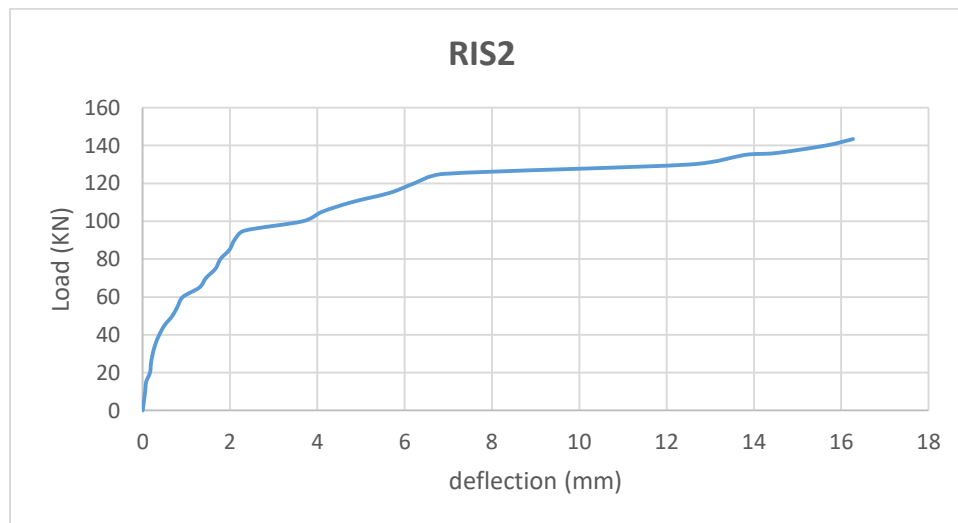


Figure 4.7 Load-deflection behavior and crack patterns for RIS2.

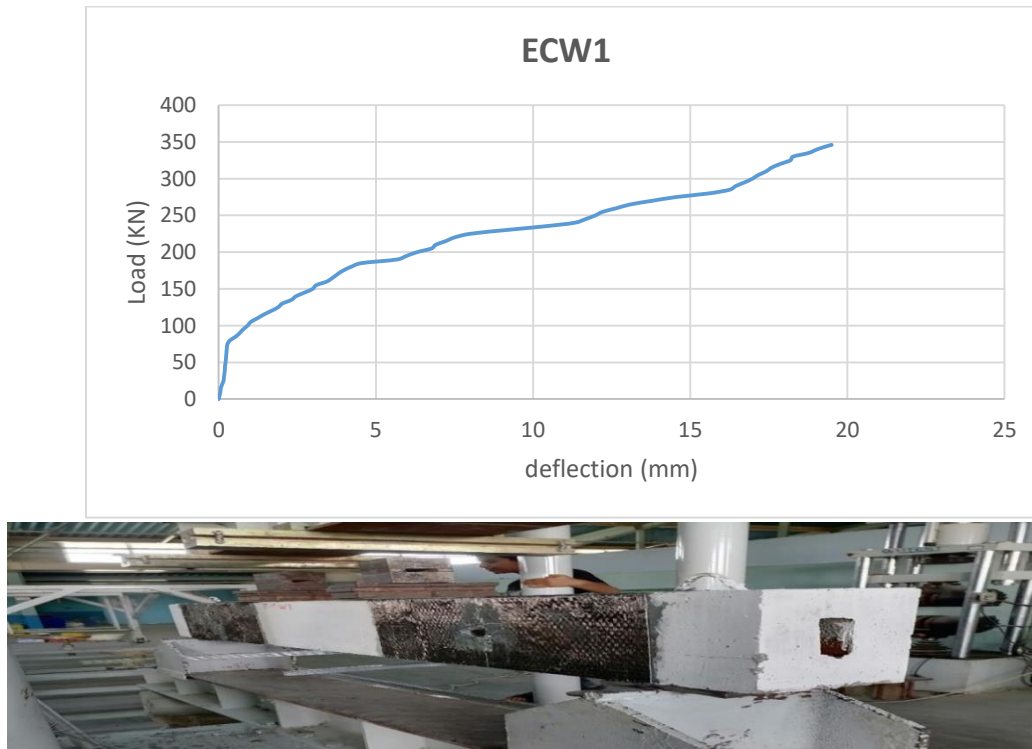


Figure 4.8 Load-deflection behavior and crack patterns for ECW1.

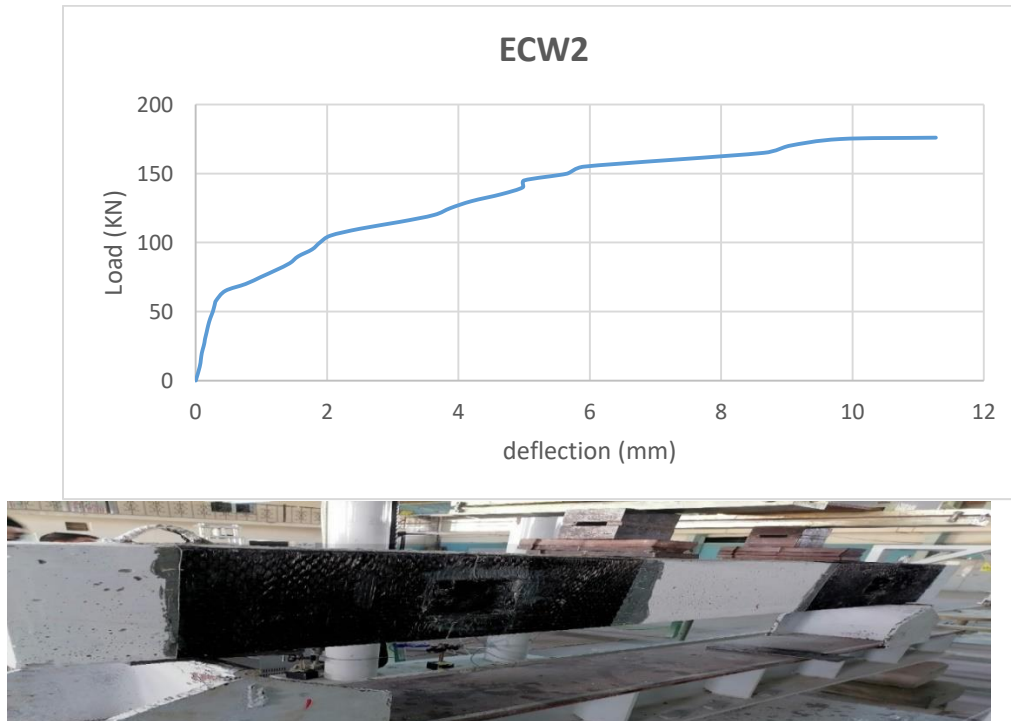


Figure 4.9 Load-deflection behavior and crack patterns for ECW2.

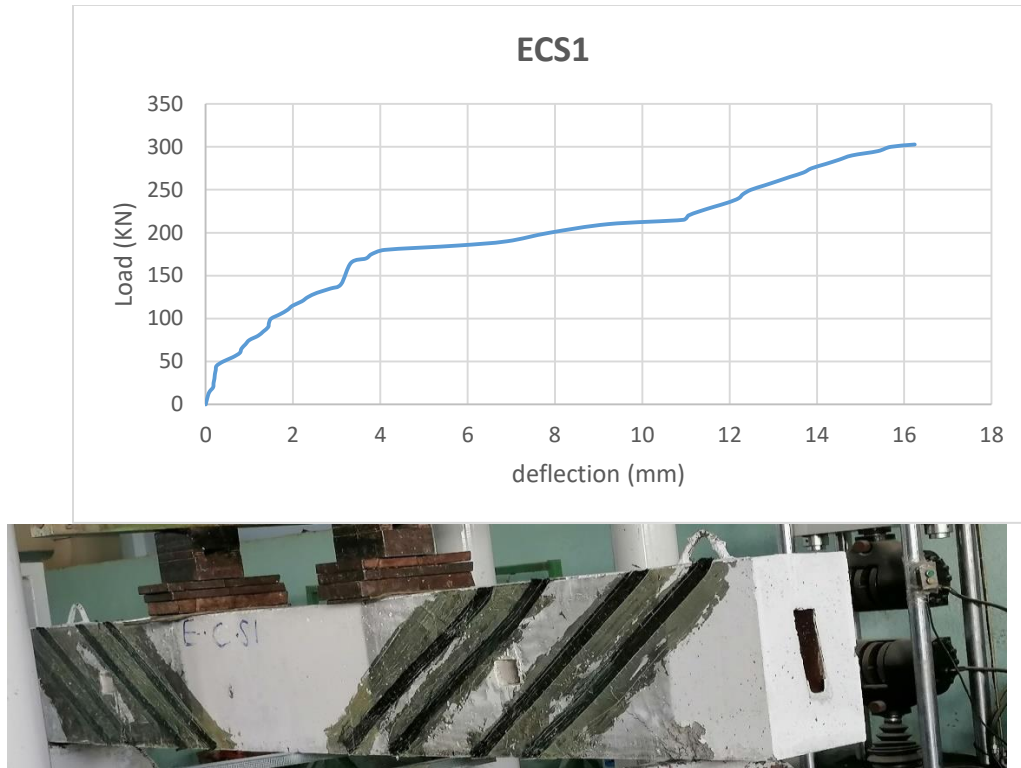


Figure 4.10 Load-deflection behavior and crack patterns for ECS1.

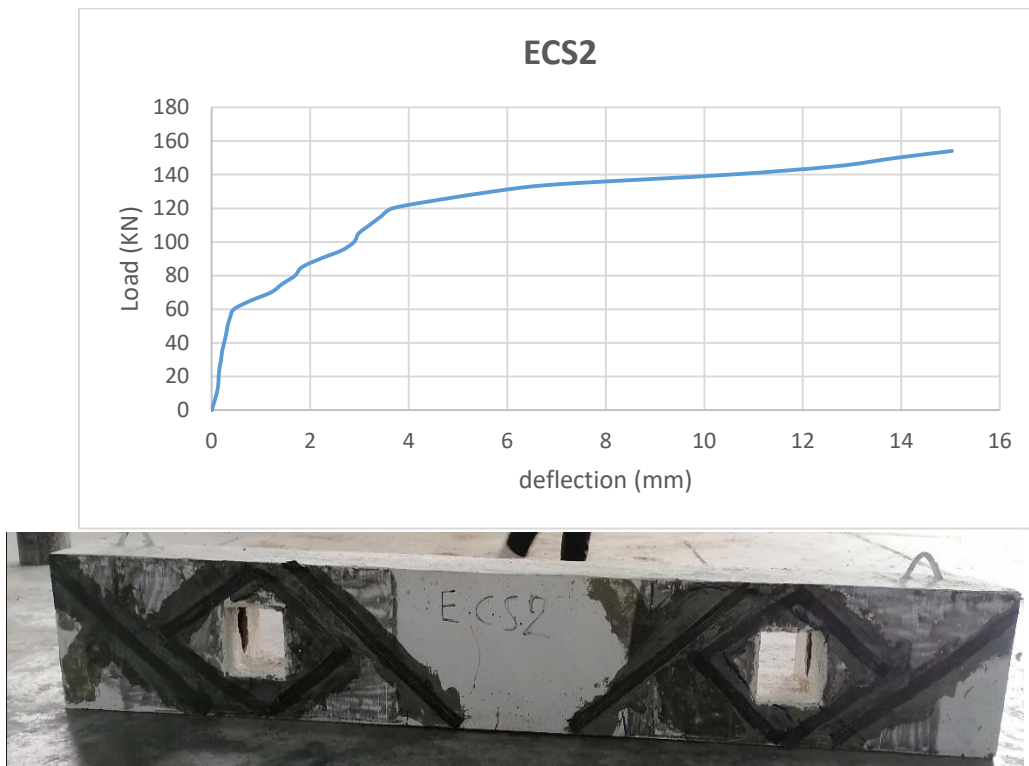


Figure 4.11 Load-deflection behavior and crack patterns for ECS2.

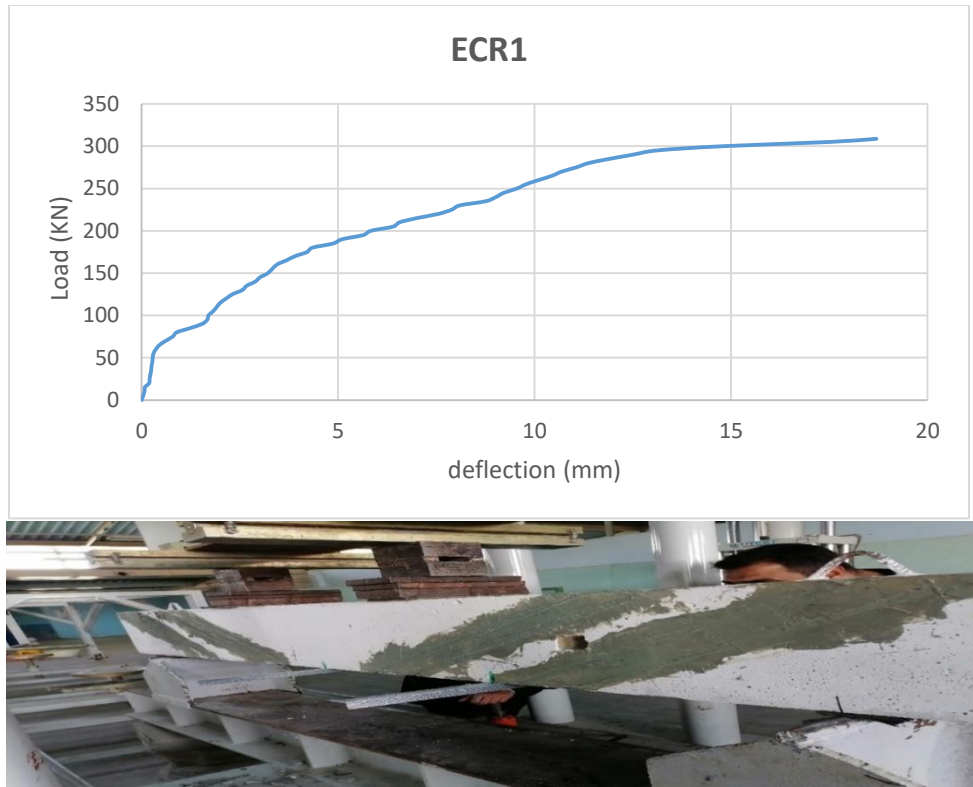


Figure 4.12 Load-deflection behavior and crack patterns for ECR1.

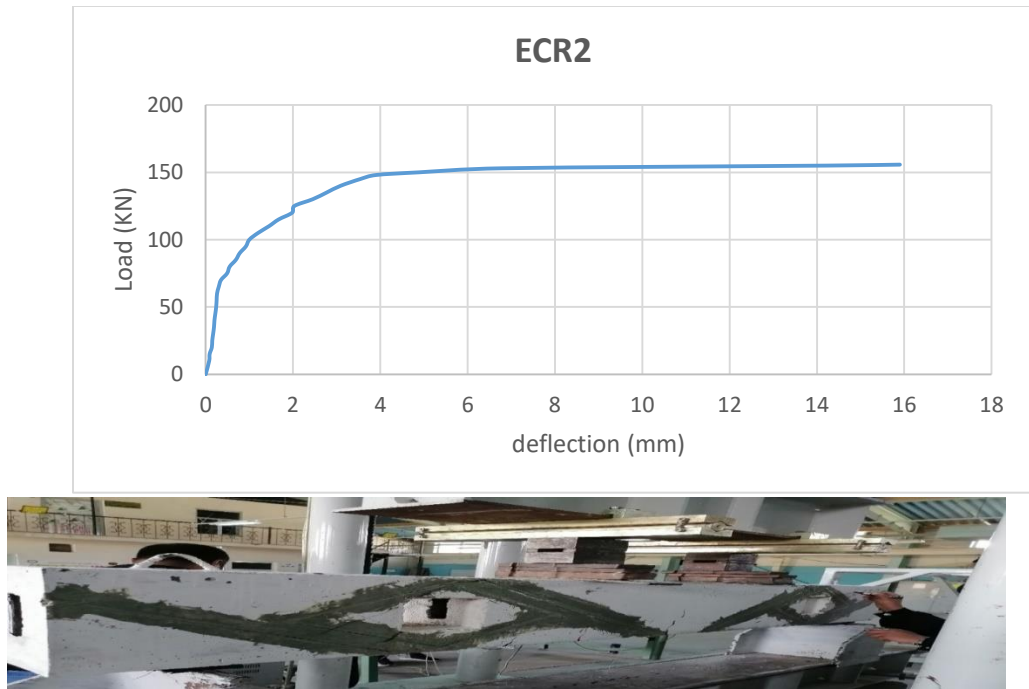


Figure 4.13 Load-deflection behavior and crack patterns for ECR2.

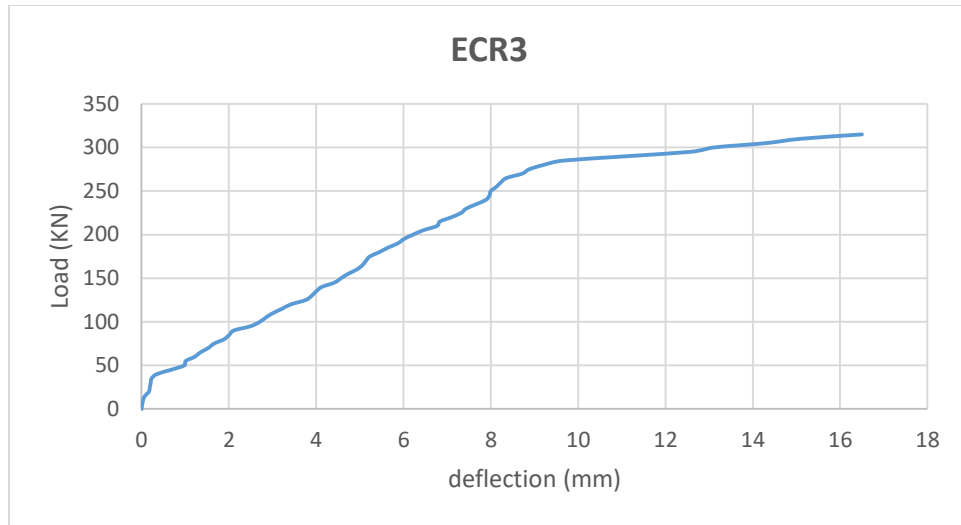


Figure 4.14 Load-deflection behavior and crack patterns for ECR3.

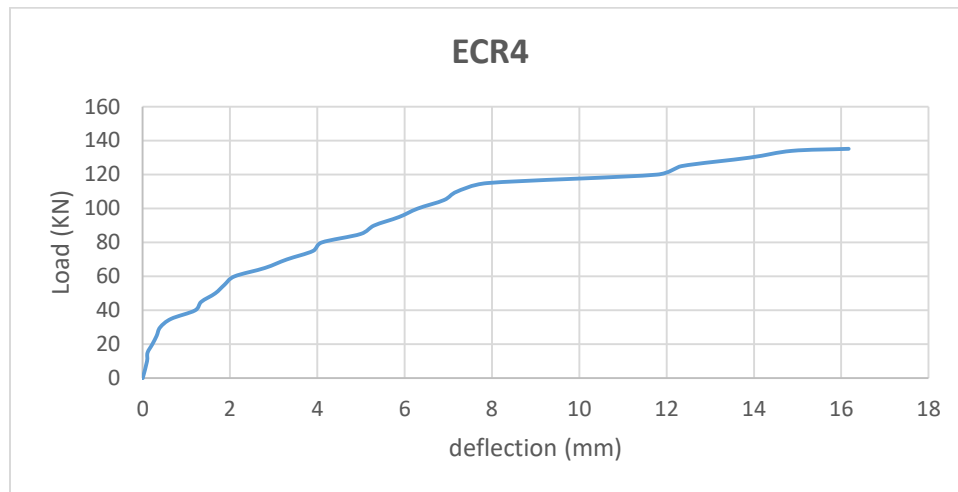


Figure 4.15 Load-deflection behavior and crack patterns for ECR4.

4.5 Ultimate load

It is noticed that the shear capacity of the composite encased steel-concrete beam with the small opening was in general slightly higher than solid beam. This increase in capacity of BW1 is due to using special reinforcement has provided in sufficient quantity with proper detailing, so the strength of BW1 improved.

For GR.No.1, in comparison with the solid beam (CB) as the control beam, it has noticed that the ultimate load of composite encased steel-concrete beam with small square openings (BW1) increased by 8%. On the other hand the load capacity of composite encased steel-concrete beam with large square openings (BW2) decrease by 48% compared with solid beam (CB). As a result that can exist small transverse opening in composite encased steel- concrete beam with using an especial reinforcement around opening.

For GR.No.2, in comparison with composite encased steel-concrete beam with small and large square openings (BW1) and (BW2); respectively as control beams. It was noticed that by the using strengthening technique of extruded encasing transversely the load capacity of the beam with small square openings (CIS1) decrease by 4% when compared with (BW1). While loading capacity of the beam with large square openings (CIS2) decrease by 17% when compared to (BW2). This suggested techniques of strengthening kept load capacity for small opening approximately equal to load capacity of control beam (BW1).

For GR.No.3, it has noticed that by the using strengthening technique of reinforcement arrangement the load capacity of the beam with small square openings (RIS1) increased by 15% when compared with control beam (BW1).

While loading capacity of the beam with large square openings (RIS2) decreased by 7% when compared with the control beam with large square openings (BW2). So the use of reinforcing bar perpendicular on the path of crack at both sides of opening this lead to increase the shear strength of beam. Generally, it is consider this suitable technique of strengthening especially for small openings.

For GR.No.4.a, using strengthening technique of CFRP sheets, it has noticed that load capacity of composite encased steel-concrete beam with small square openings strengthening by CFRP fully wrapping system around the square openings (ECW1) increased by 8% when compared with control beam (BW1). while beam with large square openings strengthening by CFRP fully wrapping system around the square openings (ECW2) load capacity increased by 14% when compared with control beam (BW2). This strengthening technique can be considered the successful technique than others.

GR.No.4.b, load capacity of the beam with small square openings strengthening by CFRP diagonal sheets (ECS1) decreased by 5% when compared with control beam (BW1). In addition to beam with large square openings strengthening by CFRP diagonal sheets (ECS2) load capacity is approximately equal to the load capacity of control beam (BW2).

For GR.No.5.a, it has noticed that load capacity of composite encased steel-concrete beam with small square openings strengthening by using CFRP diagonal bars technique (ECR1) decreased by 4% when compared with control beam (BW1). while load capacity of the beam with large square openings strengthening by CFRP diagonal bars (ECR2) is approximately equal to load capacity of control beam (BW2). This technique keeps the shear strength is constant.

GR.No.5.b, load capacity of beam with small square openings strengthening by CFRP diamond scheme bar (ECR3) approximately equal to load capacity of control beam (BW1). While beam with large square openings strengthening by CFRP diamond scheme bar (ECR4) load capacity decreased by 12% when compared with control beam (BW2).

4.6 Load-deflection comparisons for tested beam

Load-deflection curves of the tested beams at all stages of loading up to failure were shown in Figs. (4.16) to (4.20). For comparison of load-deflection, five groups of curves are established. These are [Gr.No.1 (effect of opening), Gr.No.2 (effect of extruded encasing transversely method), Gr.No.3 (effect technique of reinforcement arrangement), Gr.No.4 (effect technique of CFRP sheets) and Gr.No.5 (effect technique of CFRP bar)]. All the tested beams have approximately the same initial load-deflection behavior until reaching the first crack load.

For Gr.No.1 Figure (4.16) it is noticed composite encased steel-concrete beam with large opening (BW2) shows higher deflection compared to solid beam (CB) due to existing square opening in the shear zone which causes to high concentration of stress around opening. So this leads to excessive cracking and deflection, and reduction in beam resistance.

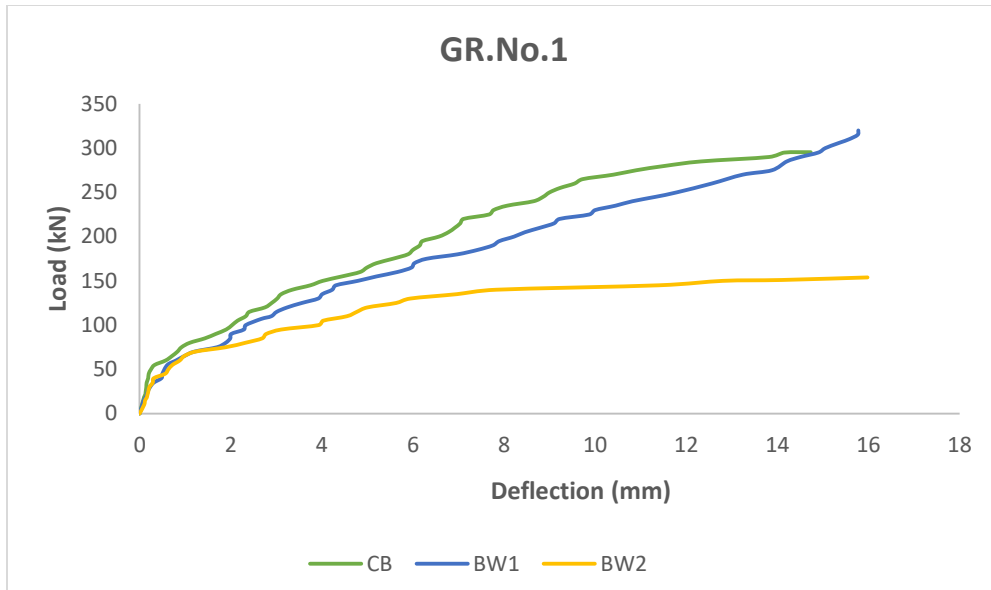


Figure 4.16 Load-deflection comparison for Gr.No.1 (effect of opening).

For Gr.No.2 Figure (4.17) it is clear that composite encased steel-concrete beam large opening strengthened by using extruded encasing transversely technique (CIS2) has maximum deflection and lower ultimate load compared to (BW1,BW2& CIS1).

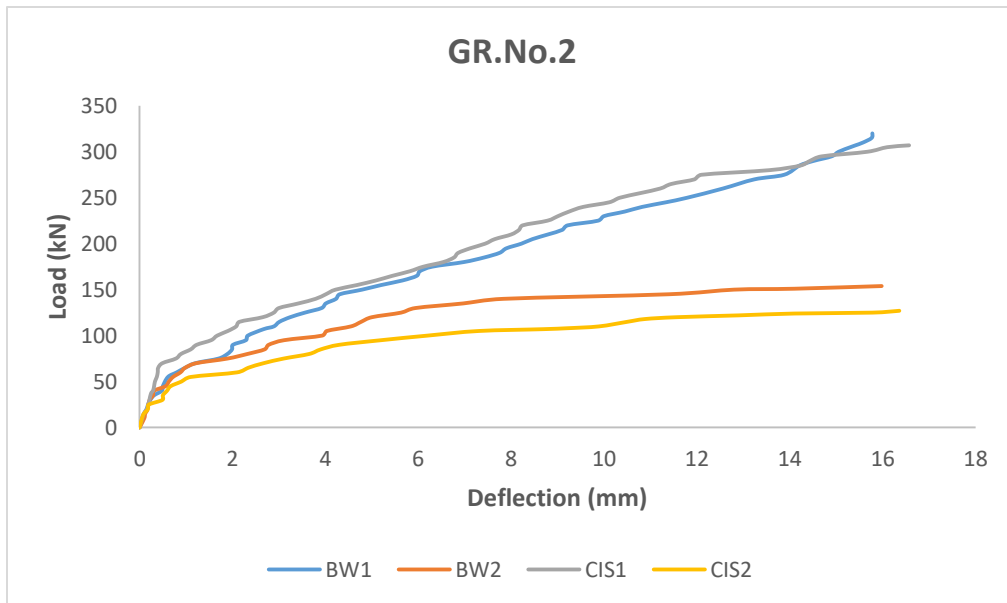


Figure 4.17 Gr.No.2 (effect of extruded encasing transversely technique) compared with control beams BW1 & BW2.

For Gr.No.3 Figure (4.18) it important to notice that the composite encased steel-concrete beam with small opening strengthened by using technique of reinforcement arrangement (RIS1) give the highest ultimate load and lower deflection compared to the rest of beams in this group. This can explained that provided additional of reinforcement bars around the opening make the section more efficient in resisting the deflection.

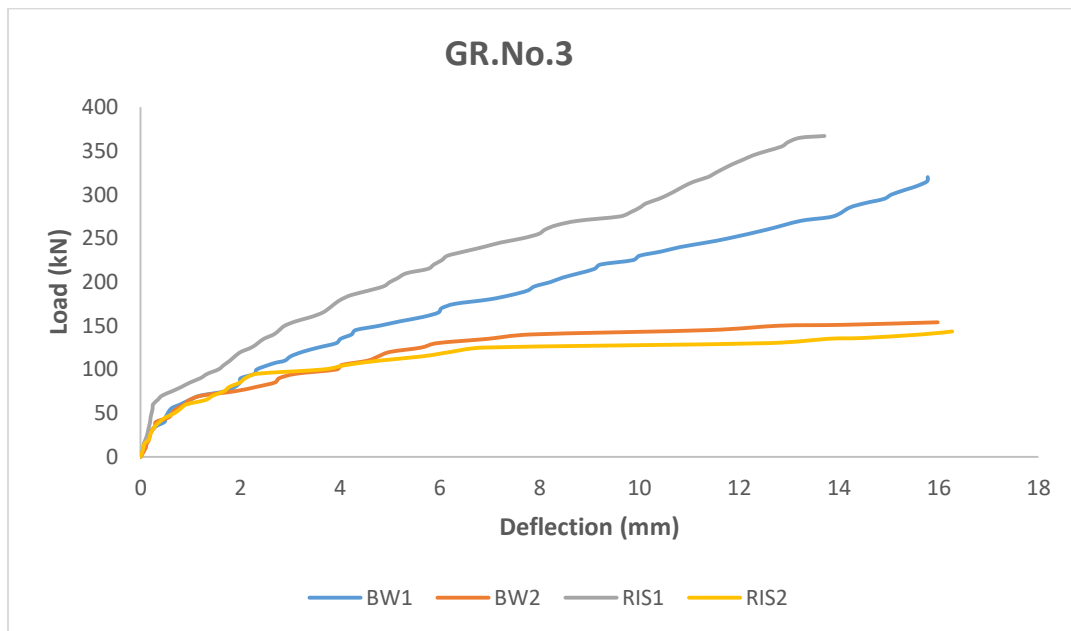


Figure 4.18 Gr.No.3 (effect technique of reinforcement arrangement) compared with control beams BW1 & BW2.

For Gr. No.4 in Figure (4.19) it is noticed clearly that composite encased steel concrete beam with large opening strengthened by using CFRP fully wrapping sheets (ECW2) has lower deflection than (BW2).

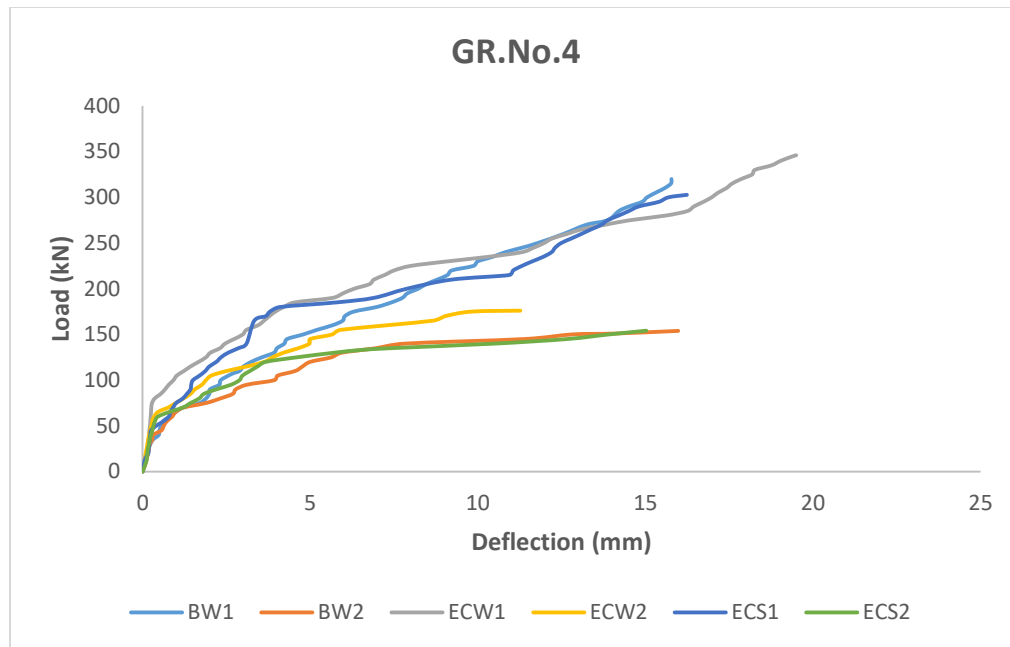


Figure 4.19 Gr.No.4 (effect technique of CFRP sheets) compared with control beams BW1 & BW2.

For Gr. No.5 in Figure (4.20) it is clear composite encased steel-concrete beam with small opening strengthened by using CFRP diagonal bars (ECR1) has maximum deflection than (BW1). In addition composite encased steel-concrete beam with large opening strengthened by using CFRP bars rhombus shape (ECR4) has maximum deflection than (BW2).

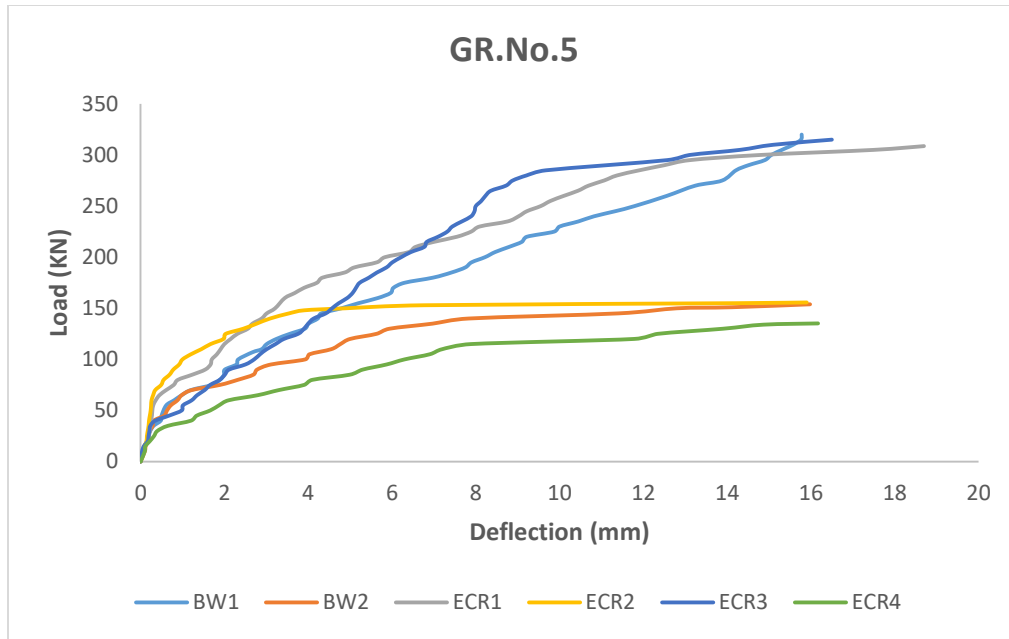


Figure 4.20 Gr.No.5 (effect technique of CFRP bar) compared with control beams BW1 & BW2.

4.7 Initial stiffness comparisons for the tested beams

Initial stiffness was calculated based on the load-deflection curve by dividing the maximum applied load (P_u) on the yield deflection (Δ_y) in the case of initial stiffness. The equations used are shown below:

$$\text{Initial stiffness} = P_y / \Delta_y$$

Stiffness calculation is carried out according to N. Priestley study[79]. The stiffness values of the tested beams are presented in Figs. (4.21 to 4.25).

For GR.No.1, it is noted that in the first group that the composite encased steel-concrete beam with small square openings (BW1) has a higher stiffness than composite encased steel-concrete beam with large square openings (BW2) by 7%. While (BW1) has a lower stiffness than the stiffness of solid beam (CB) by 29%. It indicates that stiffness value decreases with high value deflection.

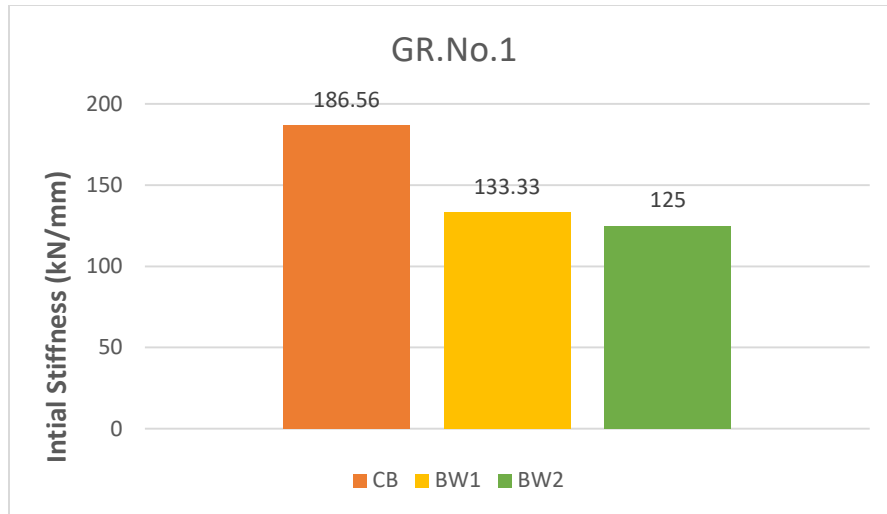


Figure 4.21 Gr.No.1 (effect of opening).

In GR.No.2 shown in Figure (4.22) It can notice that the composite encased steel-concrete beam with small square openings (CIS1) that has strengthened by extruded encasing transversely give the higher stiffness than (CIS2) and (BW2) by 17% and 4% respectively.

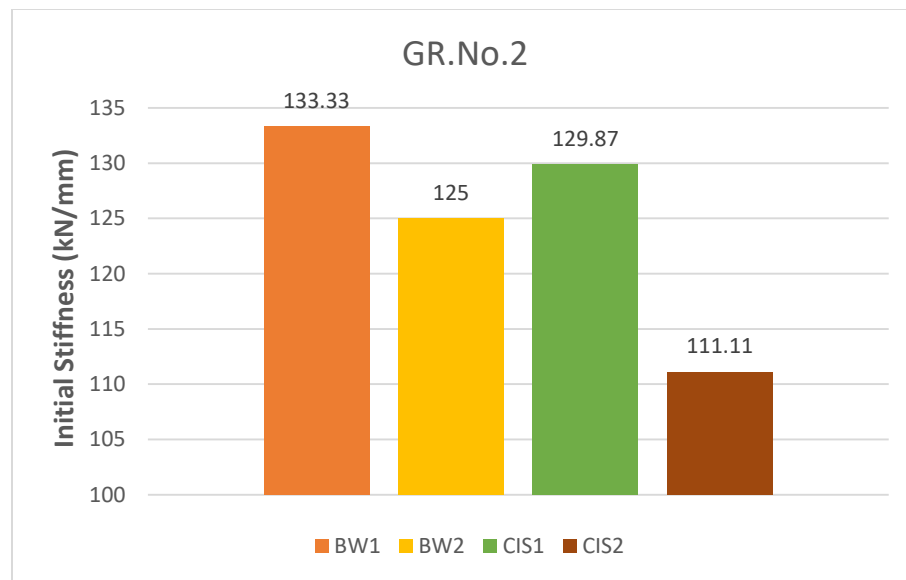


Figure 4.22 Gr.No.2 (effect of extruded encasing transversely technique) compared with control beams BW1 & BW2.

In GR.No.3 in Figure (4.23) it can notice that a composite encased steel-concrete beam with small square openings (RIS1) which have strengthened by using the technique of reinforcement arrangement has a higher stiffness than control beam (BW1) by 50%.

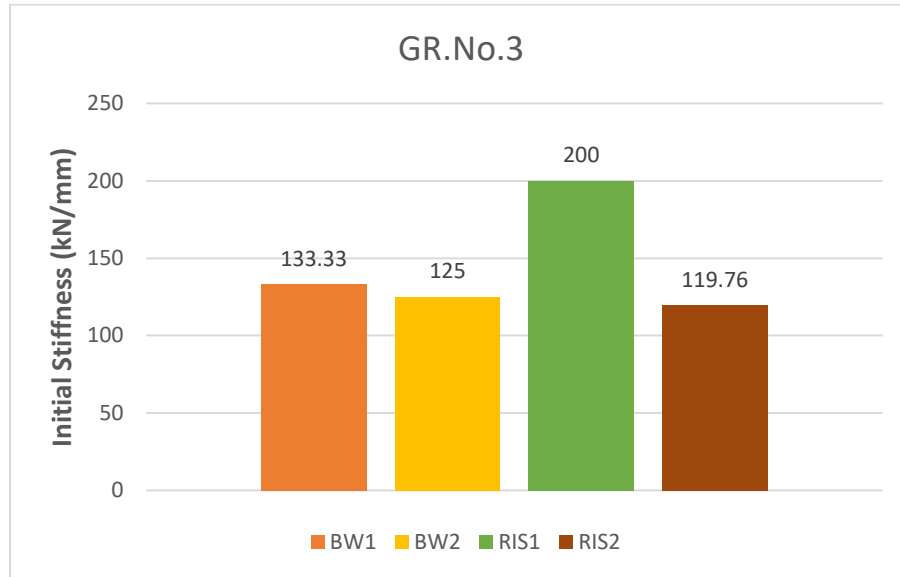


Figure 4.23 Gr.No.3 (effect technique of reinforcement arrangement) compared with control beams BW1 & BW2.

In GR.No.4 shown in Figure (4.24) it is clear that (ECW1) which has strengthened by using CFRP strips fully wrapping has the stiffness is higher by 36% than (BW1). While composite encased steel-concrete beam with large square openings (ECW2) which has strengthened by using CFRP strips fully wrapping, has the stiffness is higher by 74% than (BW2). This indicates that the stiffness of composite encased steel-concrete beams with square openings increases by using CFRP strips fully wrapping as strengthening technique.

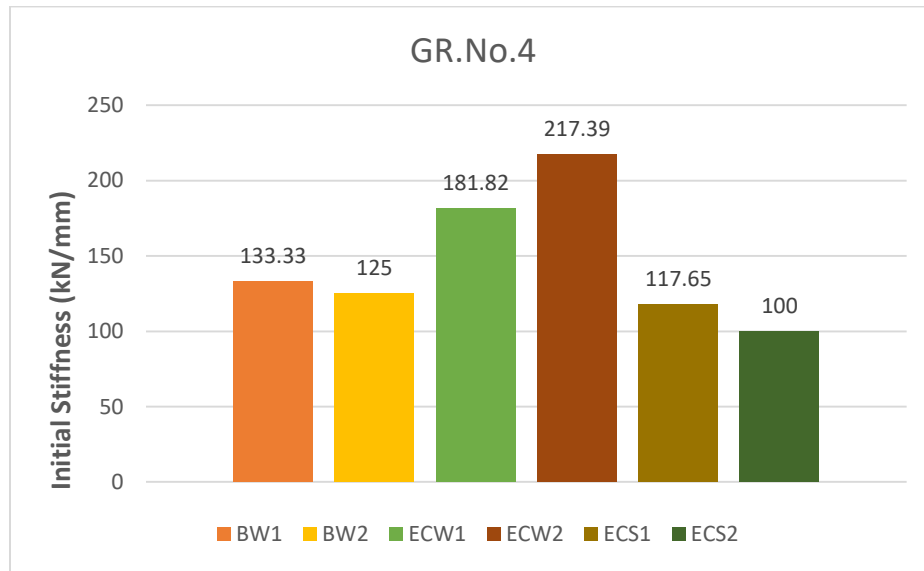


Figure 4.24 Gr.No.4 (effect technique of CFRP sheets) compared with control beams BW1 & BW2.

In GR.No.5 shown in Figure (4.25) it is noticed that for the composite encased steel-concrete beam with large square openings (ECR2) strengthened by diagonal CFRP bars around large square openings has stiffness is higher than the stiffness of control beam with large opening (BW2) by 14%.

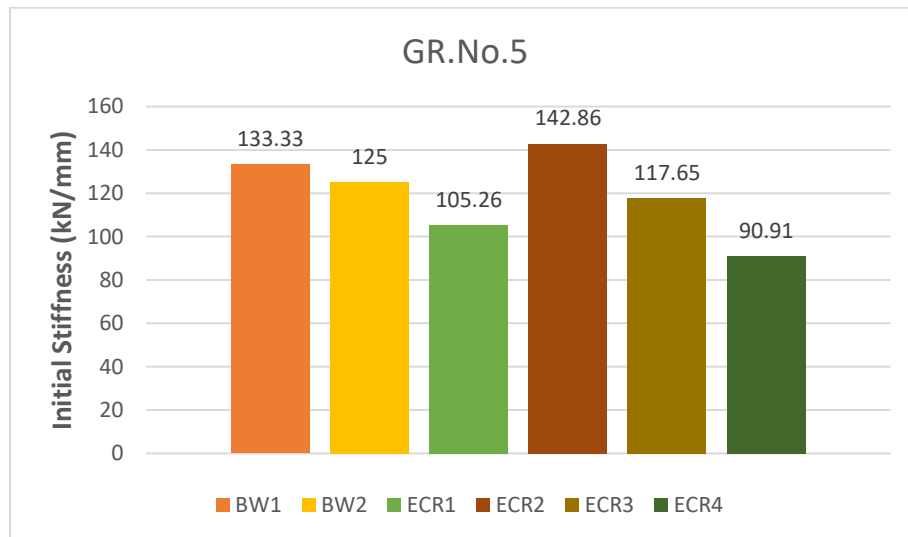


Figure 4.25 Gr.No.5 (effect technique of CFRP bar) compared with control beams BW1 & BW2.

4.8 ENERGY ABSORPTION CAPACITY COMPARISONS FOR THE TESTED BEAMS

Energy absorption capacity can be calculated through the load-deflection curve. The area under the curve represents the value of energy absorption capacity. Figs. (4.26 to 4.30) represents the energy absorption of the tested beams in this study. In Figure (4.26), we noted that the energy absorption in Group No.1. in the composite encased steel-concrete beam with small square openings (BW1) approximately equal to the solid beam (CB). while the energy absorption capacity decreased in a composite encased steel-concrete beam with large square openings (BW2) by 34% than the solid beam (CB). It seems that the use of small square openings enhanced the energy absorption capacity better than the use of large square openings in the beam. In group No.2 it is noticed that composite encased steel-concrete beam with small square openings (CIS1) which has strengthened by extruded encasing transversely give energy absorption capacity higher by 14% than (BW1). In group No.3, the use technique of reinforcement arrangement in the strengthening of the beam with small square openings has enhanced energy absorption. In group No.4 in Figure (4.29) it is noticed that the composite encased steel-concrete beam with small square openings strengthening by CFRP fully wrapping strips (ECW1) has energy absorption greater by 48% than (BW1). In group No.5 it is noticed that composite encased steel-concrete beam with small square openings (ECR1) which has strengthened by CFRP diagonal bars has energy absorption greater by 44% than (BW1).

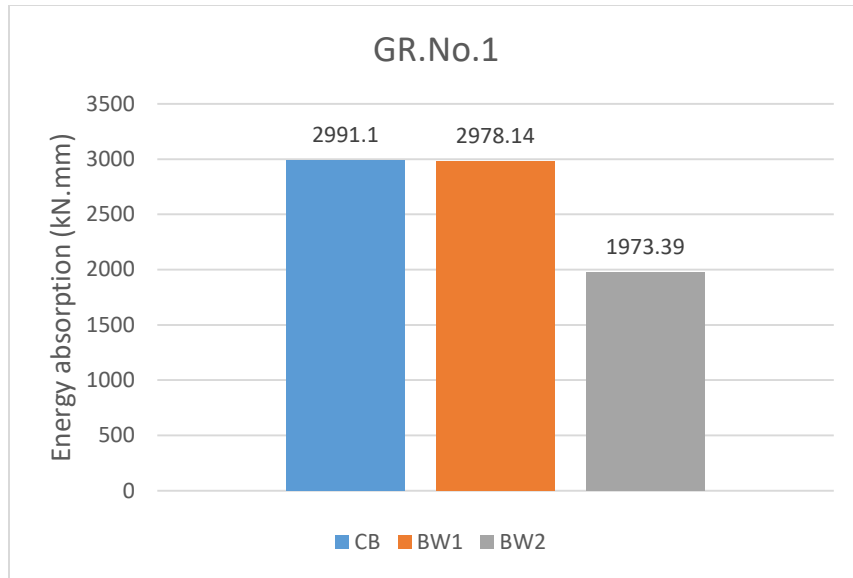


Figure 4.26 GR.No.1 (effect of openings).

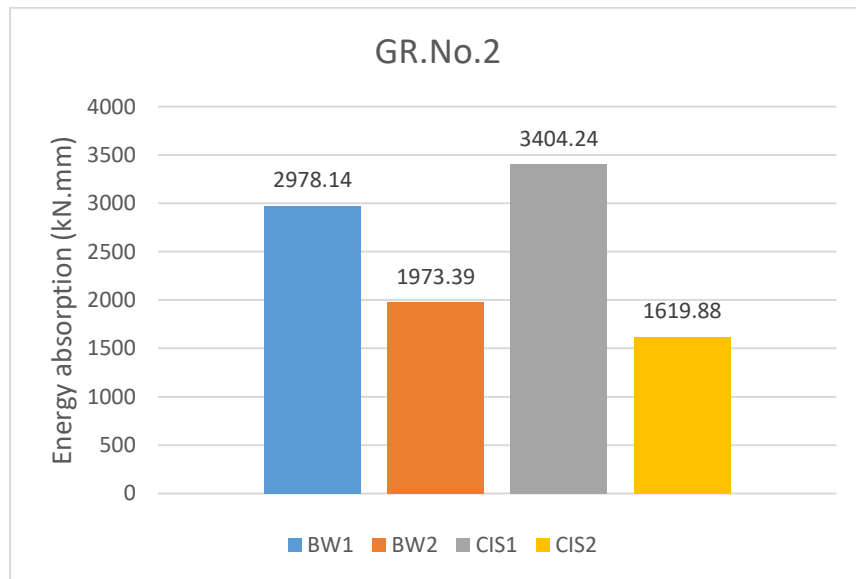


Figure 4.27 GR.No.2 (effect strengthening of extruded encasing transversely) compared with control beams BW1 & BW2.

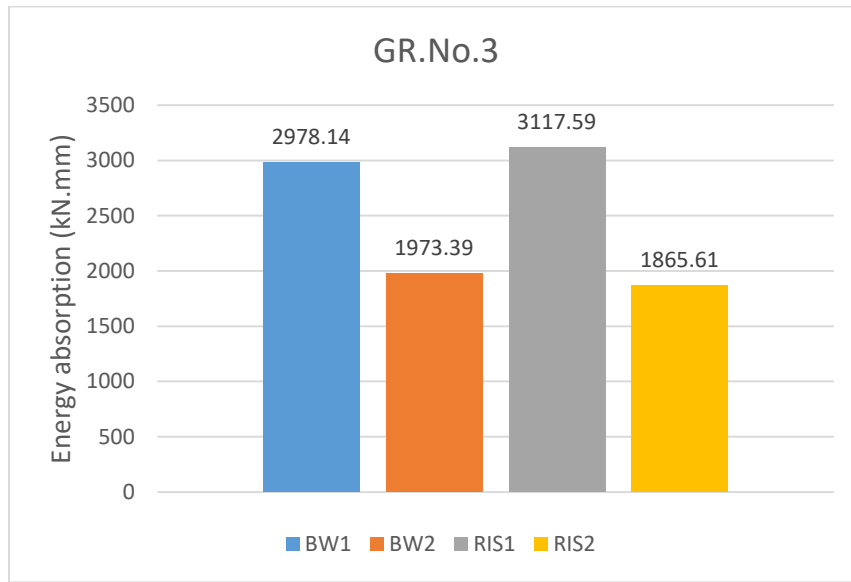


Figure 4.28 GR.No.3 (effect strengthening of reinforcement arrangement) compared with control beams BW1 & BW2.

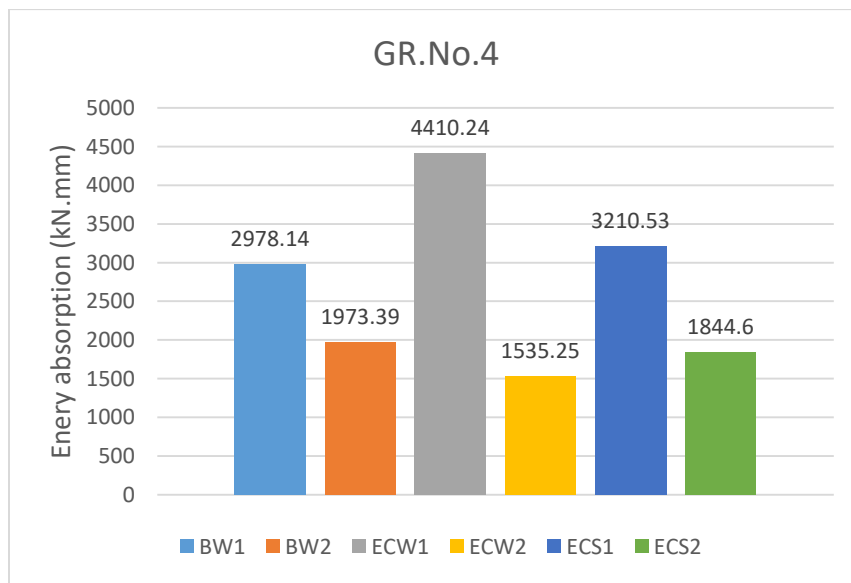


Figure 4.29 GR.No.4 (effect strengthening of CFRP sheets) compared with control beams BW1 & BW2.

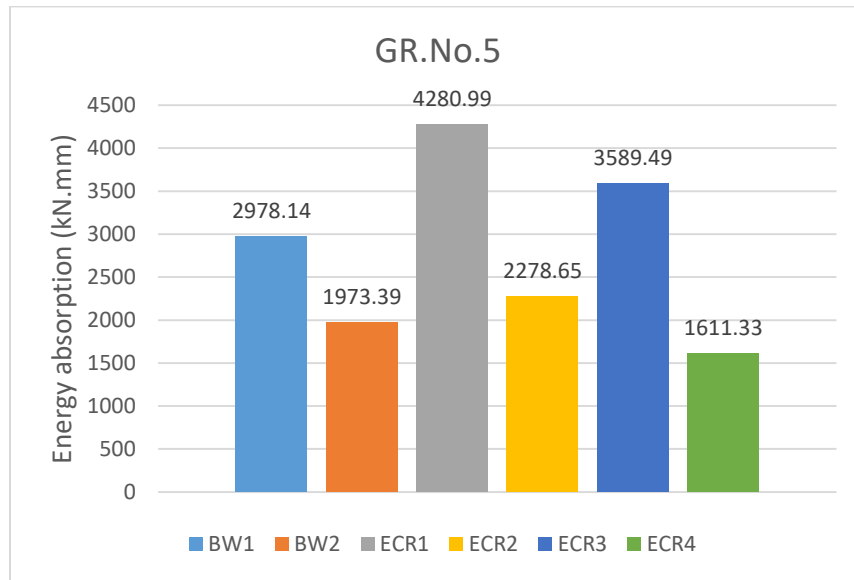


Figure 4.30 GR.No.5 (effect strengthening of CFRP bar) compared with control beams BW1 & BW2.

CHAPTER FIVE: CONCLUSIONS AND RECOMMENDATIONS

5.1 Conclusions

The current research investigates the shear behavior to new type of composite encased steel-concrete beams with transverse openings, as it is composed of a hollow steel section that is fully encased in the concrete. The main conclusions obtained in this study are as follows:

1-The existing of small transverse square openings in composite encased steel-concrete beam (BW1) increased shear capacity by 8% when compared with shear capacity of control solid beam (CB), if used special reinforcement is provided in sufficient quantity with proper detailing around openings.

2-The existing of large transverse square openings (BW2) in composite encased steel-concrete beam decreased shear capacity to half shear capacity of the control solid beam (CB).

3-The results showed that composite encased steel-concrete beam with small transverse square openings (BW1) in the shear zone increased shear capacity by 107% when compared with shear capacity of composite encased steel-concrete beam with large transverse openings in the shear zone (BW2).

4-As compared to control beam (BW1) the shear capacity increased by 15% in composite encased steel-concrete beam with small square openings in shear zone was strengthened by using technique of reinforcement arrangement (RIS1). While shear capacity decreased by 7% in composite encased steel-concrete beam with large square openings in shear zone was strengthened by using technique reinforcement arrangement (RIS2) when compared to control beam (BW2).

5-The effective strengthening technique for composite encased steel-concrete beams with small and large square openings in the shear zone, was the

external strengthening by using CFRP fully wrapping sheets around square openings. Where the results showed an increase in the ultimate load of composite encased steel-concrete beams with small (ECW1) and large square openings (ECW2) in the shear zone by 8% and 14%; respectively.

6- Using extruded encasing transversely technique as the internal strengthening, in strengthening composite encased steel-concrete beams with small (CIS1) and large transverse square openings (CIS2) in the shear zone. This technique kept shear capacity of strengthened beams approximately equal to control beams.

7-Using NSM CFRP bars in strengthening each of small and large transverse square openings in the shear zone with two different configurations around the square openings (strengthening of the specimens with diamond scheme strengthening bar and diagonal strengthening bars). The results showed that shear capacity of strengthened beams by CFRP bars kept approximately equal to shear capacity of control beams.

8-All beams failed in shear. Where diagonal shear cracks initiated in appearance from the top corner of opening toward the point load and the bottom corner of opening toward the support.

9-Mode of failure associated with CFRP application was preceded by warning signs such as snapping or peeling sounds of CFRP. In general, all beams suffered from shear failure and made a loud sound during the failure.

10-The value of stiffness of composite encased steel-concrete beam with small square openings in the shear zone (BW1) has a lower stiffness than the stiffness of solid beam (CB) by 29%. While (BW1) has stiffness higher than composite encased steel-concrete beam with large square openings (BW2) by 7%. On the other hand stiffness values increased when the internal strengthening of reinforcement arrangement used. Where the composite encased steel-concrete

beam with small square openings (RIS1) strengthening by reinforcement arrangement has higher stiffness than control beam (BW1).

11-The composite encased steel-concrete beam with small square opening in shear zone strengthening by CFRP fully wrapping sheets around openings (ECW1) has energy absorption higher than control beam (BW1) by 48%. While composite encased steel-concrete beam with small square openings (ECR1) which has strengthened by CFRP diagonal bars has energy absorption greater by 44% than (BW1).

12- With respect to strengthening techniques of CFRP diagonal sheets around small opening in composite encased steel-concrete beam the theoretical shear strength value calculated as follow:-

Shear strength for steel box

$$V_{\text{box}} = 0.6 \cdot f_{y\text{ox}} \cdot A_w \cdot c_v = 71.81 \text{ kN} \quad (\text{AISC}) \quad 5.1$$

Where $f_{y\text{box}}$ = yield stress of steel box = 220 MPa, A_w = area of steel box = 544 mm², c_v = web shear coefficient = 1.

Shear strength for stirrups

$$V_s = (d/s)(A_v)(F_y) = 37.44 \text{ kN} \quad (\text{ACI}) \quad 5.2$$

Where d = effective depth = 261.5 mm, A_v = area of stirrups = 56.52 mm², F_y = yield stress of stirrups = 380 MPa, s = spacing between stirrups = 150 mm ,

Shear strength for concrete

$$V_c = (0.16 \sqrt{f_c'}) (b_w d - (50 \cdot 50)) = 39.84 \text{ kN} \quad (\text{ACI}) \quad 5.3$$

Where f_c' = compressive strength of concrete = 25 Mpa, b_w = beam width = 200 mm, d = effective depth = 261.5 mm, (50*50) = dimension of square opening.

Shear strength for opening

$$V_{\text{so}} = V_{\text{sv}} + V_{\text{sd}} = (A_v \cdot f_{yv})/s \cdot (d_v - d_o) + A_d \cdot f_{yd} \cdot \sin \alpha = 70.56 \text{ kN} \quad (\text{AIC}) \quad 5.4$$

Where V_{sv} =shear of vertical stirrups, V_{sd} =shear of diagonal reinforcement, A_v =area of vertical stirrups=56.52mm², f_{yv} =yield stress of vertical stirrups=380MPa, s =spacing between vertical stirrups=60mm, d_v = distance between top and bottom reinforcement=230.5mm, d_o =50mm, A_d =area of diagonal reinforcement=56.52mm², f_{yd} =yield stress of diagonal reinforcement =380MPa, α =orientation angle= 45°.

Shear strength for CFRP sheets

$$V_f = (A_{fv} * F_{fe} * (\sin\alpha + \cos\alpha) d_{fv}) / s_f \quad (\text{ACI 440.2R}) \quad 5.5$$

Where t_f = thickness of CFRP sheet= 0.165mm, w_f =CFRP width= 30mm with orientation angle α 30°, effective depth of FRP shear reinforcement d_{fv} =261.5mm, area of FRP shear reinforcement $A_{fv} = 2 n * t_f * w_f = 9.9 \text{ mm}^2$, effective stress in the FRP $f_{fe} = \epsilon_{fe} * E_f = 700$, $s_f = 50\text{mm}$, Ultimate tensile strength (f_{fu}) (N/mm²)=3500, FRP strength reduction factor (Ψ_f)= 0.85, Modulus of elasticity (E_f) (N/mm²)=175000, Number of plies of FRP reinforcement (n) =1, $\phi V_n = \phi (V_c + V_s + V_{box} + V_{so} + \Psi_f V_f) = 361.04 \text{ kN}$. The table (5.1) below represents compared between theoretical and experimental value for strengthening technique of CFRP diagonal sheets:

Table 5.1 Theoretical and experimental result of CFRP sheet.

Shear force (V_f)	Theoretical results	Experimental results
Small opening strengthening by CFRP sheets	361.04 kN	302.7 kN

5.2 Recommendations for future works

Some points are recommended to be included in future work for composite encased steel-concrete beams with square openings:

1- The goal of this study is to investigate a new structural element (composite encased steel-concrete beams with web openings in shear zone). Where studied its shear behavior experimentally. So is recommended future studies to investigate flexural behavior of this new type of element.

2- In this research, the test was performed by using two point-loadings. So is proposed for future studies to use different load conditions such as distributed loads and repeated loads, etc.

3- The work included in this research is only study of the transverse square openings in shear zone and longitudinal opening fabricated by using hollow steel box. So is recommended to investigate the behavior of composite encased steel-concrete beam with opening in flexural zone or using multi openings in the composite encased steel-concrete beams.

4- It is recommended in future studies to use different types of concrete like high strength concrete.

REFERENCES

- [1] K. Fawzy, “Strengthening of Opening R . C . Beams in Shear Using Bonded External Reinforcements,” *Int. J. Eng. Sci. Innov. Technol.*, vol. 4, no. 2, pp. 11–23, 2015.
- [2] A. H. Aziz, “Experimental and Theoretical Evaluation for Effect of Openings Location on Shear Strength of Rc Beams,” *J. Eng. Dev.*, vol. 20, no. 1, pp. 1–15, 2016.
- [3] N. Q. Jassim and H. K. Jarallah, “Performance Enhancement of R.C. Beams with Large Web Openings by Using Reactive Powder Composite: An Experimental Study,” *Al-Nahrain J. Eng. Sci.*, vol. 21, no. 3, pp. 405–416, 2018, doi: 10.29194/njes.21030405.
- [4] S. S. Pillai and A. Johny, “Analytical Study on Shear Behavior of Reinforced Concrete Beam with Varying Shapes of Web Opening,” vol. 6, no. 06, pp. 2–5, 2018.
- [5] A. A. H. Abdallah, “Methodology of Bending of Rc Beams with Opening for the Usage in Construction Engineering Management,” *Civ. Eng. Res. J.*, vol. 1, no. 4, 2017, doi: 10.19080/cerj.2017.01.555569.
- [6] M. A. Mansur, “Effect of openings on the behaviour and strength of R/C beams in shear,” *Cem. Concr. Compos.*, vol. 20, no. 6, pp. 477–486, 1998, doi: 10.1016/S0958-9465(98)00030-4.
- [7] S. M. Allam, “Strengthening of RC beams with large openings in the shear zone,” *AEJ - Alexandria Eng. J.*, vol. 44, no. 1, pp. 59–78, 2005.
- [8] S. C. Chin, N. Shafiq, and M. F. Nuruddin, “Strengthening of RC beams with large openings in shear by CFRP laminates: Experiment and 2D nonlinear finite element analysis,” *Res. J. Appl. Sci. Eng. Technol.*, vol. 4, no. 9, pp. 1172–1180, 2012.

- [9] A. W. Nage and A. H. Al-zuhairi, “Strengthening of RC Beam with Large Square Opening Using CFRP,” *J. Eng.*, vol. 26, no. 10, pp. 123–134, 2020, doi: 10.31026/j.eng.2020.10.09.
- [10] B. H. Osman, E. Wu, B. Ji, and A. M. S Abdelgader, “A state of the art review on reinforced concrete beams with openings retrofitted with FRP,” *Int. J. Adv. Struct. Eng.*, vol. 8, no. 3, pp. 253–267, 2016, doi: 10.1007/s40091-016-0128-7.
- [11] M. A. E. M. Osman¹ and Kholoud Atef Sayed², “Study the Behavior of Beams with Opening in the Shear Zone Strengthened by Carbon, Glass sheet and Steel Fibers,” *Life Sci. J.*, pp. 136–146, 2019.
- [12] F. El Ame, J. N. Mwero, and C. K. Kabubo, “Openings Effect on the Performance of Reinforced Concrete Beams Loaded in Bending and Shear,” *Eng. Technol. Appl. Sci. Res.*, vol. 10, no. 2, pp. 5352–5360, 2020, doi: 10.48084/etasr.3317.
- [13] O. H. Abbas and H. A. Numan, “A state of the art review on transverse web opening for reinforced concrete beams with and without strengthening method,” *J. Phys. Conf. Ser.*, vol. 1895, no. 1, 2021, doi: 10.1088/1742-6596/1895/1/012059.
- [14] G. Ahmed and V. Gerges, “Behavior of RC Beams with Openings Strengthened with CFRP Laminates,” *Int. J. Ind. Sustain. Dev.*, vol. 1, no. 1, pp. 6–14, 2020, doi: 10.21608/ijisd.2020.73449.
- [15] M. A. Mansur, L. M. Huang, K. H. Tan, and S. L. Lee, “Deflections of reinforced concrete beams with web openings,” *ACI Struct. J.*, vol. 89, no. 4, pp. 391–397, 1992, doi: 10.14359/3019.
- [16] M. A. Mansur, “Design of Reinforced Concrete Beams with Web Openings,” *Proc. 6th Asia-Pacific Struct. Eng. Constr. Conf.*, no. September, pp. 5–6, 2006.

- [17] S. Amiri and R. Masoudnia, "Investigation of the opening effects on the behavior of concrete beams without additional reinforcement in opening region using fem method," *Aust. J. Basic Appl. Sci.*, vol. 5, no. 5, pp. 617–627, 2011.
- [18] J. V. A. Amiri and M. Hosseinalibygie, "Effect of Small Circular Opening on the Shear and Flexural Behavior and Ultimate Strength of Reinforced Concrete Beams Using Normal and High," *J. Sch. Eng.*, vol. Volume 16, no. 3239, p. Page(s) 37 To 52., 2004.
- [19] S. N. Sadik, "Strength and ductility of concrete encased composite columns," *Behav. Steel Struct. Seism. Areas*, vol. 30, no. 15, pp. 681–688, 2012, doi: 10.1201/b11396-102.
- [20] A. Y. Kamal, "Encased Beam with Variable Upper Steel," vol. 4, no. 4, pp. 60–66, 2015.
- [21] E. Ellobody and B. Young, "Behaviour and design of composite beams with stiffened and unstiffened web openings," *Adv. Struct. Eng.*, vol. 18, no. 6, pp. 893–918, 2015, doi: 10.1260/1369-4332.18.6.893.
- [22] S. Ahmad, A. Masri, and Z. Abou Saleh, "Analytical and experimental investigation on the flexural behavior of partially encased composite beams," *Alexandria Eng. J.*, vol. 57, no. 3, pp. 1693–1712, 2018, doi: 10.1016/j.aej.2017.03.035.
- [23] C. Sheets, "Flexural Strength Of Prestressed Concrete Beams With Openings And Strengthened With CFRP Sheets," *Int. J. Sci. Technol. Res.*, vol. 4, no. 6, pp. 161–172, 2015.
- [24] M. B. Dawood and D. H. Al-Saffar, "Flexural behavior of steel concrete composite beam with web openings and strengthened by cfrp laminates," *Proc. 8th Int. Conf. Comput. Plast. - Fundam. Appl. COMPLAS 2015*, pp. 507–518, 2015.

- [25] M. A.-B. Abdo, “Analysis of Steel Bridges With Rectangular Web Openings: Finite Element Investigation,” *JES. J. Eng. Sci.*, vol. 38, no. 1, pp. 1–17, 2010, doi: 10.21608/jesaun.2010.123766.
- [26] J. G. Teng, T. Yu, and D. Fernando, “Strengthening of steel structures with fiber-reinforced polymer composites,” *J. Constr. Steel Res.*, vol. 78, pp. 131–143, 2012, doi: 10.1016/j.jcsr.2012.06.011.
- [27] M. H. Makhoul and H. M. Refat, “Strengthening of Composite Steel-Concrete Beams Openings by Adopting Different Reinforcement Methods,” *Adv. Res.*, vol. 19, no. 2, pp. 1–17, 2019, doi: 10.9734/air/2019/v19i230119.
- [28] G. Kim, J. Sim, and H. Oh, “Shear strength of strengthened RC beams with FRPs in shear,” *Constr. Build. Mater.*, vol. 22, no. 6, pp. 1261–1270, 2008, doi: 10.1016/j.conbuildmat.2007.01.021.
- [29] K.-H. Yang, A. F. Ashour, and Jin-Kyu Song, “Shear Capacity of Reinforced Concrete Beams Using Neural Network,” *Int. J. Concr. Struct. Mater.*, vol. Vol.1, No., p. pp.63~73.
- [30] P. D. Zararis and G. C. Papadakis, “DIAGONAL SHEAR FAILURE AND SIZE EFFECT IN RC BEAMS WITHOUT WEB REINFORCEMENT,” *Struct. Eng.*, vol. 127, pp. 733–742, 2001.
- [31] A. Carolin and B. Täljsten, “Theoretical Study of Strengthening for Increased Shear Bearing Capacity,” *J. Compos. Constr.*, vol. 9, no. 6, pp. 497–506, 2005, doi: 10.1061/(asce)1090-0268(2005)9:6(497).
- [32] G. Martinola, A. Meda, G. A. Plizzari, and Z. Rinaldi, “Strengthening and repair of RC beams with fiber reinforced concrete,” *Cem. Concr. Compos.*, vol. 32, no. 9, pp. 731–739, 2010, doi: 10.1016/j.cemconcomp.2010.07.001.
- [33] A. Pimanmas, “Strengthening R/C beams with opening by externally installed FRP rods: Behavior and analysis,” *Compos. Struct.*, vol. 92, no. 8, pp. 1957–1976, 2010, doi: 10.1016/j.compstruct.2009.11.031.

- [34] A. Ahmed, S. Naganathan, K. Nasharuddin, M. M. Fayyadh, and S. Jamali, “Repair effectiveness of damaged RC beams with web opening using CFRP and steel plates,” *Jordan J. Civ. Eng.*, vol. 10, no. 2, pp. 163–183, 2016, doi: 10.14525/jjce.10.1.3534.
- [35] L. de Lorenzis, A. Rizzo, and A. La Tegola, “2.9 Anchorage length of near-surface mounted FRP rods in concrete,” *Adv. Polym. Compos. Struct. Appl. Constr.*, pp. 135–142, 2002, doi: 10.1680/apcfsaic.31227.0014.
- [36] A. H. Abdel-Kareem, “Shear strengthening of reinforced concrete beams with rectangular web openings by FRP Composites,” *Adv. Concr. Constr.*, vol. 2, no. 4, pp. 281–300, 2014, doi: 10.12989/acc.2014.2.4.281.
- [37] K. N. Rahal and H. A. Rumaih, “Tests on reinforced concrete beams strengthened in shear using near surface mounted CFRP and steel bars,” *Eng. Struct.*, vol. 33, no. 1, pp. 53–62, 2011, doi: 10.1016/j.engstruct.2010.09.017.
- [38] H. H. Kammona, “Estimation of Maximum Shear Capacity of RC Deep Beams Strengthened by NSM Steel Bars,” no. 3, pp. 13–22, 2018.
- [39] B. Täljsten, A. Carolin, and H. Nordin, “Concrete structures strengthened with near surface mounted reinforcement of CFRP,” *Adv. Struct. Eng.*, vol. 6, no. 3, pp. 201–213, 2003, doi: 10.1260/136943303322419223.
- [40] M. S. Abdel-Jaber, P. R. Walker, and A. R. Hutchinson, “Shear strengthening of reinforced concrete beams using different configurations of externally bonded carbon fibre reinforced plates,” *Mater. Struct.*, vol. 36, no. 5, pp. 291–301, 2003, doi: 10.1007/bf02480868.
- [41] A. Khalifa, W. J. Gold, A. Nanni, and A. A. M.I., “Contribution of Externally Bonded FRP to Shear Capacity of RC Flexural Members,” *J. Compos. Constr.*, vol. 2, no. 4, pp. 195–202, 1998, doi: 10.1061/(asce)1090-0268(1998)2:4(195).
- [42] H. A. Abdalla, A. M. Torkey, H. A. Haggag, and A. F. Abu-Amira, “Design

- against cracking at openings in reinforced concrete beams strengthened with composite sheets,” *Compos. Struct.*, vol. 60, no. 2, pp. 197–204, 2003, doi: 10.1016/S0263-8223(02)00305-7.
- [43] S. Amiri, R. Masoudnia, and M. A. Ameri, “A review of design specifications of opening in the web for simply supported RC beams,” *J. Civ. Eng. Constr. Technol.*, vol. 2, no. 4, pp. 82–89, 2011.
- [44] S. B. Kudatini, “Experimental Investigation on Internally Strengthened RC Beam with Rectangular,” pp.15410–15417, 2016, doi: 10.15680/IJIRSET.2016.0508175.
- [45] N. K. Oukaili and A. H. Shammari, “Response of reinforced concrete beams with multiple web openings to static load,” *Proc. 4th Asia-Pacific Conf. FRP Struct. APFIS 2013*, no. December, pp. 11–13, 2013.
- [46] W. E. El-demerdash, “Design of Reinforced Concrete, ” by a thesis Submitted in Partial Fulfillment for the Requirements of the Degree of Master of Science Under the Supervision of Ahmed Amin Ghaleb Associate Prof ., Structural Engrg . Dept ., Mohamed El-Said El-Zoughiby Associat,,” no. February 2014, 2018.
- [47] T. Almusallam, Y. Al-Salloum, H. Elsanadedy, A. Alshenawy, and R. Iqbal, “Behavior of FRP-Strengthened RC Beams with Large Rectangular Web Openings in Flexure Zones: Experimental and Numerical Study,” *Int. J. Concr. Struct. Mater.*, vol. 12, no. 1, 2018, doi: 10.1186/s40069-018-0272-5.
- [48] C. C. Weng, S. I. Yen, and C. C. Chen, “SHEAR STRENGTH OF CONCRETE-ENCASED COMPOSITE STRUCTURAL MEMBERS,” *Struct. Eng.*, vol. 127, pp. 1190–1197, 2001.
- [49] ACI Committee 315, “Details and Detailing of Concrete Reinforcement Reported by ACI 315,” *Am. Concr. Inst.*, pp. 1–44, 1999.
- [50] ACI 440.2R, *Guide for the Design and Construction of Externally Bonded*

FRP Systems. 2008.

- [51] C. Paper *et al.*, “Prestressing Systems for Strengthening of Concrete and Metallic Structures, ”Recent developments at ... Eighth International Conference on Fibre-Reinforced Polymer (FRP) Composites in Civil Engineering,” no. December, 2016.
- [52] ACI Committee 440.1R-06, “Guide for the design and construction of concrete reinforced with FRP bars,” *Am. Concr. Inst.*, p. 44, 2006, [Online]. Available: www.concrete.org.
- [53] S. J. E. Dias and J. A. O. Barros, “Performance of reinforced concrete T beams strengthened in shear with NSM CFRP laminates,” *Eng. Struct.*, vol. 32, no. 2, pp. 373–384, 2010, doi: 10.1016/j.engstruct.2009.10.001.
- [54] S. J. E. Dias and J. A. O. Barros, “NSM shear strengthening technique with CFRP laminates applied in high T cross section RC beams,” *Compos. Part B Eng.*, vol. 114, pp. 256–267, 2017, doi: 10.1016/j.compositesb.2017.01.028.
- [55] Z. Zhang and C.-T. T. Hsu, “Shear Strengthening of Reinforced Concrete Beams Using Carbon-Fiber-Reinforced Polymer Laminates,” *J. Compos. Constr.*, vol. 9, no. 2, pp. 158–169, 2005, doi: 10.1061/(asce)1090-0268(2005)9:2(158).
- [56] A. Khalifa and A. Nanni, “Improving shear capacity of existing RC T-section beams using CFRP composites,” *Cem. Concr. Compos.*, vol. 22, no. 3, pp. 165–174, 2000, doi: 10.1016/S0958-9465(99)00051-7.
- [57] L. De Lorenzis and A. Nanni, “Shear strengthening of reinforced concrete beams with near-surface mounted fiber-reinforced polymer rods,” *ACI Struct. J.*, vol. 98, no. 1, pp. 60–68, 2001, doi: 10.14359/10147.
- [58] H. S. Ghali and H. S. Ghali, “Shear Strengthening of RC Beams Using NSM GFRP Bars or CFRP U- Wrap Sheets,” vol. 19, no. 1, pp. 85–102, 2019.
- [59] V. Jayanthi and C. Umarani, “Performance evaluation of different types of

- shear connectors in steel-concrete composite construction,” *Arch. Civ. Eng.*, vol. 64, no. 2, pp. 97–110, 2018, doi: 10.2478/ace-2018-0019.
- [60] P. S. Shraddha, C. Sudha, and M. Lakshmipathy, “Study on ductility behavior of different types of shear connectors in composite structural elements,” *Int. J. Civ. Eng. Technol.*, vol. 8, no. 4, pp. 339–353, 2017.
- [61] M. Titoum, A. Mazoz, A. Benanane, and D. Ouinas, “Experimental study and finite element modelling of push-out tests on a new shear connector of I-shape,” *Adv. Steel Constr.*, vol. 12, no. 4, pp. 487–506, 2016, doi: 10.18057/IJASC.2016.12.4.7.
- [62] R. Balasubramanian and B. Rajaram, “Study on behaviour of angle shear connector in steel-concrete composite structures,” *Int. J. Steel Struct.*, vol. 16, no. 3, pp. 807–811, 2016, doi: 10.1007/s13296-015-0094-0.
- [63] M. Shariati, N. H. Ramli Sulong, M. Suhatri, A. Shariati, M. M. Arabnejad Khanouki, and H. Sinaei, “Comparison of behaviour between channel and angle shear connectors under monotonic and fully reversed cyclic loading,” *Constr. Build. Mater.*, vol. 38, pp. 582–593, 2013, doi: 10.1016/j.conbuildmat.2012.07.050.
- [64] T. M. C. Neto, “Analysis and Design of Composite Beams with Web Openings,” *T. M. Cameira Neto / Inst. Super. Técnico*, pp. 1–10, 2014.
- [65] Y. N. A. C, “Experimental Study on Concrete Encased Composite Beam with Web Opening,” vol. 6, no. 02, pp. 2973–2978, 2018.
- [66] B. El-Taly, M. Hamdy, K. Kandil, and A. Bashandy, “Structural Behavior of Strengthened Concrete-Encased Steel Beams with Web Openings,” *Int. J. Civ. Eng.*, vol. 19, no. 3, pp. 245–263, 2021, doi: 10.1007/s40999-020-00552-1.
- [67] Kirijaa A/P Ratanarajah, “SHEAR STRENGTHENING OF BEAMS WITH LARGE OPENING IN CRITICAL SHEAR ZONE (STATIC

- CONDITIONS),” 2010.
- [68] W. A. Jasim, A. A. Allawi, and N. K. Oukaili, “Strength and Serviceability of Reinforced Concrete Deep Beams with Large Web Openings Created in Shear Spans,” *Civ. Eng. J.*, vol. 4, no. 11, p. 2560, 2018, doi: 10.28991/cej-03091181.
- [69] A. M. Morsy and A. M. Barima, “Behavior of R . C . Beams with Openings using Different Strengthening Techniques,” *Int. J. Sci. Basic Appl. Res.*, vol. 46, no. 1, pp. 195–219, 2019.
- [70] H. H. KAMONNA and L. R. ALKHATEEB, “STRENGTHENING OF REINFORCED CONCRETE DEEP BEAMS WITH OPENINGS BY NEAR SURFACE MOUNTED STEEL BAR,” *J. Eng. Sci. Technol.*, vol. 15, pp. 2559–2579, 2020.
- [71] Y. Gatia Abtan and H. Dhafer AbdulJabbar, “Experimental Study to Investigate the effect of Longitudinal and Transverse Openings on the Structural Behavior of High Strength Self Compacting Reinforced Concrete Beams,” *J. Eng. Sustain. Dev.*, vol. 2019, no. 01, pp. 66–79, 2019, doi: 10.31272/jeasd.23.1.5.
- [72] A. I. el-kassas, H. M. Hassan, and M. A. E. S. Arab, “Effect of longitudinal opening on the structural behavior of reinforced high-strength self-compacted concrete deep beams,” *Case Stud. Constr. Mater.*, vol. 12, p. e00348, 2020, doi: 10.1016/j.cscm.2020.e00348.
- [73] A. A. G. Abu Altemen, A. A. K. Sharba, R. A. N. Al Ameri, M. K. Ibrahim, and M. Ozakca, “Effect of Laying Service longitudinal and Transverse Openings on Reinforced Concrete Hollow Beam Web under Flexural Loadings,” *IOP Conf. Ser. Mater. Sci. Eng.*, vol. 1076, no. 1, p. 012121, 2021, doi: 10.1088/1757-899x/1076/1/012121.
- [74] M. Dinesh Kanna and M. Arun, “Effects of Longitudinal and Transverse

- Direction Opening in Reinforced Concrete Beam: The State of Review,” *IOP Conf. Ser. Mater. Sci. Eng.*, vol. 1059, no. 1, 2021, doi: 10.1088/1757-899X/1059/1/012049.
- [75] A.C.I. Committee, “318-19 Building Code Requirements for Structural Concrete and Commentary,” *318-19 Build. Code Requir. Struct. Comment.*, 2019, doi: 10.14359/51716937.
- [76] ASTM A 370-05, “Standard Test Method and Definition for Mechanical Testing of Steel Products,” 2005 Annual Book of ASTM Standards, Vol.01.01, ASTM, Philadelphia, PA., 2005.
- [77] T. El Maaddawy and S. Sherif, “FRP composites for shear strengthening of reinforced concrete deep beams with openings,” *Compos. Struct.*, vol. 89, no. 1, pp. 60–69, 2009, doi: 10.1016/j.compstruct.2008.06.022.
- [78] L. De Lorenzis and J. G. Teng, “Near-surface mounted FRP reinforcement: An emerging technique for strengthening structures,” *Compos. Part B Eng.*, vol. 38, no. 2, pp. 119–143, 2007, doi: 10.1016/j.compositesb.2006.08.003.
- [79] T. J. Sullivan, G. M. Calvi, and M. J. N. Priestley, “Initial stiffness versus secant stiffness in displacement based design,” *13th World Conf. Earthq. Eng.*, vol. 65, no. 2888, pp. 581–626, 2004.

APPENDIX A



PRODUCT DATA SHEET

Sikadur®-330

2-COMPONENT EPOXY IMPREGNATION RESIN

PRODUCT DESCRIPTION

Sikadur®-330 is a 2-component, thixotropic epoxy based impregnating resin and adhesive.

USES

Sikadur®-330 may only be used by experienced professionals.

Sikadur®-330 is used as:

- Impregnation resin for SikaWrap® fabric reinforcement for the dry application method
- Primer resin for the wet application system
- Structural adhesive for bonding Sika® CarboDur® plates into slits

CHARACTERISTICS / ADVANTAGES

- Easy mix and application by trowel and impregnation roller
- Manufactured for manual saturation methods
- Excellent application behaviour to vertical and overhead surfaces
- Good adhesion to many substrates
- High mechanical properties
- No separate primer required

APPROVALS / STANDARDS

- Adhesive for structural bonding tested according to EN 1504-4, provided with the CE-mark

PRODUCT INFORMATION

Chemical Base	Epoxy resin	
Packaging	5 kg (A+B)	Pre-batched unit
Colour	Component A: white paste Component B: grey paste Components A + B mixed: light grey paste	
Shelf Life	24 months from date of production	
Storage Conditions	Store in original, unopened, sealed and undamaged packaging in dry conditions at temperatures between +5 °C and +30 °C. Protect from direct sunlight.	
Density	1.30 ± 0.1 kg/l (component A+B mixed) (at +23 °C)	
Viscosity	Shear rate: 50 /s	
	Temperature	Viscosity
	+10 °C	~10 000 mPas
	+23 °C	~6 000 mPas
	+35 °C	~5 000 mPas

TECHNICAL INFORMATION

Flexural E-Modulus	~ 3 800 N/mm ² (7 days at +23 °C)	(DIN EN 1465)		
Tensile Strength	~ 30 N/mm ² (7 days at +23 °C)	(ISO 527)		
Tensile Modulus of Elasticity	~ 4 500 N/mm ² (7 days at +23 °C)	(ISO 527)		
Elongation at Break	0.9 % (7 days at +23 °C)	(ISO 527)		
Tensile Adhesion Strength	Concrete fracture (> 4 N/mm ²) on sandblasted substrate	(EN ISO 4624)		
Coefficient of Thermal Expansion	4.5 × 10 ⁻⁵ 1/K (Temperature range -10 °C – +40 °C)	(EN 1770)		
Glass Transition Temperature	Curing time	Curing temperature	TG (EN 12614)	
	30 days	+30 °C		+58 °C
Heat Deflection Temperature	Curing time	Curing temperature	HDT (ASTM D 648)	
	7 days	+10 °C		+36 °C
	7 days	+23 °C		+47 °C
	7 days	+35 °C		+53 °C
Resistant to continuous exposure up to +45 °C.				
Service Temperature	-40 °C to +45 °C			

SYSTEM INFORMATION

System Structure	Substrate primer - Sikadur®-330. Impregnating / laminating resin - Sikadur®-330. Structural strengthening fabric - SikaWrap® type to suit requirements.
-------------------------	---

APPLICATION INFORMATION

Mixing Ratio	Component A : component B = 4 : 1 by weight When using bulk material the exact mixing ratio must be safeguarded by accurately weighing and dosing each component.			
Consumption	See the "Method Statement for SikaWrap® manual dry application" Ref 850 41 02. Guide: 0.7 - 1.5 kg/m ²			
Ambient Air Temperature	+10 °C min. / +35 °C max.			
Dew Point	Beware of condensation. Substrate temperature during application must be at least 3 °C above dew point.			
Substrate Temperature	+10 °C min. / +35 °C max.			
Substrate Moisture Content	< 4 % pbw			
Pot Life	Temperature	Pot life	Open time	(EN ISO 9514)
	+10 °C	~90 minutes (5 kg)	~90 minutes	
	+23 °C	~60 minutes (5 kg)	~60 minutes	
	+35 °C	~30 minutes (5 kg)	~30 minutes	
The pot life begins when the resin and hardener are mixed. It is shorter at high temperatures and longer at low temperatures. The greater the quantity mixed, the shorter the pot life. To obtain longer workability at high temperatures, the mixed adhesive may be divided into portions. Another method is to chill components A+B before mixing them (not below +5 °C).				

APPLICATION INSTRUCTIONS

SUBSTRATE QUALITY

Product Data Sheet
Sikadur®-330
May 2017, Version 02.01
020206040010000004



Substrate must be sound and of sufficient tensile strength to provide a minimum pull off strength of 1.0 N/mm² or as per the requirements of the design specification.
See also the "Method Statement for SikaWrap® manual dry application" Ref 850 41 02.

SUBSTRATE PREPARATION

Also refer to SikaWrap® Technical Information Manual for dry application method" Ref 850 41 02.

MIXING

Pre-batched units:
Mix components A+B together for at least 3 minutes with a mixing spindle attached to a slow speed electric drill (max. 300 rpm) until the material becomes smooth in consistency and a uniform grey colour. Avoid aeration while mixing. Then, pour the whole mix into a clean container and stir again for approx. 1 more minute at low speed to keep air entrapment at a minimum. Mix only that quantity which can be used within its pot life.

Bulk packing, not pre-batched:
First, stir each component thoroughly. Add the components in the correct proportions into a suitable mixing pail and stir correctly using an electric low speed mixer as above for pre-batched units.

APPLICATION METHOD / TOOLS

Also refer to SikaWrap® Technical Information Manual for dry application method" Ref 850 41 02.

CLEANING OF TOOLS

Clean all equipment immediately with Sika® Thinner C. Cured material can only be removed mechanically.

LIMITATIONS

Sikadur®-330 must be protected from rain for at least 24 hours after application.

Ensure placement of fabric and laminating with roller takes place within open time.

At low temperatures and / or high relative humidity, a tacky residue (blush) may form on the surface of the cured Sikadur®-330 epoxy. If an additional layer of fabric or a coating is to be applied onto the cured epoxy, this residue must first be removed with warm, soapy water to ensure adequate bond. In any case, the surface must be wiped dry prior to application of the next layer or coating.

For application in cold or hot conditions, pre-condition material for 24 hours in temperature controlled storage facilities to improve mixing, application and pot life limits.

For further information on over coating, number of layers or creep, please consult a structural engineer for calculations and see also the "Method Statement for SikaWrap® manual dry application" Ref 850 41 02. Sikadur® resins are formulated to have low creep under permanent loading. However due to the creep behaviour of all polymer materials under load, the long term structural design load must account for creep. Generally the long term structural design load must be lower than 20-25% of the failure load. Please consult a structural engineer for load calculations for the specific application.

VALUE BASE

All technical data stated in this Product Data Sheet are based on laboratory tests. Actual measured data may vary due to circumstances beyond our control.

LOCAL RESTRICTIONS

Please note that as a result of specific local regulations the performance of this product may vary from country to country. Please consult the local Product Data Sheet for the exact description of the application fields.

ECOLOGY, HEALTH AND SAFETY

For information and advice on the safe handling, storage and disposal of chemical products, users shall refer to the most recent Safety Data Sheet (SDS) containing physical, ecological, toxicological and other safety-related data.

LEGAL NOTES

The information, and, in particular, the recommendations relating to the application and end-use of Sika products, are given in good faith based on Sika's current knowledge and experience of the products when properly stored, handled and applied under normal conditions in accordance with Sika's recommendations. In practice, the differences in materials, substrates and actual site conditions are such that no warranty in respect of merchantability or of fitness for a particular purpose, nor any liability arising out of any legal relationship whatsoever, can be inferred either from this information, or from any written recommendations, or from any other advice offered. The user of the product must test the product's suitability for the intended application and purpose. Sika reserves the right to change the properties of its products. The proprietary rights of third parties must be observed. All orders are accepted subject to our current terms of sale and delivery. Users must always refer to the most recent issue of the local Product Data Sheet for the product concerned, copies of which will be supplied on request.

SIKA LIMITED
Watchmead
Welwyn Garden City
Hertfordshire, AL7 1BQ
Tel: 01707 394444
Web: www.sika.co.uk
Twitter: @SikaLimited

SIKA IRELAND LIMITED
Ballymun Industrial Estate
Ballymun
Dublin 11, Ireland
Tel: +353 1 862 0709
Web: www.sika.ie
Twitter: @Sikaireland



Sikadur-330_en_GB_(05-2017)_2_1.pdf

Product Data Sheet
Sikadur®-330
May 2017, Version 02.01
020206040010000004

APPENDIX B

Shear strength for CFRP by using Near Surface (NS)

$$\begin{aligned} E_b &= 175000 \\ \tau_{\text{bond}} &= 0.001 ((E_b * d_b)/L_i) = 2.046784 \\ L_i &= 513 \\ d_r &= 300 \\ d_{\text{net}} &= d_r - 2C = 260\text{mm} \\ S &= 50 \text{ mm} \\ L_{\text{tot-min}} &= d_{\text{net}} - S = 210\text{mm} \quad \text{if } d_{\text{net}}/3 < S < d_{\text{net}} \end{aligned}$$

$$\begin{aligned} L_{\text{tot-min}} &= 2.d_{\text{net}} - 4.S = 320\text{mm} \\ \text{if } d_{\text{net}}/4 < S < d_{\text{net}}/3 \end{aligned}$$

$$\theta = 30 \text{ degree}$$

$$V_f = [2 \pi d_b \tau_{\text{bond}} L_{\text{tot-min}}] \sin\theta = 8.1 \text{ kN}$$

تقنيات التقوية للفتحات في منطقة فضاء القص للعتبات المركبة من الحديد المغطى بالخرسانة

درس هذا البحث تقنيات تقوية للعتبات المركبة من الحديد المغطى بالخرسانة والتي لها فتحات مستعرضة مربعة في منطقة القص تحت تأثير التحميل من أربع نقاط. تمت دراسة فتحتين مربعتين (50 × 50) مم و (136 × 136) مم تحت تأثير استخدام تقنيات تقوية مختلفة. يتألف البرنامج التجريبي من اختبار خمسة عشر عتبة ذات فتحات مربعة عرضية في منتصف منطقة القص ، وكانت ثلاثة من العتبات بمثابة عتبات تحكم ، بما في ذلك عتبة واحدة بدون فتحات ، في حين أن العتبتين الأخرتين بهما فتحتان تقعان بشكل متماثل في منطقة القص ، وتم تقوية اثنتا عشر عتبة بتقنيات مختلفة في منطقة الفتح مثل تقنية التغليف المبتوق المستعرض (EET) ، وترتيب التسليح ، وصفائح البوليمر المقوى بألياف الكربون (كان تكوين تقوية CFRP الذي تم النظر فيه في هذه الدراسة عبارة عن نظام تغليف كامل حول الفتحات المربعة وصفائح تقوية قطرية حول الفتحات المربعة) وقضبان CFRP المثبتة بالقرب من السطح في تكوينين مختلفين حول الفتحات المربعة (تقوية العينات بشكل معيني من قضبان CFRP وقضبان CFRP تقوية قطري). تمت مناقشة الاستجابة الهيكلية من حيث حمل التكسير الأول ، والحمل النهائي ، وأقصى انحراف ، وأنماط الفشل ، وأنماط الشقوق ، والصلابة الأولية ، وامتصاص الطاقة. أشارت نتائج الاختبار إلى أن تقنية ترتيب التسليح المستخدمة لتقوية الفتحة الصغيرة سجلت زيادة في قدرة الحمل القصوى والصلابة بحوالي 15% و 50% ؛ على التوالي مقارنة بعتبة التحكم ذات الفتحة الصغيرة. بالإضافة إلى العتبة المركبة من الحديد المغطى بالخرسانة مع فتحة مربعة صغيرة في منطقة القص المقواة بواسطة صفائح ملفوفة بالكامل من البوليمر المقوى بألياف الكربون (CFRP) حول الفتحات ، فقد أدى ذلك إلى تحسين مقاومة القص فيما يتعلق بسعة الحمل القصوى وامتصاص الطاقة بنسبة 8% و 48% مقارنةً بعتبة التحكم مع فتحة صغيرة على التوالي.



جمهورية العراق
وزارة التعليم العالي والبحث العلمي
جامعة ميسان / كلية الهندسة
قسم الهندسة المدنية

تقنيات التقوية للفتحات في منطقة فضاء القص للعتبات المركبة من الحديد المغطى
بالخرسانة

من قبل

الاسم: ختام سالم حسين

بكالوريوس هندسة مدنية, 2018

أطروحة

مقدمة الى كلية الهندسة - جامعة ميسان

كجزء من متطلبات الحصول على درجة الماجستير

في علوم الهندسة المدنية

(الإنشاءات)

إيار 2022

بإشراف: د. ناصر حكيم طعمه